

https://dspace.org/

3D geophysical modelling of the Bethlehem sub-basin, Free State, South Africa

Naidoo, Ansuya

2020
https://hdl.handle.net/10539/30187

Downloaded from a DSpace repository. https://dspace.org/

3D Geophysical modelling of the Bethlehem Sub – basin, Free State, South Africa

A dissertation submitted to the Faculty of Science, University of the Witwatersrand in fulfilment of the requirements for the degree of
Master of Science

Johannesburg, March 2019

School of Geosciences, University of the Witwatersrand

Ansuya Naidoo



Declaration

I declare that this dissertation is my own, unaided work. It is being submitted for the Degree of Master of Science at the University of the Witwatersrand, Johannesburg. It has not been submitted before for any degree or examination in any other university



_____

Signature

29 March 2019

_____

Date

Abstract

Extensions to the Witwatersrand Basin have been widely examined, with many geophysical surveys being carried out in the early 1990s. One of these areas is the Bethlehem sub-basin, located on the south eastern edge of the Witwatersrand basin.

The aim of the study is to integrate old geophysical datasets to create a 3D geological and a 3D gravity forward model of the Bethlehem Sub - basin. A re – interpretation of the Bethlehem sub-basin was done using the latest geophysical software and techniques. The study also investigates the cause of the Bethlehem gravity high. The outcome of this study provides a more constrained interpretation of the structure of the Bethlehem sub-basin and its relationship to the Witwatersrand Basin.

The resultant 3D gravity model shows the Bethlehem Sub - basin is structurally controlled by north northwest trending horsts and grabens of granite and West Rand Group rocks respectively. These grabens preserve large-scale West Rand Group sediments of the Witwatersrand Supergroup. The horst and graben structures creates a change in density from low density granite to high density West Rand Group, causing the gravity high seen in the Bethlehem area.

Four major structures were interpreted in the seismic and gravity data. These are labelled as fault B, C, D and E. Normal faults B and C trending north northwest create a granite ridge underlying the Karoo Supergroup. Normal faults D and E create a smaller granite ridge overlain by West Rand Group sediments.

This study investigates the ability to integrate existing 2D datasets into a 3D space and the significance of viewing data in a 3D environment to better understand and constrain lithological structures and boundaries.

Contents

3D Geophysical modelling of the Bethlehem Sub – basin, Free State, ... 1
South Africa 1
Abstract ii
List of Figures v
List of Tables ix
1. Introduction 1
1.1 Study area and history of the Bethlehem Sub-basin 3
1.2 Prospectus 5
2 Geological setting 6
2.1 Stratigraphy of the Witwatersrand basin 6
2.2 Structural Setting 10
2.3 Geological setting of the Bethlehem study area 11
3 Data sets 13
3.1 Borehole data 15
3.2 Seismic data 19
3.3 Gravity data 23
3.4 Magnetic data 26
4 Methodology 27
4.1 Seismic reflection method 29
4.1.1 Background 29
4.1.2 Survey design 29
4.1.3 Seismic Interpretation 30
4.1.4 Justification for lithological boundaries - All densities and velocities shown in table 5 31
4.2 Magnetic Method 33
4.2.1 Background 33
4.2.2 Magnetic Interpretation 33
4.3 Gravity Method 34
4.3.1 Background 34
4.3.2 Forward Modelling Methods 34
4.3.3 Gravity Interpretation 37
5 Results 40

5.1 Seismic Results 40
5.1.1 Seismic results of south western region 41
5.1.2 Seismic results of north eastern region 52
5.2 Gravity Results 55
6 3D Modelling 67
6.1 3D Geological Model 67
6.2 Geological Volumes 69
6.2.1 Basement volume 69
6.2.2 West Rand Group Volume 71
6.2.3 Central Rand Group Volume 73
6.2.4 Ventersdorp Supergroup Volume 75
6.3 3D Gravity Model 77
6.4 Gravity Volumes 80
6.4.1 Basement Volume 80
6.4.2 West Rand Group Volume 82
6.4.3 Central Rand Group Volume 83
6.4.4 Ventersdorp Supergroup Volume 84
7 Discussion 85
7.1 Stratigraphy of the Bethlehem study area 85
7.2 Structural Features 86
7.3 3D gravity forward model 87
7.4 Timeline of events 88
7.5 Bethlehem gravity anomaly 90
8 Conclusion 92
References 93
Appendix A 99

List of Figures

Figure 1.1 Map (A) Locality map of the Bethlehem study area with reference to the map of South Africa (black outline), Kaapvaal Craton (red outline), Karoo Basin (green outline) and Witwatersrand basin (yellow outline). The Witwatersrand basin overlies the Kaapvaal Craton and is in turn overlain by the Karoo Basin. Map (B) shows a simplified geological map of the Witwatersrand basin showing the main groups in the Basin and the Karoo cover over the Witwatersrand basin. Note that the south eastern boundary is poorly constrained as it is overlain by the Karoo Supergroup (redrafted from Pretorius, 2003 and Dankert and Hein, 2010). 2

Figure 1.2Map A - Location and inspiration for the study of the Bethlehem anomaly. Map B - The Bouguer Gravity Map published by Corner et al., (1986), showing the spatial relationship between the Witwatersrand basin and the Bethlehem gravity high outlined by black box. These data inspired an era of exploration as the possibility of the Bethlehem region being part of the Witwatersrand basin and gold bearing rocks were explored. Map C - The magnetic map modified from McCarthy et al., (2018) shows the relationship of the Witwatersrand basin (yellow) and Bethlehem area outline in black box with the shape of the Bethlehem gravity high outlined in blue. The Vredefort structure is shown on Map B and C. 3

Figure 2.1 Locality map of the Bethlehem study area with simplified geology of the Karoo Basin that covers more than half of the Witwatersrand basin (yellow outline). Location of 13 boreholes (white triangles) and 10 seismic lines (black dotted lines) used for this study. Outcrops of dolerite sills (red) within the Karoo Supergroup which covers the Bethlehem area 9

Figure 2.2 Map A – Bethlehem area in comparison to South Africa, Karoo Basin, Witwatersrand Basin and Vredefort structure. Map B – The Bethlehem area, with a gravity backdrop. Shows the town of Bethlehem (black dot), seismic lines and boreholes. Bethlehem anomaly Pink area (Modified from Council of Geoscience) 11

Figure 3.1 Map (A) Location map for the Bethlehem gravity anomaly in relation to the Kaapvaal Craton (red line), Witwatersrand basin (yellow line) and Karoo Basin (green line). Map (B) shows the data used to constrain the Bethlehem region and black dot represents town of Bethlehem. A section of the Bouguer gravity map of South Africa that covers the Bethlehem study area. 10 Reflection seismic lines (black dotted lines) with the town of Bethlehem at the center and borehole data (white triangles). The boreholes linked with a black line were used to create a north – south profile to determine a general understanding of the geology beneath the Karoo cover 14

Figure 3.2 North - south profile through the western side of the Bethlehem study area, showing 7 out of 13 wells. The wells were numbered in Table 3.1 and gravity map showing the location of boreholes with the dotted line representing the profile shown above. Each lithology is represented by a different colour; Karoo (green), Ventersdorp (orange), Central Rand (yellow), West Rand (brown) and basement (pink). Stratigraphic boundaries are marked with a dotted line were possible as some boreholes do not have enough information. Blue dotted line represents 1 km above sea level to represents where seismic sections begin. 17

Figure 3.3 Borehole data of Karoo Supergroup showing dolerite sills in red. The Borehole data shows dolerite sills range in thickness from 10 m to 200 m. These boreholes were used to constrain the dolerite sills interpreted in the seismic sections. 18

Figure 3.4 Bouguer Gravity map of South Africa with Bethlehem study area outlined in black box (above). Bouguer gravity map of Bethlehem study area (below). Seismic lines (dotted lines) and boreholes (white triangles) are overlain on map (Modified from Council of Geoscience). 25

Figure 3.5 Map of magnetic data in the Bethlehem area showing, outline of Bethlehem gravity anomaly (solid black line), seismic lines (dotted black lines) and borehole locations (white triangles). Black dot represents town of Bethlehem 26

Figure 4.1 Flow chart outlining the process for each borehole, magnetic, 2D seismic and gravity data sets used in this study to a 3D geological model and 3D gravity model. Arrows are used to show the order of each step in the process and when datasets were integrated and used as constraints for a more accurate interpretation. 28

Figure 4.2 The geometry of a 2D source used to determine the Talwani method et al., (1959) algorithm to describe the gravitational anomaly created by the source. The top diagram shows the source has been elongated into the y-axis and the bottom diagram shows how the smooth outline of the cross-section is simplified to a n-sided polygon. Diagram modified from Blakely (1995) 35

Figure 4.3 The geometry of a 3D rectangular prism method, approximating a 3-dimensional mass. Diagram modified from Blakely (1995). 36

Figure 4.4 Map A – original Bouguer gravity map, Map B – residual Bouguer gravity map, Map C – calculated regional Bouguer gravity map and Map D – crustal thickness map, overlain with borehole data (white triangles and seismic lines (black lines). Profile line X - Y (black) used for forward modelling in figure 4.5. 38

Figure 4.5 Profile X-Y showing the removal of regional gravity data. Above image shows Profile X-Y of the original gravity data (green line) compared to regional gravity data (blue line) and residual gravity data (red line). The residual gravity map was used for 2D and 3D forward modelling for this study. 39

Figure 5.1 Location map of seismic lines interpreted for this study overlaid on the residual gravity map (left) and magnetic map (right) of the Bethlehem region. Seismic lines are centered on the town of Bethlehem. Most of the lines end at the town, crossing one side of the anomaly except for EB310 which runs across the anomaly. EB310 is also split into 3 parts A, B and C. The boreholes are represented by green triangles. The south western region and north eastern regions are separated by dashed line 41

Figure 5.2 Gravity map (A) shows location of the seismic line. Seismic section EB330 with no interpretation (B) and interpretation (C). There are no boreholes close to this seismic line. Fault B uplift granite and tilts West Rand Group 44

Figure 5.3 Gravity map (A) shows location of seismic section EB332. Seismic section EB332 with no interpretation (B) and interpretation (C). This line was separated into A and B. There are no boreholes close to this seismic line 45

Figure 5.4 Gravity map (A) and magnetic map (B) shows location of seismic line and borehole for EB310. Seismic section EB310 C and B with no interpretation (C) and interpretation (D).This line was split into 3 parts section EB310 C and B on the south western side and EB310 A on the north eastern side. Boreholes 9 and 6 go deeper than the Karoo and are shown in the interpreted seismic section. Boreholes 9, 6, 4 and 5 also show dolerites which are shown in (E). 46

Figure 5.5 Gravity map (A) shows the location of seismic section and boreholes. Seismic section EB335 with no interpretation (B) and interpretation (C). Borehole 7 which overlies seismic section EB335 is shown in (C). 47

Figure 5.6 Gravity map (A) and magnetic map (B) shows the location of seismic section and boreholes. Borehole1 which overlies. Seismic section EB337 with no interpretation (C) and interpretation (D). Seismic section EB335 is shown in (D). Borehole 1 also shows dolerite intrusions and is shown in image (E). 48

Figure 5.7 Gravity map (A) shows the location of seismic section and boreholes. Seismic section EB334 with no interpretation (B) and interpretation (C). Borehole 6 which overlies seismic section EB334 is shown in (C). 49

Figure 5.8 Gravity map (A) shows location of seismic line. Seismic section WB491 with no interpretation (B) and interpretation (C). There are no boreholes close to this seismic line. 50

Figure 5.9 Gravity map (A) shows location of seismic line. Seismic section EB331 with no interpretation (B) and interpretation (C). Borehole 11 is shown in interpreted seismic section (B). 51

Figure 5.10 Gravity map (A) shows location of seismic line. Seismic section EB310A with no interpretation (B) and interpretation (C). There are no boreholes near his section. 53

Figure 5.11 Gravity map (A) shows location of seismic line. Seismic section EB311 with no interpretation (B) and interpretation (C). Boreholes near this seismic line do not go deeper than the Karoo and are not shown. 54

Figure 5.12 Location map of the 4 gravity profiles (Black lines) overlying the residual gravity map of the Bethlehem study area. Boreholes are represented by green triangles. 55

Figure 5.13 Location of gravity profile 1 overlain on the residual gravity map of Bethlehem (A). Location of seismic section EB331 and WB491 which corresponded with the gravity profile (B). First panel (C) shows 2D gravity profile with observed gravity anomaly and calculated gravity anomaly of model (thin black line). Second panel (D) shows correlating seismic sections used to constrain model. Third panel (E) shows 2D gravity model corresponding to the calculated gravity profile in first panel. 56

Figure 5.14 Location of gravity profile 2 overlain on the residual gravity map of Bethlehem (A). Location of seismic section EB310 which corresponded with the gravity profile (B). First panel (C) shows 2D gravity profile with observed gravity anomaly and calculated gravity anomaly of model (thin black line). Second panel (D) shows correlating seismic sections used to constrain model. Third panel (E) shows 2D gravity model which corresponds to calculated gravity profile in first panel. 58

Figure 5.15 Location of gravity profile 3 overlain on the residual gravity map of Bethlehem (A). Location of seismic sections EB332 EB310 which corresponded with the gravity profile (B). First panel (C) shows 2D gravity profile with observed gravity anomaly and calculated gravity anomaly of model (thin black line). Second panel (D) shows correlating seismic sections used to constrain model. Third panel (E) shows 2D gravity model corresponding to the calculated gravity profile in first panel. 60

Figure 5.16 Location of gravity profile 4 overlain on the residual gravity map of Bethlehem (A). Location of seismic section EB330 which corresponded with the gravity profile (B). First panel (C) shows 2D gravity profile with observed gravity anomaly and calculated gravity anomaly of model (thin black line). Second panel (D) shows correlating seismic sections used to constrain model. Third panel (E) shows a 2D gravity model corresponding to the calculated gravity profile in first panel. 62

Figure 5.17 Location of seismic lines fault B and C and 2D gravity model faults C – E overlain on the residual gravity map (left) and Magnetic map (right). Green triangles are borehole locations and white lines are seismic line locations. 65

Figure 5.18 Google earth image of all seismic sections (top), the south western region (left) and north eastern region (right). Residual gravity map and Fault B, C shows how seismic section interpretation corresponds to observed data. Fault D and E interpreted only in 2D forward modelling and not in seismic sections are also drawn on map..... 66

Figure 6.1 A 3D view of interpreted seismic lines, looking north and plunging at 35°shown in image (A). The imported seismic horizons which define the lithological boundaries. Key; pink – granite, brown – Central Rand, Orange – Ventersdorp, yellow – Karoo shown image (B). 4 Major faults interpreted from the 2D seismic lines and redrawn in Leapfrog Geo faults B and C shown in image (C)..... 68

Figure 6.2 Model of basement volume. Upper contact wireframe (above). Pink lines represent the unconformable lithological contacts. Interpolated volume (below) with faults B and C labelled in dashed lines..... 70

Figure 6.3 Model of West Rand Group volume. Upper contact wireframe of West Rand Group and Central Rand Group (above). Brown lines represent the unconformable lithological contacts. Interpolated volume (below) with faults shown in dashed lines..... 72

Figure 6.4 Model of Central Rand Group volume. Upper contact wireframe of Central Rand Group and Ventersdorp (above). Brown lines represent the unconformable lithological contacts. Interpolated volume (below) with faults shown in dashed lines..... 74

Figure 6.5 Model of Ventersdorp volume. Upper contact wireframe of Ventersdorp and Central Rand Group (above). Brown lines represent the unconformable lithological contacts. Interpolated volume (below) with faults shown in dashed lines. 76

Figure 6.6 Map of observed gravity (above) and calculated gravity from forward model (below). Lines 7, 68, 55, 34, and 90 are the locations of profiles shown in figure 6.7. 78

Figure 6.7 2D profiles from the 3D gravity model. Green dotted line shows observed residual gravity and blue line represents calculated gravity from model. Faults B, C and D correspond to seismic and 2D forward modelling interpretation. 79

Figure 6.8 3D Model of basement volume. Dotted black lines show faults B, C and D. 81

Figure 6.9 3D gravity West Rand Group volume with underlying basement (pink). Dotted black lines shows faults B, C, and D. 82

Figure 6.10 3D gravity model of Central Rand Group volume (yellow), with underlying West Rand Group (brown) and basement (pink). 83
Figure 6.11 3D gravity model of the Ventersdorp Supergroup (orange), with underlying Central Rand Group (yellow), West Rand Group (brown) and basement (pink). 84

Figure 7.1 Chart showing the deposition of the Witwatersrand basin, Bethlehem tectonic events which have occurred and tectonic events in the Witwatersrand basin in literature. Areas shaded in grey shows deposition that did not occurred in the Bethlehem study area (Johnson et al., 2006; Dankert and Hein, 2010; Manzi et al., 2013; Molezzi, 2017). 89

Figure 7.2 Residual gravity map of the Bethlehem study area, TMI map of the Bethlehem study area and a greater region surrounding the Bethlehem study area. Seismic lines shown in (white), boreholes (green triangles) and faults B, C, D and E in dashed white lines. 91

List of Tables

Table 1 Simplified stratigraphy of the Witwatersrand basin and overlying Karoo Basin, The units identified from boreholes in the Bethlehem study area are highlighted in blue (Johnson et al., 2006; Frimmel and Minter, 2002; Catuneanu,2001). 7

Table 2 Borehole database used to help constrain either the top or base of each lithology in the Bethlehem region (Karoo Supergroup, Ventersdorp Supergroup, Witwatersrand Supergroup and Granite basement). Coordinates are converted relative to the WGS84 ellipsoid, Grey blocks represent a lithology that was not seen in the borehole due to the borehole not going deep enough or the specific lithology is not being present in that borehole. 16

Table 3 Summary of the acquisition parameters used for the 2D seismic data between 1990 and 1993 (Pretorius, 1994). 20

Table 4 Summary of the processing parameters used for the 2D seismic data sets acquired in 1994 (Pretorius, 1994). 21

Table 5 Velocity of each Stratigraphic group found in the Bethlehem region. This is a collection of velocities from literature across the Witwatersrand basin. 22

Table 6 Density of each stratigraphic group found in the Bethlehem region. This is a collection of densities from literature across the Witwatersrand basin. 24

Acknowledgements

I would like to thank Thuthuka Foundation NRF (National Research Foundation) and CIMERA (Centre of Excellent for Integrated Mineral and Energy Resource Analysis) for providing financial support. The Council for Geoscience for providing access to borehole, gravity and magnetic data. AngloGold Ashanti for providing the 2D reflection seismic data. Acknowledgments to Patrick Cole from CGS for providing and updating PyGMI software. Thank you to my supervisor Prof. Susan Webb for patience, support and continuous encouragement. Finally thank you to my parents for giving me the opportunity to pursue a masters.

Introduction

The Witwatersrand Basin hosts one of the greatest gold-bearing conglomerate units in the world. Understanding the structure and extent of the Witwatersrand basin became essential for exploration throughout the 20th Century. However, this was complicated by the fact that most of the basin was buried beneath younger rocks of the Ventersdorp, Transvaal and Karoo Supergroups (figure 1.1). During this golden age the main basin as well as possible extensions to the basin were explored and depending on their mining potential the area was either explored further for geological and structural information or left unexplored (de Beer, 2015; Pretorius, 2003).

The north western margin of the Witwatersrand basin is the most exposed section of the basin whereas the interior region, sections of the western margin and the southwestern margin are overlain by younger sediments. These areas were mapped using magnetic, gravity and reflection seismic geophysical techniques. To determine the presence of gold bearing strata at depth mining companies used the density contrasts between the strata, gravity was used to show the density contrast between the less dense Central Rand Group quartzites compared to the overlying more dense Ventersdorp lavas. Magnetic susceptibility showed a contrast of the strongly magnetized ferruginous shales of the West Rand Group sediments compared to the less magnetized basement rocks and overlying Central Rand Group sediments. This was what led to the discovery of the West Witwatersrand Goldfield by Dr. R. Krahmann (Krahmann, 1936; Roux et al., 1967; Wilsher, 1987).

In the early 1980s the 2D reflection seismic method was used to explore for gold and base metal deposits in hard rock environments. The 2D reflection method was capable of mapping more detailed deeply buried strata compared to the gravity and magnetic methods. Thus a new era of exploration began. The gold bearing strata of the Witwatersrand basin are usually less than 1 m thick and do not have a large impedance contrast within the rock layer consisting mainly of quartzite. However the reflection seismic method uses the contrast of overlying and underlying reefs known as marker horizons. Another importance of the reflection seismic method is to create structural maps. Structures such as horst and grabens, synclines and anticlines could determine if a reef was brought closer to surface and possible to mine. South Deep is an example of a mine discovered through the reflection seismic method (Roux et al., 1967).

At the same time as the 2D reflection seismic exploration was growing, advanced techniques which could enhance images of magnetic and gravity data were introduced (de Beer, 2015). The reinterpretation of airborne magnetic and gravity surveys which were flown 10 to 20 years earlier, led to the discovery of

magnetic and gravity anomalies on the south eastern edge of the Witwatersrand basin. Magnetic anomalies situated around the town of Bethlehem were indicative of West Rand Group magnetic sediments found in the main Witwatersrand basin. Corner and Wilsher (1989) and Corner et al. (1986) suggested that the gravity anomalies around the town of Bethlehem represented small basins of Witwatersrand sediments separated by basement granite due to its alternating high and low readings. In light of new information mining companies such as Anglo American carried out several 2D reflection seismic surveys around the south western margin of the Witwatersrand basin as well as drilling of deep boreholes (>2 km). However investigation showed limited mining potential and research into the structure and geology of these anomalies was left unresolved.

In this study a compilation of borehole, 2D reflection seismic images, gravity and magnetic data is used to investigate the Bethlehem region and the gravity anomaly known as the Bethlehem gravity high that sits beneath extensive Karoo sediments (Cantuneau et al., 2005). A 3D gravity forward model of the Bethlehem region is produced and interpreted in a modern structural environment to test ideas of the structural history of the Bethlehem region and causes of the Bethlehem gravity high.

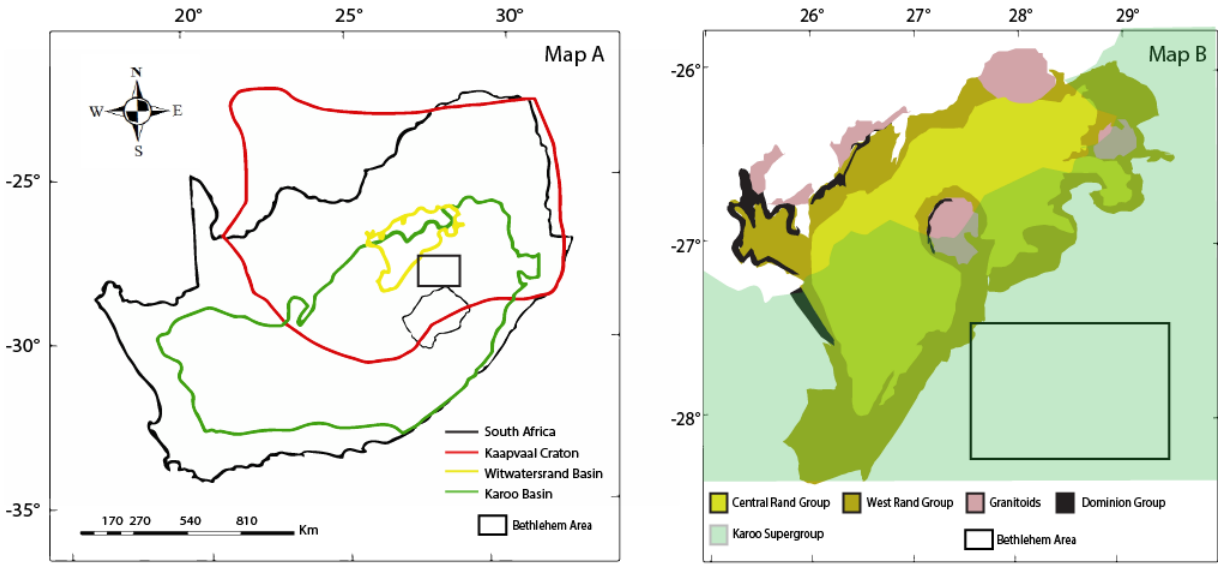


Figure 0.1 Map (A) Locality map of the Bethlehem study area with reference to the map of South Africa (black outline), Kaapvaal Craton (red outline), Karoo Basin (green outline) and Witwatersrand basin (yellow outline). The Witwatersrand basin overlies the Kaapvaal Craton and is in turn overlain by the Karoo Basin. Map (B) shows a simplified geological map of the Witwatersrand basin showing the main groups in the Basin and the Karoo cover over the Witwatersrand basin. Note that the south eastern boundary is poorly constrained as it is overlain by the Karoo Supergroup (redrafted from Pretorius, 2003 and Dankert and Hein, 2010).

1.1 Study area and history of the Bethlehem Sub-basin

The Bethlehem sub-basin is situated on the south eastern edge of the Witwatersrand basin, in the Free State Province, South Africa (Figure 1.2). Geologically Bethlehem is situated on the Kaapvaal Craton and approximately 150 km southeast of the Vredefort structure. The area is also covered by Karoo sediments which are Phanerozoic in age and vary in thickness from 500 m in the north to 1500 m in the south (Johnson *et al.*, 1991; SACS, 1980). The structure of the Bethlehem gravity high and thereafter study of the Bethlehem sub-basin has been debated since the 1960s.

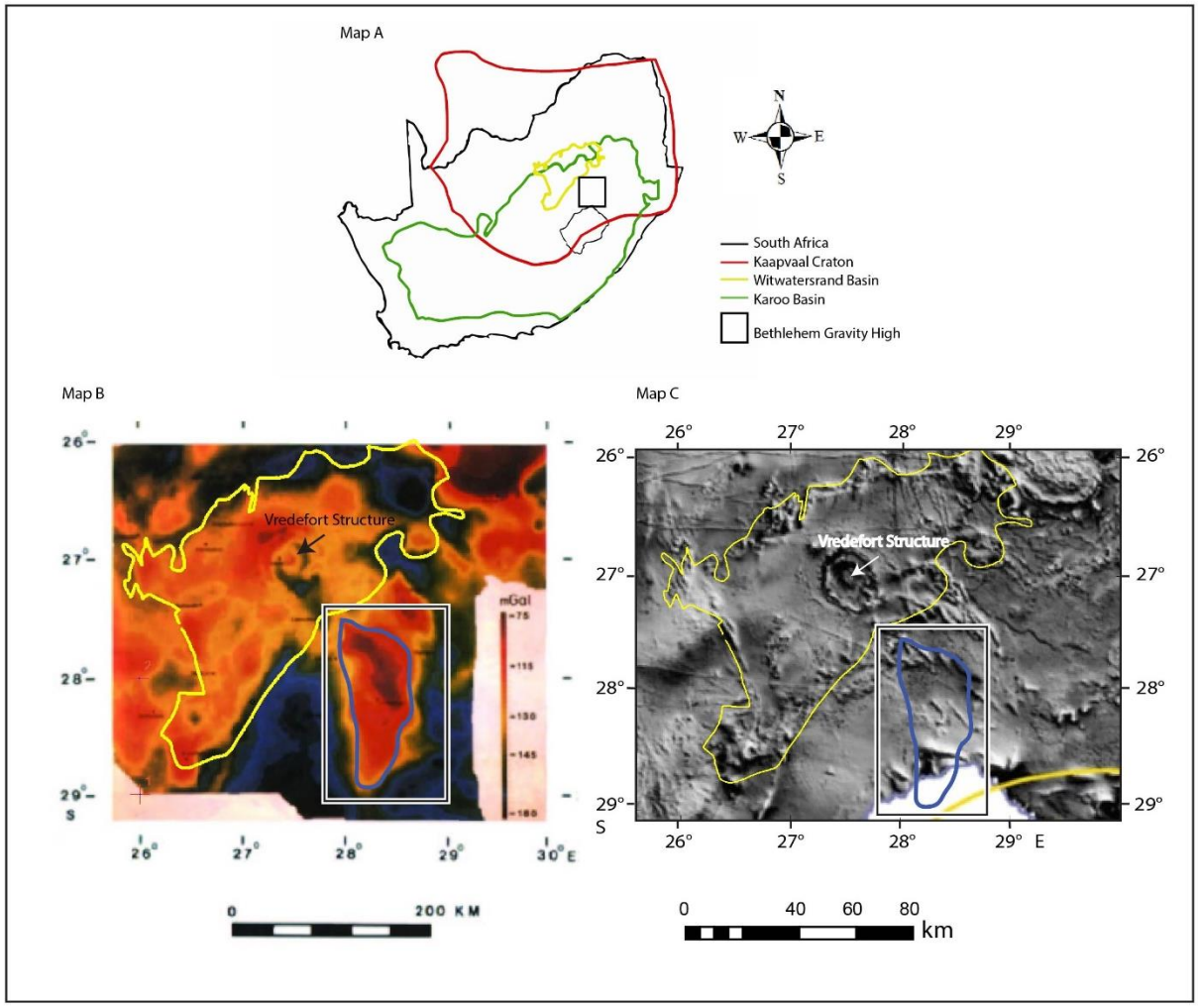


Figure 0.2Map A - Location and inspiration for the study of the Bethlehem anomaly. Map B - The Bouguer Gravity Map published by Corner et al., (1986), showing the spatial relationship between the Witwatersrand basin and the Bethlehem gravity high outlined by black box. These data inspired an era of exploration as the possibility of the Bethlehem region being part of the Witwatersrand basin and gold bearing rocks were explored. Map C - The magnetic map modified from McCarthy et al., (2018) shows the relationship of the Witwatersrand basin (yellow) and Bethlehem area outline in black box with the shape of the Bethlehem gravity high outlined in blue. The Vredefort structure is shown on Map B and C.

Hales and Gough (1962) suggested that the Bethlehem gravity anomaly could be due to an intrusion similar to that of the Bushveld Complex, due to its similar wavelength and amplitude. However, the Bethlehem gravity high has a larger wavelength compared to that seen in the Bushveld complex. In fact borehole data and enhanced geophysical interpretation in later studies shows Witwatersrand type rocks in the Bethlehem region (Ainslie, 1994 and Mcarthy et al., 2018). Corner et al, (1986a, 1986b and 1986) interpreted magnetic and gravity data in the southern region of the Kaapvaal Craton. They identified the Bethlehem area as possible outliers of Witwatersrand basin lithology. As techniques for gravity imaging improved Wilsher, (1987) interpreted gravity and magnetic data for the whole of the Witwatersrand Basin. Wilsher suggested that the gravity anomaly surrounding Bethlehem is due to the uplift of denser intermediate and lower crustal material, which has been brought close to surface. The upward warping of lower crust occurred along an axis called the Vredefort axis. The magnetic anomalies were suggested to be West Rand Group and greenstone belt relicts which have been brought closer to surface. During this time extensive geophysical studies were conducted around the Bethlehem region. Further research from Corner et al. (1989), into the relationship between the Vredefort structure and the Witwatersrand basin, suggested a similar model but with possible mafic sills within the granulitic lower crust which has been warped upwards along the Vredefort axis contributing to the denser lower crust producing a gravity high. Ainslie et al. (1989) who also looked at gravity and magnetics over the Vredefort structure agreed with the Vredefort axis and that the Bethlehem gravity high extends from the Vredefort structure in a south east direction.

A report by the Ainslie et al. (1994) provided an overview of the geophysical research conducted in the Bethlehem area. This research was conducted to provide information to mining company Anglo American. At the time Anglo American were motivated to drill boreholes in excess of 2 km, due to the new interpretations of gravity and magnetic data discussed previously. The aim of the report was to determine if the Bethlehem region could become a gold and uranium producer.

The south eastern edge of the Witwatersrand basin shows many differences to that of the rest of the main Witwatersrand basin. Ainslie et al. (1994), proposed the Bethlehem sub-basin is controlled by major fault systems, which does not agree with the Vredefort axis model produced by Corner et al, (1986).

Ainslie et al. (1994) proposes that the Bethlehem region is structurally controlled by N – NNW trending grabens and half-grabens within the granite basement. These grabens preserve large-scale Witwatersrand sediments. Added on to this are N-S and E-W trending faults creating a mosaic pattern only seen on the south eastern edge of the Witwatersrand basin. However, their result showed little economical potential for mining and exploration in the Bethlehem region ceased.

The source of the Bethlehem gravity anomaly has remained unclear despite numerous geological and geophysical studies. This dissertation presents a fully integrated borehole, gravity, seismic and magnetic geophysical dataset to produce a 3D geology and a 3D gravity model of the Bethlehem area. The result shows consistent large scale faulting of basement and Witwatersrand rocks, with horst and graben structures creating ridges of granite and thick West Rand Group grabens producing the Bethlehem gravity high.

1.2 Prospectus

A brief summary of chapters 2 – 8. Chapter 2 presents a geological and structural overview of the Witwatersrand basin. As well as borehole data which provided a general stratigraphic interpretation of the Bethlehem region. Chapter 3 presents borehole, seismic, magnetic and gravity data provided for this study. Chapter 4 describes the theory of the seismic reflection method, gravity method and magnetic method. This includes a summary of the acquisition, processing and interpretation theory behind the geophysical methods used in the Bethlehem region. In Chapter 5 the results of the seismic, gravity and magnetic interpretation are presented. Chapter 6 presents the 3D geological and gravity models. A final discussion to explain how the Bethlehem Sub-basin is connected to its surroundings, in addition to cause of the Bethlehem gravity high are presented in Chapter 7. A summary of the discussion and final conclusion are incorporated in Chapter 8.

2 Geological setting

Understanding the geological setting of the Bethlehem study area is an essential step in the interpretation of seismic, gravity and magnetic data. Analyses of borehole data will allow a better understanding of geological boundaries which are expected in the Bethlehem study area. Contrast in velocity, density or magnetic susceptibility are used to determine what boundaries are expected to produce a strong reflector for seismic data.

2.1 Stratigraphy of the Witwatersrand basin

The Witwatersrand basin is a 50 000 km^2 Archean basin situated centrally on the Kaapvaal Craton. The basin formed between 3074 and 2714 Ma, over a period of 360 Ma (Robb and Meyer, 1995). Table 1 outlines the stratigraphy of the Witwatersrand basin produced from previous literature. The basement granite is overlain by the Dominion Group quartzite, conglomerate and volcanic lava units. The Witwatersrand basin overlies the Dominion Group and consists of the Witwatersrand and Ventersdorp Supergroups. The basin is overlain by the Transvaal and Karoo Supergroup.

The Bethlehem region is situated on the south eastern edge of the Witwatersrand basin, covered by 1 km thick Karoo Supergroup sediments (see figure 2.1). Only small portions of the basin stratigraphy are recorded in borehole data, which are discussed in Chapters 3 and 4. The borehole data consists of Karoo Supergroup sediments, Klipriviersberg Group of the Ventersdorp Supergroup, the Central and West Rand Groups of the Witwatersrand Supergroup and the basement. Only these groups are discussed further as detailed information about the Kaapvaal Craton and the basins within it are readily available in many geology textbooks such as Johnson et al. (2006) etc.

Table 1 Simplified stratigraphy of the Witwatersrand basin and overlying Karoo Basin, The units identified from boreholes in the Bethlehem study area are highlighted in blue (Johnson et al., 2006; Frimmel and Minter, 2002; Catuneanu,2001).

Supergroup	Group	Rock types	Age (Ga)	Tectonic environment
Karoo Supergroup	Drakensberg Stormberg		0.30 – 0.18	Breakup of Gondwana Retro-arc Foreland system
	Beaufort Ecca Dwyka	Shale Sandstone Tillite		
Transvaal Supergroup	Pretoria Chuinespoort		2.59 – 2.20	Intracratonic And Extensional
Ventersdorp Supergroup	Pniel Platberg		2.72 – 2.63	Extensional
	Klipriviersberg	Lava		
Witwatersrand Supergroup	Central Rand	Quartzite Conglomerate	2.90 – 2.85	Rectro - arc And Foreland system
	West Rand	Shale Magnetic shale	2.98 – 2.90	
Dominion			3.07	Extensional
Basement			3.60 – 3.20	

The West Rand Group is a sequence of clastic and marine sediments, deposited between 2.98 – 2.90 Ga (Frimmel and Minter, 2002). It was deposited on a stable tectonic craton and is approximately 4.5 km thick and covers an area of 42 000 km^2 (Frimmel et al., 2005). The West Rand Group is divided into 3 subgroups, the Hospital Hill, Government and Jeppestown Subgroup. The lower most subgroups; Hospital Hill and Government subgroups are characterized mainly by shallow marine shales, quartzites and shale, conglomerate and diamictites (Frimmel and Minter, 2002; Beach and Smith, 2007). The uppermost subgroup, the Jeppestown subgroups consists mainly of quartzites and conglomerates.

The Central Rand Group is a sequence of quartzites, conglomerates and minor shale units, deposited between 2.90 – 2.85 Ga (Frimmel and Minter, 2002). It was deposited in a braided river system which then combined to form alluvial fans. Over time these alluvial fans narrowed allowing fluvial sediments to move from the basin margins into the center of the basin (Wronkiewics and Condie, 1987; Moon and Whateley, 1989). Gold was deposited in the conglomerate units of the Central Rand Group. The Central Rand Group is divided into the Johannesburg Subgroup and Turrfontein Subgroup.

The Ventersdorp Supergroup (2.72 – 2.63) Ga (Frimmel and Minter, 2002) underlies the Transvaal Supergroup in the main Witwatersrand basin. The lower Ventersdorp Supergroup comprises the Klipriviersberg Group consisting of basaltic lavas and the Platberg Group consisting of boulders, amygdaloidal lava fragments, quartzite, shale and chert units. The upper Ventersdorp Supergroup comprises the Pniel Group. The Ventersdorp Supergroup shows an undulating topography caused by the compressional tectonic environment at the time. In the Bethlehem region we encounter a thin layer of the Klipriviersberg Group, which overlies the Central Rand Group, recorded in borehole data.

The Karoo Supergroup deposited between 0.30 and 0.18 Ga is defined by a base of glacial deposits known as the Dywka Group. Overlying the Dwyka Group, is a sedimentary sequence conssting of Beaufort, Ecca and Stormberg Groups. The topmost group of the Karoo Supergroup occurred during the breakup of Pangea and basaltic lava extruded forming the Drakensberg Group (see Figure 2.1). There is an extensive network of dolerite sills, dykes and sheets forming part of the Karoo Igneous Province (Duncan and Marsh, 2016). This dolerite intrusion occurred over a short period of time, dating between 190 – 178 Ma around the same time as the Drakensberg lava.

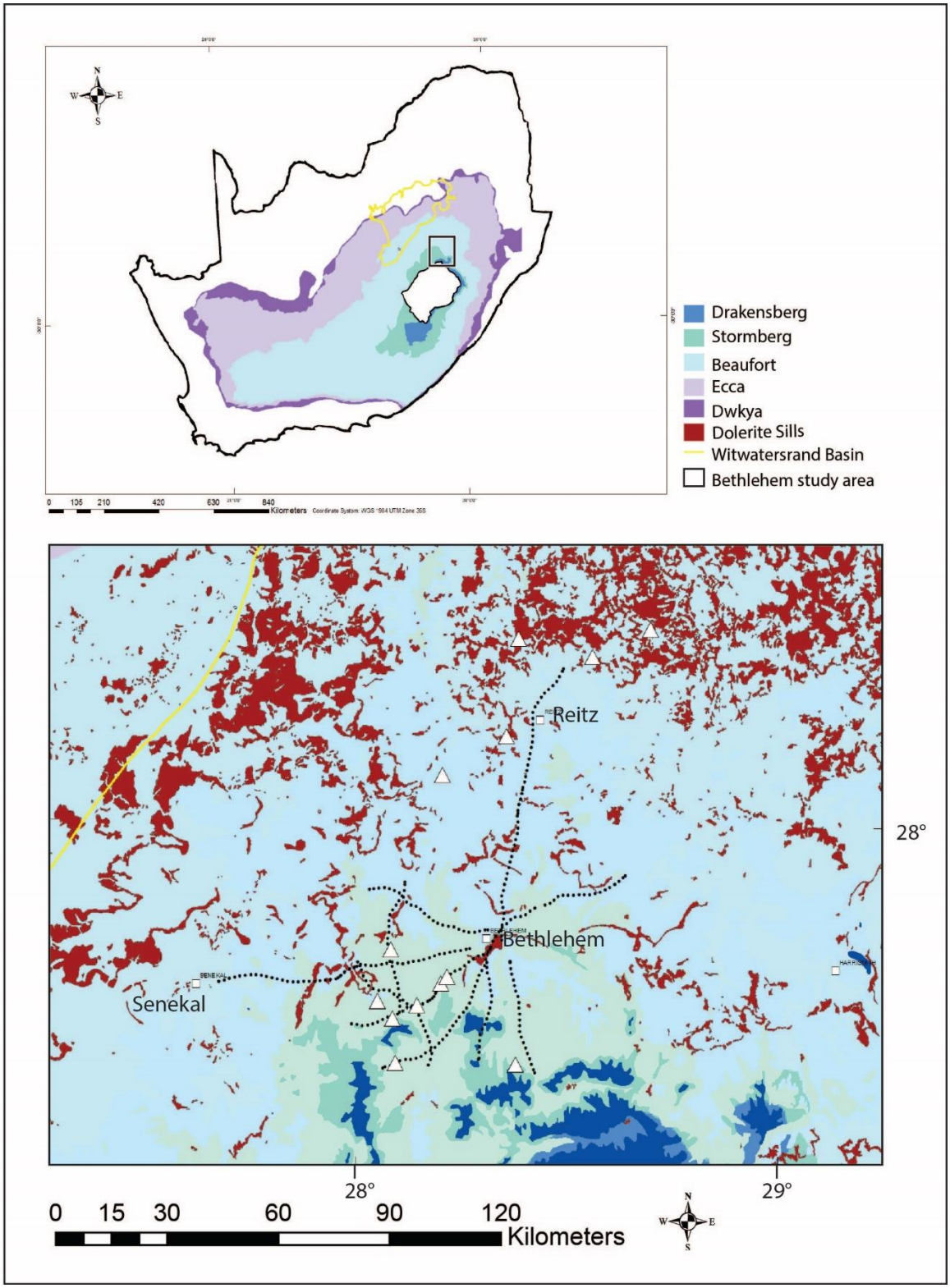


Figure 2.1 Locality map of the Bethlehem study area with simplified geology of the Karoo Basin that covers more than half of the Witwatersrand basin (yellow outline). Location of 13 boreholes (white triangles) and 10 seismic lines (black dotted lines) used for this study. Outcrops of dolerite sills (red) within the Karoo Supergroup which covers the Bethlehem area

2.2 Structural Setting

The main Witwatersrand basin has gone through several stages of deformation which can be observed in distinct lithostratigraphic units. Frimmel (2014) suggested deposition of the Dominion Group volcanics was the result of continental rifting at 3.09 Ga to 3.07 Ga.

The West Rand Group sediment were deposited in a passive margin through transgression and regression cycles, which formed during the period 2. 99 Ga to 2.90 Ga (Dankert and Hein, 2010; Johnson et al., 2006). The West Rand Group deposition terminated with the Asazi event described by Manzi et al. (2013) which uplifted and tilted the West Rand Group sediments syn to post erosion. The Asazi event resulted in local faulting and block tilting. An angular unconformity was also formed with the overlying Central Rand Group (Dankert and Hein, 2010; Manzi et al., 2013).

Synchronous with the deposition of the Central Rand Group 2.90 – 2.85 Ga (Frimmel and Minter, 2002) is the Umzawami event described by Dankert and Hein (2010). The Umzawami event was a compressive deformation event. Frimmel (2014) describes this as the formation of a retroarc, creating a fold thrust belt formation. West Wits Line, Welkom and Klerksdorp Goldfields are areas which identified north to northwest trending folds with thrust, reverse and flexural-slip faults in the Central Rand Group. North to northeast folds in the Central Rand Group, were identified in West Wits Line and West and Central Rand Goldfields (Dankert and Hein, 2010).

Following the Unzawami event and end to rectroarc development, major continental rifting resulted in volcanism of the Klipriviersberg Group (2.73 – 2.72 Ga) across the Kaapvaal Craton. Further extensional collapse associated with the sedimentation of the Platberg Group shows major graben formation and listric faulting of existing structures. This major continental rift system created first-, second- and third- order faults such as the Bank Fault, a north northeast trending listric fault. This extensional event is described by Manzi et al., (2013) as the Hlukana-Platberg Event at 2.70 to 2.64 Ga.

During the period 2.2 Ga to 2.0 Ga several events took place. Dankert and Hein (2010) described the deposition of the Transvaal Supergroup. As well as several structural indicators during this time such as, the Bushveld Complex intrusion (2.05 Ga) and the Vredefort Impact (2.02 Ga).

The deposition of the Karoo Supergroup occurred 1.7 billion years after deposition of the Pretoria Group. During this time the Pilanesberg Complex Dyke swarm occurred at 1.3 – 1.1 Ga which is described by

Dankert and Hein (2010). The Karoo dykes are spread throughout the Witwatersrand basin and were feeders to the flood basalts that cap the Karoo Supergroup.

2.3 Geological setting of the Bethlehem study area

The Bethlehem region is situated on the border of the Witwatersrand basin map and approximately 150 km south west of the center of the Vredefort impact (Figure 2.2). The size of the Bethlehem study area is 100 km x 100 km. What is known of the geology beneath the Karoo cover is based on a few boreholes and magnetic, gravity and seismic data. This data is discussed in Chapter 3. The most notable feature of the Bethlehem region is the Bethlehem gravity high. This is one of the most distinguished gravity anomalies on the Kaapvaal craton.

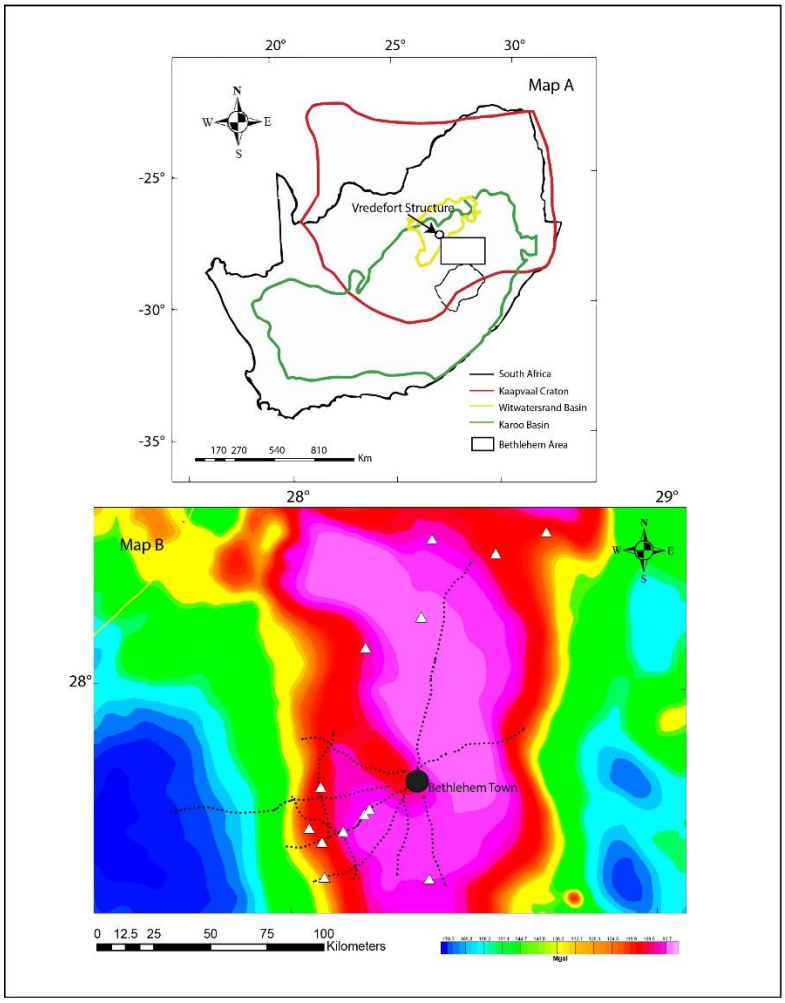


Figure 2.2 Map A – Bethlehem area in comparison to South Africa, Karoo Basin, Witwatersrand Basin and Vredefort structure. Map B – The Bethlehem area, with a gravity backdrop. Shows the town of Bethlehem (black dot), seismic lines and boreholes. Bethlehem anomaly Pink area (Modified from Council of Geoscience)

The location of the Bethlehem Sub - basin and Bouguer gravity anomaly has brought much complexity to the origin and structure of this region and its anomalies. Wilsher (1987), Corner et al. (1989) and Ainslie et al. (1994) present the most detailed theories of the structure of the Bethlehem region mainly interpreted from gravity and magnetic data describe in Chapter 1.

Corner and Wilsher, (1989) describe the Vredefort axis as a northwest trending structural axis, located along the crest of the Bethlehem gravity high and extending through the Vredefort dome. Corner and Wilsher, (1989) attributes the Vredefort axis to compression from the southwest of the Witwatersrand basin producing a northwest fold structure.

The latest research from corner et al. (2017) interprets the Bethlehem Sub – basin to be separated from the main Witwatersrand basin by the Bloemfontein arch. Corner also describes major successions of Transvaal and Witwatersrand Basin rocks extending from Bloemfontein west of Bethlehem possible into the Bethlehem area. Boreholes close to the Bethlehem area containing Transvaal Supergroup sediments were also interpreted by McCarthy et al. (2018). However, the boreholes provided for this study do not show any Transvaal sediments.

Ainslie, (1994) describes the Bethlehem area as a complex fault system that does not agree with the Vredefort axis theory. Ainslie interpreted two major fault systems in the Bethlehem region and surrounding areas as follows; (1) Lindley fault, which appears to follow a pattern in respect to the Vredefort dome and has displaced several kilometers of pre-Karoo sediments. This caused granite to underlie the Karoo strata and allow for preservation of large blocks of Witwatersrand sediments. (2) The Bethlehem fault system shows a number of fractures visible in Karoo Strata which correlate to faults in the granite basement mapped with magnetic data. These faults also appear radial to the Vredefort dome.

3 Data sets

Datasets used for this study are borehole, gravity, and magnetic data, provided by the Council of Geoscience and 2D reflection seismic data provided by AngloGold Ashanti. Understanding the limits of each dataset were important in making sure the integrity of the data and interpretations were kept to a high standard. The gravity map of Bethlehem shown in Figure 3.1 will be used as a backdrop for all data.

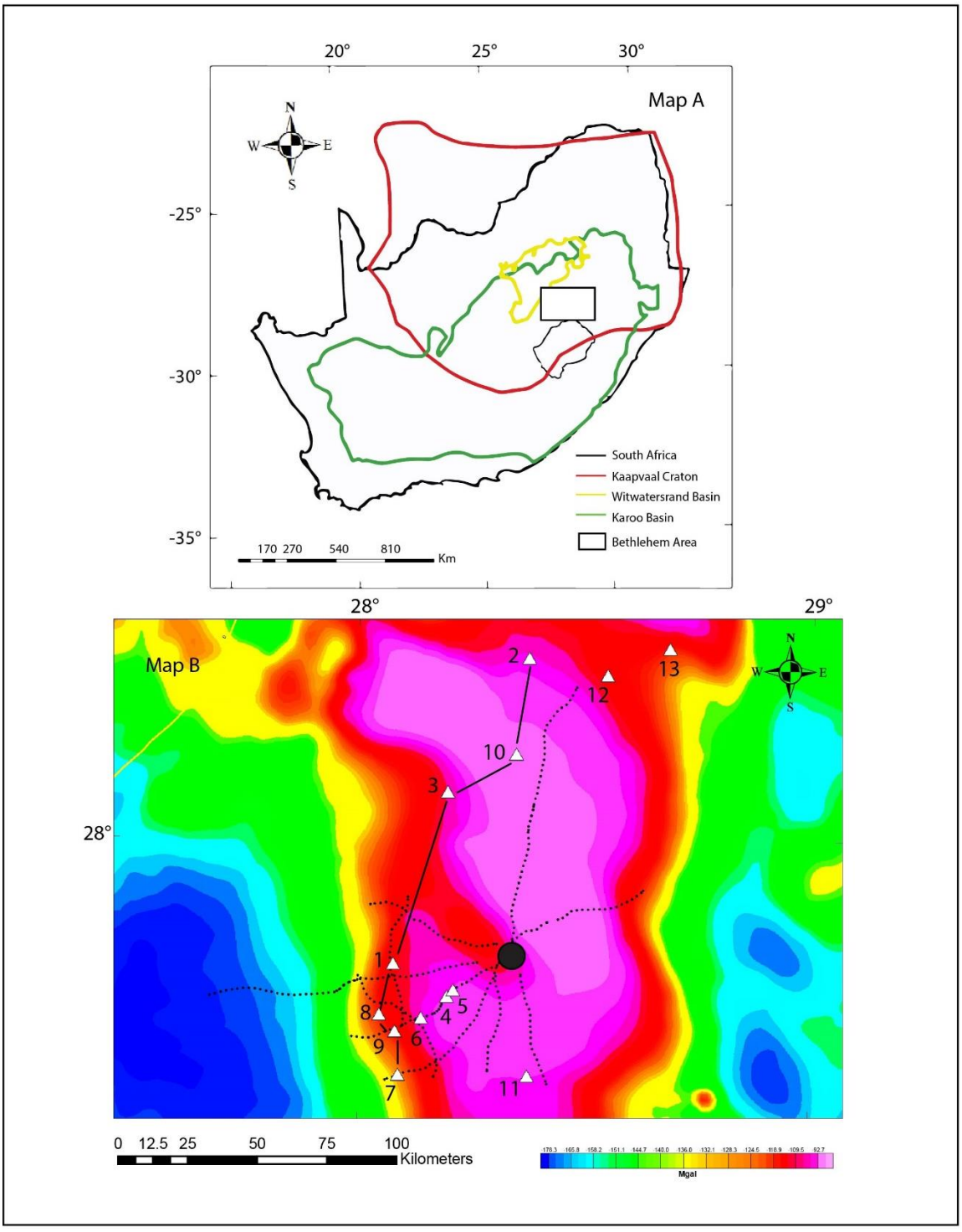


Figure 3.1 Map (A) Location map for the Bethlehem gravity anomaly in relation to the Kaapvaal Craton (red line), Witwatersrand basin (yellow line) and Karoo Basin (green line). Map (B) shows the data used to constrain the Bethlehem region and black dot represents town of Bethlehem. A section of the Bouguer gravity map of South Africa that covers the Bethlehem study area. 10 Reflection seismic lines (black dotted lines) with the town of Bethlehem at the center and borehole data (white triangles). The boreholes linked with a black line were used to create a north – south profile to determine a general understanding of the geology beneath the Karoo cover.

3.1 Borehole data

Borehole data was provided by the Council for Geoscience (CGS). Boreholes were drilled by Anglo American and Goldfields during the 80s and 90s. Thirteen Boreholes closest to the Bethlehem study area and seismic lines are shown in Table 2.

This study is most interested in the structures and geology below the Karoo Supergroup, borehole data was used to interpret dolerite sills in the Karoo Supergroup and as a constraint on the depth of reflectors in the seismic interpretation (Figure 3.2) and (Figure 3.3).

Limitations to the borehole data collected for this study are as follows: The boreholes are clumped together in the north eastern and south western sections of the Bethlehem study area (figure 3.1). There are no boreholes on the eastern side of the gravity anomaly. This means that some sections of the Bethlehem region do not have any borehole data to correlate with the seismic sections or gravity profiles. Most boreholes do not go deeper than 2100 m and the Karoo Sediments range from 1 km to 1.7 km (Table 2).

Table 2 Borehole database used to help constrain either the top or base of each lithology in the Bethlehem region (Karoo Supergroup, Ventersdorp Supergroup, Witwatersrand Supergroup and Granite basement). Coordinates are converted relative to the WGS84 ellipsoid, Grey blocks represent a lithology that was not seen in the borehole due to the borehole not going deep enough or the specific lithology is not being present in that borehole.

	Borehole	Date borehole drilled	UTM35S N	UTM35S E	Elevation (m)	Base Karoo (m)	Top Ventersdorp (m)	Base Ventersdorp (m)	Top Witwatersrand (m)	Top Granite (m)	End of borehole (m)
1	4003246	8/21/1992	605729.68	6875037.365	1648	1103.35	1103.35	1555.3	1555.3		3082.1
2	4003296	7/23/1959	635469.168	6941282.22	1615	822.05				822.05	916.53
3	4003297	11/18/1959	617674.781	6912273.699	1660	947.01				947.01	991.21
4	4038581	9/6/1991	617365.926	6867847.027	1477	1320.21			1320.21		1755.3
5	4038591	3/13/1989	618767.077	6869260.67	1735	1436.71			1436.71		2643.9
6	4038593	1/17/1991	611793.033	6863202.029	1729	1284.9	1284.9	2224.22	2224.22		3663.9
7	4038594	3/2/1993	606753.432	6850921.57	1657	1697.31	1697.31	2653	2653		3603.65
8	4038595	9/16/1987	602679.494	6864047.99	1628	1234.87	1234.87				2160.4
9	4038596	3/26/1992	606117.132	6860340.606	1725	1303.79	1303.79	1964.54	1964.54		3135.35
10	4062235	3/26/1959	632631.397	6920479.093	1598	866.42				866.42	935.74
11	4064826	4/8/1994	634697.899	6850537.034	1799	1713.19			1713.19		2081.7
12	4213250	12/27/1959	652505.417	6937430.823	1667	845					845.52
13	4213251	5/29/1959	666002.596	6943127.734	1565	781.2					781.2

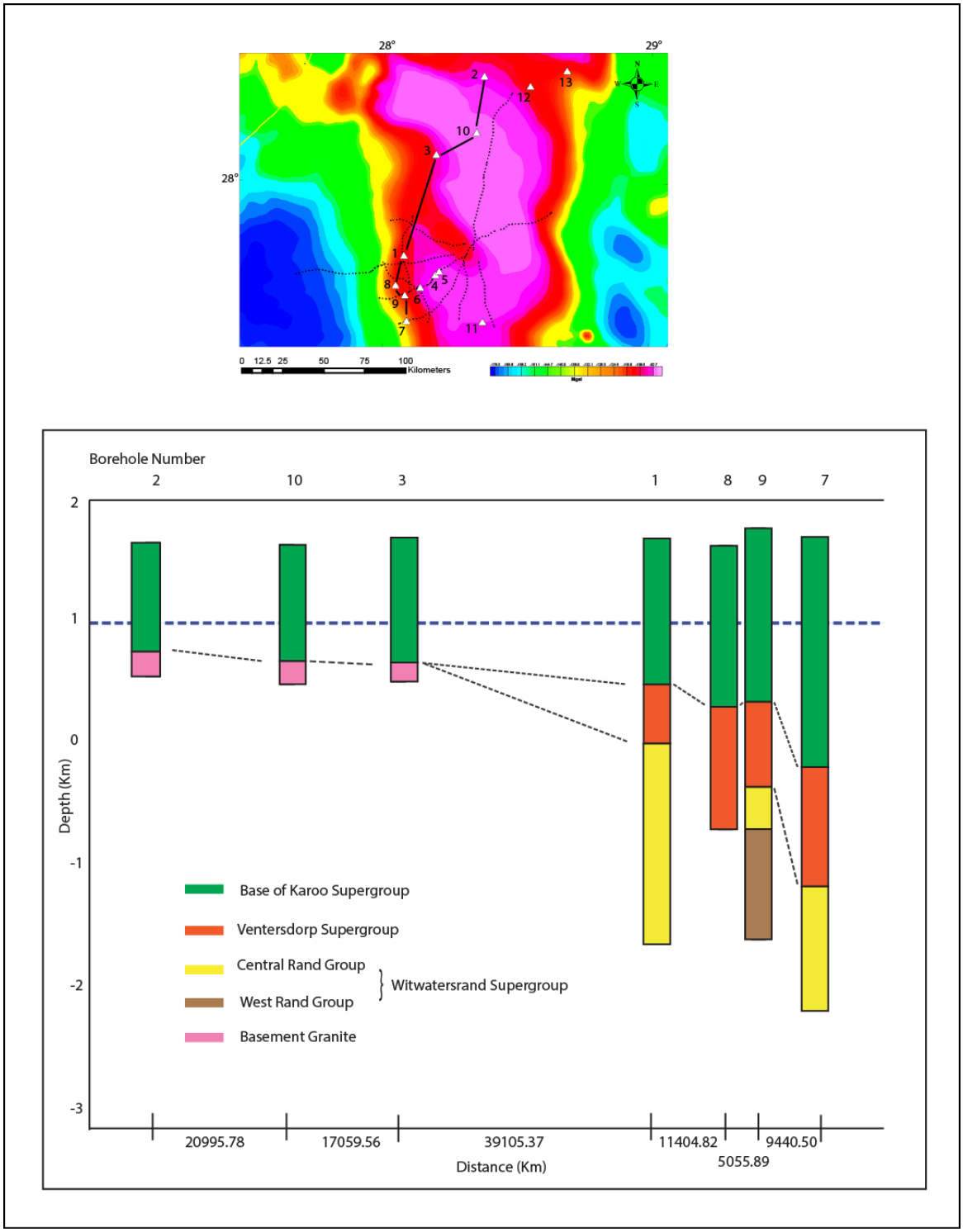


Figure 3.2 North - south profile through the western side of the Bethlehem study area, showing 7 out of 13 wells. The wells were numbered in Table 2 and gravity map showing the location of boreholes with the dotted line representing the profile shown above. Each lithology is represented by a different colour; Karoo (green), Ventersdorp (orange), Central Rand (yellow), West Rand (brown) and basement (pink). Stratigraphic boundaries are marked with a dotted line were possible as some boreholes do not have enough information. Blue dotted line represents 1 km above sea level to represents where seismic sections begin.

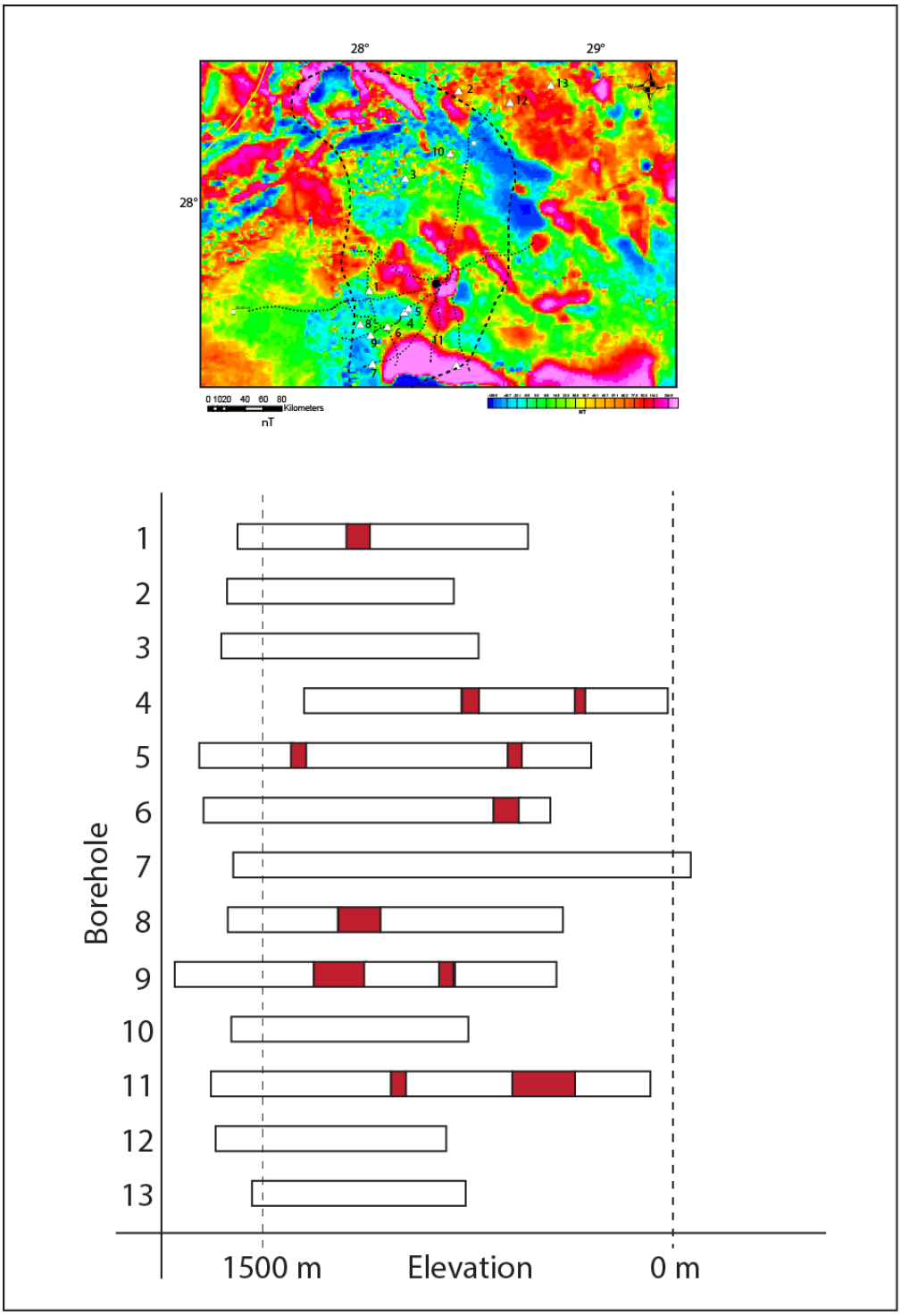


Figure 3.3 Borehole data of Karoo Supergroup showing dolerite sills in red. The Borehole data shows dolerite sills range in thickness from 10 m to 200 m. These boreholes were used to constrain the dolerite sills interpreted in the seismic sections.

3.2 Seismic data

Vibroseis reflection seismic data were collected between the 1980s and 1990s by AngloGold Ashanti (Pretorius, 1994). The aim was to determine (1) the extent of the Witwatersrand basin and if gold bearing strata discovered in the main Witwatersrand basin sediments continued to the edge of the basin. (2) Exploration of uranium deposits. The study included investigation into the structure of the Bethlehem gravity anomaly and structure below the Karoo. However, no economically minable resources were discovered and all these investigations were shut down by 1995.

To interpret the Bethlehem geology and structures beneath the Karoo surface, as well as dolerite sills within the Karoo sediments, 10 seismic lines where interpreted, stretching approximately 100 km across the Bethlehem anomaly see Figure 3.1. The acquisition parameters used for recording these seismic lines are shown in Table 3, and the processing parameters are shown in Table 4. The processing parameters for these data are taken from (Pretorius et al., 2003) as no record could be obtained for this specific set of seismic lines.

Limitations to interpreting the 2D reflection seismic lines are as follows: (1) No velocity data were collected in the area that is known of and therefore the time to depth conversion was an approximation using a constant velocity of 3000 $m.s^{-1}$. The constant velocity time to depth conversion meant deeper horizons were difficult to correlate with borehole data. Table 5 shows velocities of each different layer taken from literature mainly based in the main Karoo basin. (2) Few deep boreholes (Table 3.1) used to constrain the horizons and continuity across each seismic line, meant many parts of the seismic horizons had to be picked without borehole data. Despite these limitations the dataset provides us with a unique look into the lithology and structural information beneath the Bethlehem region which has had very little exploration thus far.

Table 3 Summary of the acquisition parameters used for the 2D seismic data between 1990 and 1993 (Pretorius, 1994).

Seismic acquisition parameters	
Instruments	
Vibrators	4 x Failing Y1100
	27000 Ib each
Recording instrument	SN368/I/O CS
No. of Channels	120
Geophones	SM4
Vibrator Quality Control system	Vigil/Valid
Sweep Parameters	
Sweep Length	24 s
Sweeps per Vibroseis Pattern	3
Frequencies	10 – 61 Hz linear up
Listening period	6 s
Sample rate	2 ms
Geometric Parameters	
Field spread	Split straddle
	2975-25-x-25-2975 m
Station interval	50 m
Vibroseis Pattern interval	50 m
Common Mid Point interval	25 m
Vibroseis pattern	50 m linear
Receiver pattern	50 m linear
Fold of cover	30

Table 4 Summary of the processing parameters used for the 2D seismic data sets acquired in 1994 (Pretorius, 1994).

Steps	**Processing Work flow**
1	Demultiplex – including gain removal and minimum – phase conversion
2	Trace editing
3	Amplitude recovery
4	Source – domain deconvolution
5	Receiver – domain sort, f-k filter and deconvolution
6	Trace normalization and sort into source domain
7	Dip moveout
8	Common mid-point sort
9	NMO correction
10	Surface consistent gain correction
11	Residual statics correction
12	Stack
13	Migration
14	Frequency filter

Table 5 Velocity of each Stratigraphic group found in the Bethlehem region. This is a collection of velocities from literature across the Witwatersrand basin.

Supergroup	Group	Velocity (m/s) (P-wave)	Reflection Coefficient	Reference
Karoo		3200 3195 3000		De Wet and Hall, 1994 Pretorius et al., 1987 Weder, 1994
				This Study
Ventersdorp	Klipriviersberg	6400 6300 6230		De Wet and Hall, 1994 Weder, 1994 Pretorius et al., 1987
			-0.065	Pretorius et al., 1987
Witwatersrand	Central Rand	5779 5750 5550		Pretorius et al., 1987 De Wet and Hall, 1994 Weder, 1994
			+0.025	Pretorius et al., 1987
	West Rand	5748		Pretorius et al., 1987
			-0.032	Tinker, 2002
Basement		5693		Pretorius et al., 1987

3.3 Gravity data

The Gravity data set was provided by the Council for Geoscience. In 1994 the Council created a database of Bouguer gravity data. This is data which has been continuously collected and compiled since 1939 (Gordon – Welsh et al., 1986). Most readings were collected using LaCoste and Romberg geodetic gravity meters. A grid spacing of 1 km was used for imaging, although the original data points were mainly focused around main roads with various spacing.

In older parts of the data set, barometers were used to measure elevation and were not well constrained. These poorly constrained measurements can result in an error of between 2 – 5 mgal in the gravity data (Leaman, 1984; Hales and Gough, 1960). For this study a more accurate higher resolution data set is not available. The resolution of the gravity data set was taken into account during the forward modelling process. During forward modelling the densities used for each lithology were taken from literature results for the main Witwatersrand basin and modified. Table 6 outlines the densities used.

Table 6 Density of each stratigraphic group found in the Bethlehem region. This is a collection of densities from literature across the Witwatersrand basin.

Supergroup	Group	Density (g/cm^3)	Lithology	No of samples	Reference	Density used for this study (kg/m^3)	Reason for change - in this study
Karoo		2.38 2.54 2.55	Sandstone Mudstone Sediments	15 25	Jones, 2003 Jones, 2003 Maré, 2012	2.55	Increase inconsideration of dolerites present from borehole data.
		2.96	Dolerite	9	Jones, 2003		
Ventersdorp	Klipriviersberg	2.88 2.89	Lava Basalt	40 5	Jones, 2003 Maré, 2012	2.88	Within range
Witwatersrand	Central Rand	2.69 2.63 2.61	quartzite/conglomerate quartzite ferruginious shale	308 285 2	Jones, 2003 Maré, 2012 Maré, 2012	2.61	Used lower densities as less quartzite conglomerate observed in boreholes
	West Rand	2.95 2.91	Iron rich shale quartzite	2 2	Maré, 2012 Maré, 2012	2.91	Within range
Basement		2.65 2.67	Granitoids (Vredefort) Granite/gneiss (Vredefort)	71 1	Henkel and Reimold, 1996 Maré, 2012	2.67	Within range

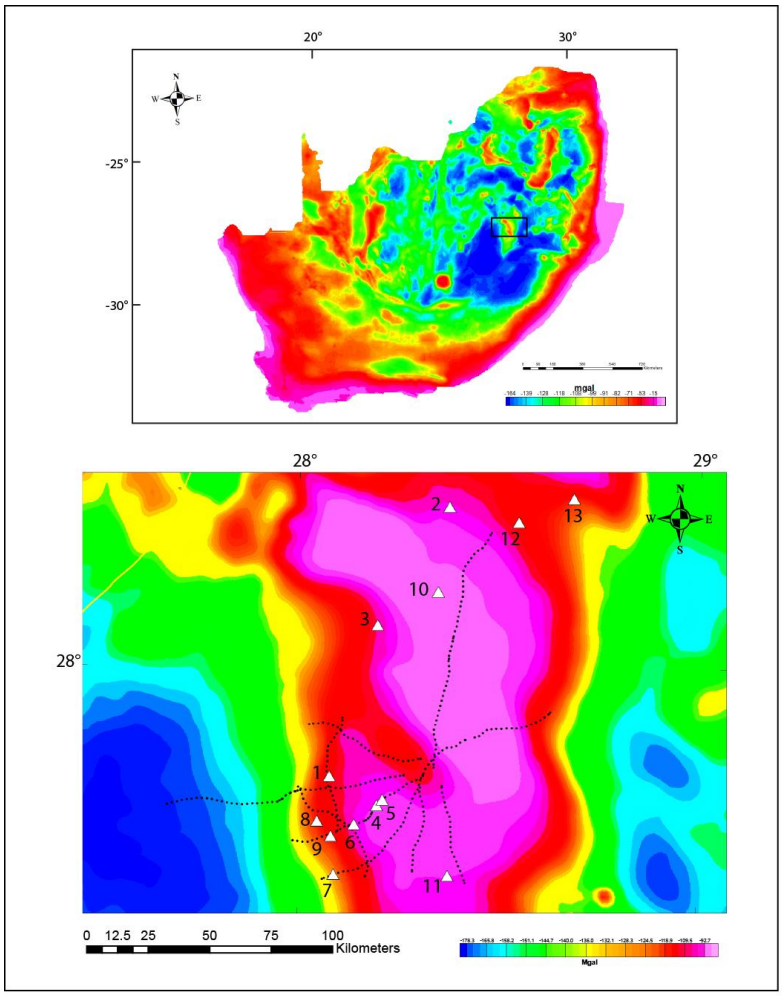


Figure 3.4 Bouguer Gravity map of South Africa with Bethlehem study area outlined in black box (above). Bouguer gravity map of Bethlehem study area (below). Seismic lines (dotted lines) and boreholes (white triangles) are overlain on map (Modified from Council of Geoscience).

3.4 Magnetic data

The Council of Geoscience collected and compiled the regional aeromagnetic dataset during the 1980s and 1990s. Data was collected using the Cesium-vapor magnetometers. The dataset was flown at a flight height of 100 – 150 m at a line spacing of 1 km and sample spacing of 60 m. The Council of Geoscience has compiled data for most of southern Africa and has gridded the data at 1 km grid spacing (Stettler *et al.*, 2000).

The limitations of using aeromagnetic data with a large line spacing (1 km) are as follows; it is not suited for quantitative and calculated small scale interpretations. It is best suited for qualitative, large scale interpretations such as, magnetic lineaments, boundaries and lithology differences. For this study magnetic data is used to determine dolerite sills within the Karoo sediments which are observed in borehole data see Figure 3.5.

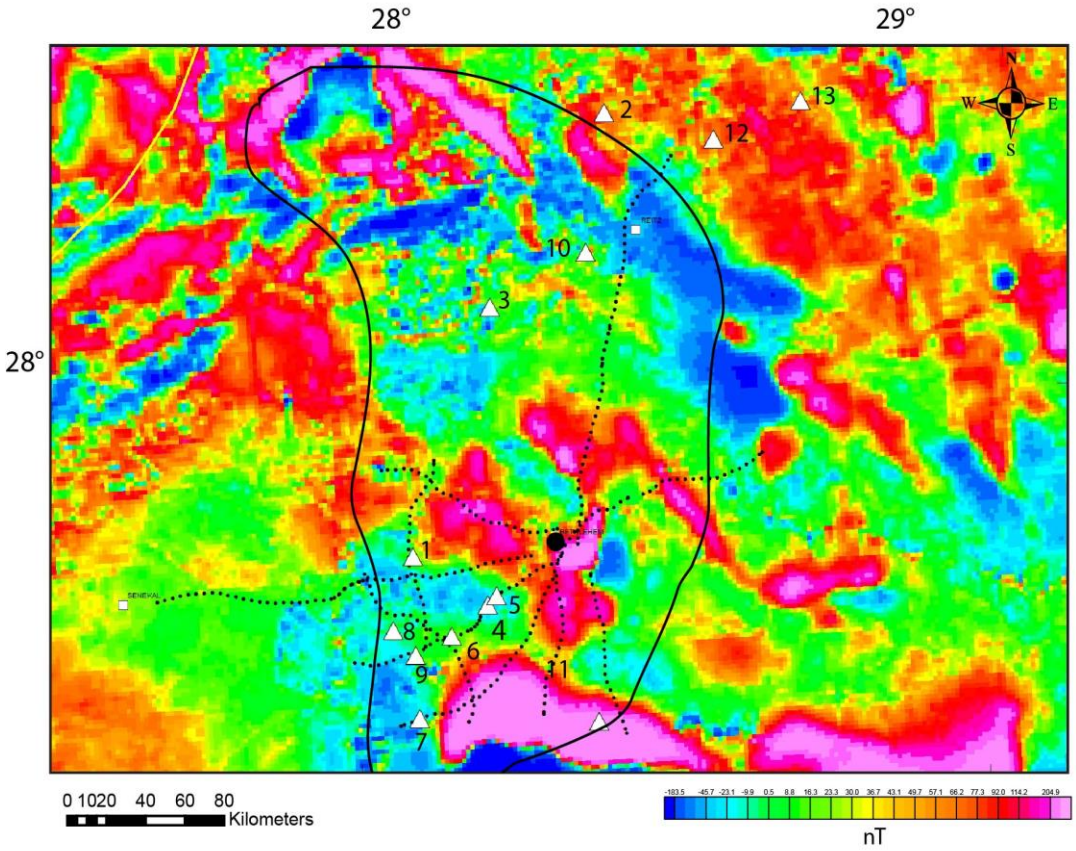


Figure 3.5 Map of magnetic data in the Bethlehem area showing, outline of Bethlehem gravity anomaly (solid black line), seismic lines (dotted black lines) and borehole locations (white triangles), town of Bethlehem (black dot).

4 Methodology

To achieve a constrained 3D geological model and 3D gravity model of the Bethlehem region a multidisciplinary geophysical approach was used. This study involved the following procedures: borehole analysis, magnetic interpretation, 2D reflection seismic section analysis, 2D forward modelling of gravity profiles and 3D geological and gravity modelling.

In this chapter we outline the process taken for each method to create the 3D geological model and 3D gravity model, indicating at what points these methods integrated with each other, see Figure 4.1. We summarize the background theory behind the 2D reflection seismic method and provide detailed outline on the method used during the interpretation process of the seismic sections. We then outline the method used for the magnetic qualitative interpretation. The background theory of the gravity data is also discussed in detail on the 2D and 3D forward modelling method.

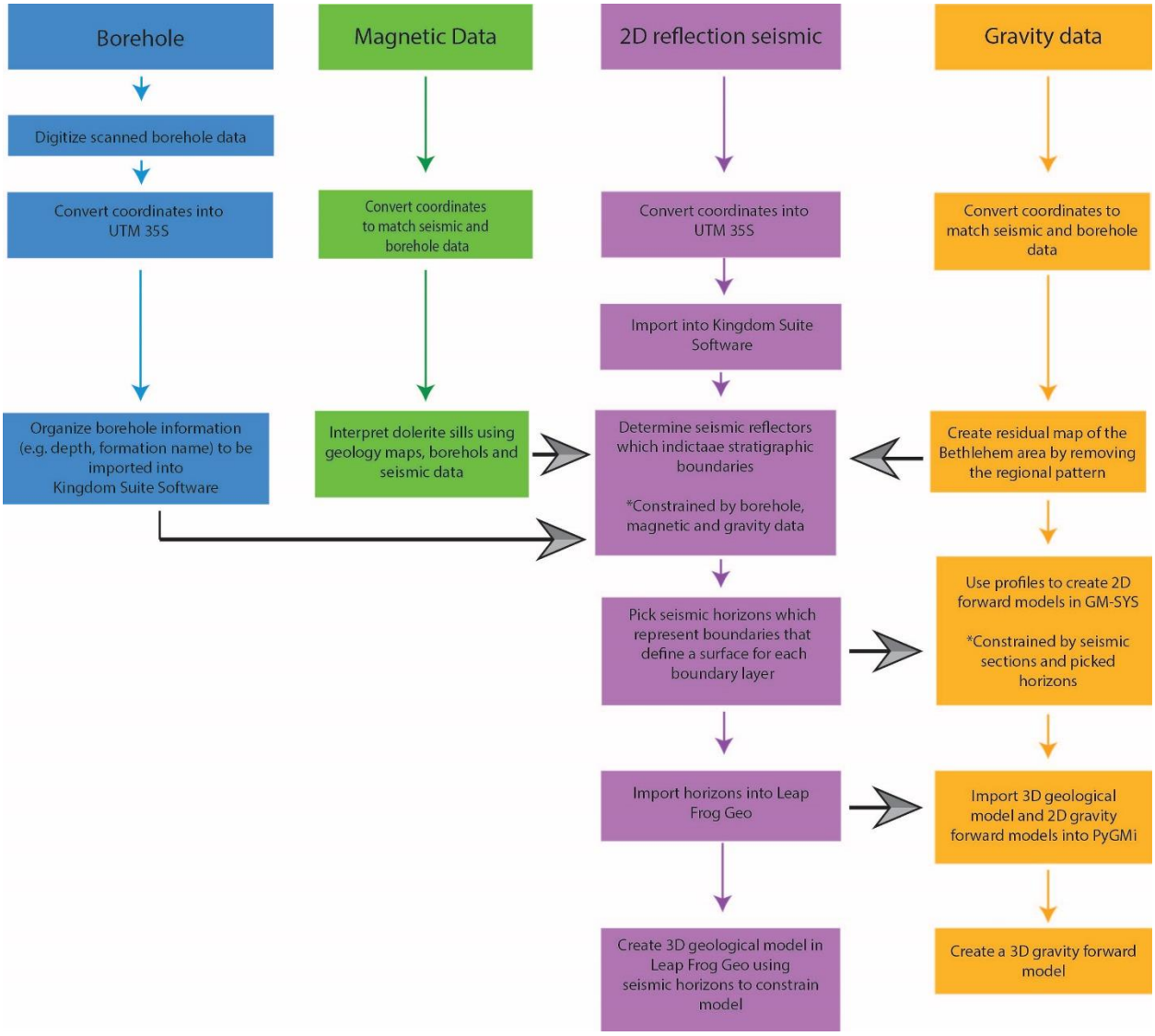


Figure 4.1 Flow chart outlining the process for each borehole, magnetic, 2D seismic and gravity data sets used in this study to a 3D geological model and 3D gravity model. Arrows are used to show the order of each step in the process and when datasets were integrated and used as constraints for a more accurate interpretation.

4.1 Seismic reflection method

4.1.1 Background

There are a number of methods used in mapping the subsurface which have been very successful in determining mineral bodies and geological boundaries. The seismic reflection method provides high resolution imaging of subsurface structures and lithological boundaries. The reflection seismic method estimates the physical properties of the earth's subsurface such as their density and seismic velocity, using the principles of seismology (Musset and Khan, 2000). This method has become a key tool in determining structures at depth while still maintaining high resolution. Currently 3D seismic is the leading method in mine planning and deep exploration (Pretorius et al., 1994; Salisbury and Snyder, 2007; Malehmir et al., 2012)

4.1.2 Survey design

Snell's Law describes the behavior and path a wave will take when it crosses an interface between two mediums with different refraction indices (Kearey et al., 2002). The reflection seismic technique is based on this principle. During a reflection seismic survey an energy source (e.g. explosive or Vibroseis system) produces a compressional wave which travels through the subsurface. When this compressional wave interacts with an interface between two mediums with different physical properties, it will either refract and continue through the media or reflect back to the surface. These reflected waves are measured using geophones which are placed on the ground.

To observe and image a reflector, two factors are considered. The acoustic impedance contrast between 2 rock types and the geometry (Salisbury and Snyder, 2007). Each geological layer has an acoustic impedance. The difference in acoustic impedance contrast between each layer is used to determine the energy of a reflection from a boundary. It is calculated using the velocity and density of the rock layer and is defined by:

$$Z = v * \rho \quad (1)$$

where (Z) is the acoustic impedance, (v) is the velocity and (ρ) is the density of the rock (Veeken, 2007). The acoustic impedance contrast between two geological layers will determine if a reflection from the geological interface is strong enough to be observed. The same applies for a reflection from any structure (e.g. faults) and its surrounding medium. A strong reflector implies a high acoustic impedance contrast between rocks and therefore better interpretations can be made. Whereas, a poor reflector implies a low acoustic impedance contrast (Salisbury and Snyder, 2007).

A reflection is strong enough to be observed if the impedance contrast between two layers is 2.5 x 10^5 g/cm^2. This is equivalent to a reflection coefficient of 0.06. The reflection coefficient (RC) is defined by the difference between two rock types having a density $\rho 1$ and $\rho 2$ and velocity $v1$ and $v2$.

$$RC = \frac{\rho 2v2 - \rho 1v1}{\rho 2v2 + \rho 1v1} = \frac{Z2 - Z1}{Z2 + Z1} \quad (2)$$

The second factor that will determine how well the seismic technique can map the subsurface at a specific depth and resolution is the geometry, which involves the size and depth of the reflector or structure being surveyed. The vertical resolution limit describes the smallest interval at which you can identify the top and bottom of a horizon or deposit at certain depths. This is also known as the tuning thickness. The horizontal resolution limit describes the ability to identify the diameter of a deposit at depth.

The tuning thickness is used to estimate the minimum thickness for which a tabular deposit can be determined. The tuning thickness also known as the vertical resolution limit or Rayleigh limit and, is defined as the interval of constructive interference between seismic waves reflecting off the top and bottom of the deposit or horizon. The tuning thickness (t) is expressed as the average velocity of the rocks (v) divided by 4 times the dominant frequency (f) of the survey.

$$t = \frac{v}{4f} \quad (3)$$

The horizontal resolution limit is determined by the width of the first Fresnel zone. This is the area where reflected waves constructively interfere by less than half a wavelength. The width of the first Fresnel zone is determined by the dominant wavelength and depth of deposit (Salisbury and Snyder, 2007).

4.1.3 Seismic Interpretation

The seismic data were interpreted in HIS Kingdom Suite. Interpreting seismic data is dependent on the vertical and horizontal resolution of the data and the geological constraints used (e.g. borehole and surface data).

The seismic data in the Bethlehem study area is legacy data but the quality is good enough to produce continuous reflectors. Seismic horizons are the reflectors that are picked by the interpreter. They are based on continuity and strong seismic amplitudes. When picking a horizon in the amplitude based interpretation,

the trough or peak is chosen, based on the polarity of the seismic data. By showing the change of the acoustic impedance contrast between layers, the amplitude attribute indicates a change in lithology. The amplitude display is one of the most common used attributes to interpret seismic sections and was the main attribute used for picking horizons from the Bethlehem seismic sections. These horizons can represent a lithological boundaries or structural events such as faults or unconformities.

Using all the concepts described above the Bethlehem seismic sections were interpreted with the best possible constraints and approximations possible, with the available data. The next section will describe in detail a justification for each of the horizons which were picked and the constraints used.

4.1.4 Justification for lithological boundaries - All densities and velocities shown in Table 5

Karoo Contact

The Karoo Supergroup has a p and Vp range of 2.3 – 2.5 g/cm3 and 3000 – 3500 m/s. This is much lower than the underlying rock groups with a p and Vp range greater than 2.5 g/cm^3 and 5000 m/s. This contrast will produce a high RC and strong amplitude reflection. Within the Karoo Supergroup most of the layers consist of sandstone (2.38 g/cm^3) and shale (2.54 g/cm^3). This variation in p will produce an acoustic impedance contrast at each contact. The dolerite intrusions within the Karoo Supergroup will also produce a strong reflector, as dolerites have a much higher velocity (6, 200 m/s), compared to that of the Karoo Supergroup rocks in that area. The strength of the reflector may fluctuate according to the thickness of the dolerite (Fatti 1970).

Ventersdorp Supergroup (Klipriviersberg lava) – Witwatersrand Supergroup (Central Rand Group)

The Ventersdorp Supergroup in the Bethlehem region consists of the Klipriviersberg Group with a Vp and p of (6300 m/s and 2.89 g/cm^3). The underlying lithology is the quartzite and conglomerate layers of the Central Rand Group, with a Vp and p of (5700 m/s and 2.76 g/cm^3) for the quartzite layers. The drop in Vp and p at the interface between the Klipriviersberg and Central Rand Group will produce a strong amplitude reflection with a negative RC. The Klipriviersberg and Central Rand Groups individually are fairly homogeneous layers, with little change in p. Therefore transparent or weak reflectors will be seen within each layer.

West Rand Group Contact

The Central Rand Group as previously stated consists of mostly quartzite and conglomerate layers and minor shale and volcanic layers. The range in Vp and p for the Central Rand Group is (5000 – 5800 m/s and 2.67 – 2.87 g/cm^3). The West Rand Group has a rock sequence consisting of shales, ironstones,

quartzites, conglomerates and volcanic layer. The Vp average is (5750 m/s) and p range of (2.86 – 3.15 g/cm^3). This variation in density, will image the West Rand Group package as a series of closely spaced reflections with varying amplitude. This will be contrasting to the homogeneous Central Rand Group. Due to the Vp and p change, it will be possible to image the unconformity between the two groups as the dominant quartzites of the Central Rand Group overlie the shale units of the West Rand Group.

Basement Contact

The basement suite and greenstones have a Vp and p of 5693 m/s and 2.8 g/cm^3. According to borehole data the basement interface underlies the West Rand Group and the Karoo. The base of the West Rand Group rocks have a very similar Vp and p to the basement rock and therefore may not be imaged. However, the basement rock has a more homogeneous layer compared to that of the West Rand Group package. This contrast will define the appearance of a change in rock type but will not give the exact depth of the interface. Where the basement rock underlies the Karoo lithology, the change in Vp and p will allow an interface to be imaged.

4.2 Magnetic Method

As stated in Chapter 3 the magnetic data are only used for a qualitative interpretation, due to the large flight and line spacing. The magnetic data were integrated with borehole and seismic data to interpret dolerites in the Bethlehem region.

4.2.1 Background

The magnetic method has been a major geophysical method used in determining the extent of the Witwatersrand basin. Magnetic shales in the West Rand Group of the Witwatersrand Supergroup were used as a marker to determine gold bearing strata found in the overlying Central Rand Group. The magnetic method has also played a big part in determining dolerites in the Karoo Supergroup (de Beer, 2015).

4.2.2 Magnetic Interpretation

Magnetic data were used to understand the distribution of dolerites across the Bethlehem region. In doing so a qualitative analysis of magnetic anomalies could be done to determine which anomalies were associated with dolerites and which could be related to structures beneath the Karoo or structures related to the Bethlehem gravity high.

A qualitative analysis of dolerites within the borehole data were used to confirm the trend and distribution of dolerites within a few seismic sections which had a borehole that coincided with its location. IHS Kingdom Suite was used to interpret seismic data to better understand geometry of subsurface dolerites. An explanation of seismic interpretation is described in Section 4.1.

4.3 Gravity Method

A brief summary outlining the principles of forward modelling is discussed in this section. These algorithms were the main methods used in the software to create the 2D and 3D models of the Bethlehem region. Oasis Montaj was used for 2D forward modelling and PyGMI was used for 3D forward modelling of gravity data.

4.3.1 Background

The gravity method is a widely used technique which detects lateral density contrast in subsurface rocks. It can be used in small scale surveys, detecting minute density contrast on structures of a few meters, as well as large scale surveys, capable of identifying faults, intrusions and more (Mussett and Khan, 2000). Forward modelling is made up of a three step process which are; (1) create an initial source body based on geological and geophysical information, (2) calculate anomaly of created model and compare it to the observed anomaly and (3) correct model making adjustment on all parameters to determine a suitable fit between observed and calculated anomalies.

4.3.2 Forward Modelling Methods

4.3.2.1 Two and two and a half dimensional Talwani Methods

The Talwani algorithm describes a two dimensional body with a gravitational attraction, where at least one dimension can be infinitely long. This would describe the real life situation of a dyke or fracture. As one dimension is infinite, integration is only performed on the cross-section, which has been simplified to approximating the wavy outline as an n-sided polygon. The Talwani et al. (1959) algorithm is widely used in many 2D forward modelling programs (Figure 4.2). The equation for the vertical component gravity, g_z, is given by:

$$g_z = 2G\Delta\rho \sum_{n-1}^{N} \frac{\beta_n}{1+\alpha_n^2} \left[log \frac{r_{n+1}}{r_n} - \alpha_n(\theta_{n+1} - \theta_n) \right] \quad (4)$$

$$\alpha_n = \frac{x_{n+1} - x_n}{z_{n+1} - z_n} \quad \text{and} \quad \beta_n = x_n - \alpha_n z_n \quad (5)$$

where r_n is the distance from the polygon corner (x_n z_n) to the point of calculation P, and θ_n is the angle between P and polygon corner, G is the gravitational constant and $\Delta\rho$ is the density contrast.

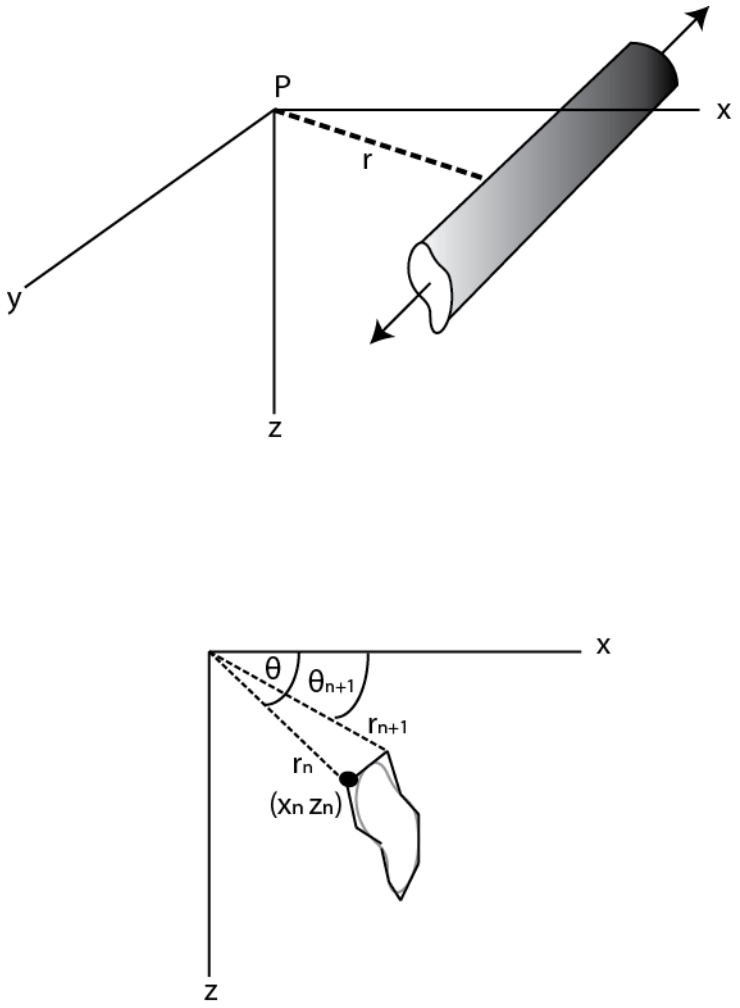


Figure 4.2 The geometry of a 2D source used to determine the Talwani method et al., (1959) algorithm to describe the gravitational anomaly created by the source. The top diagram shows the source has been elongated into the y-axis and the bottom diagram shows how the smooth outline of the cross-section is simplified to a n-sided polygon. Diagram modified from Blakely (1995).

4.3.2.2 Rectangular prism method

The rectangular prism method uses a simple shape like a rectangular prism which has a known solution to determine the gravitational effect of an object. This simple shape can be used to build up a complex source and determine its 3D gravitational effect by summing the solution of each rectangular prism (Figure 4.3). A complete derivation for the rectangular prism method can be found in Blakely (1995). Below is a short summary following this derivation. The gravitational anomaly due to a point source P is given by:

$$\bar{g}(P) = -\nabla U = -G \int p \frac{\hat{r}}{r^2} dv \tag{4.6}$$

where P has a density p, and volume v, P is located at the origin a distance r away, U is the gravitational potential and G is the gravitational constant.

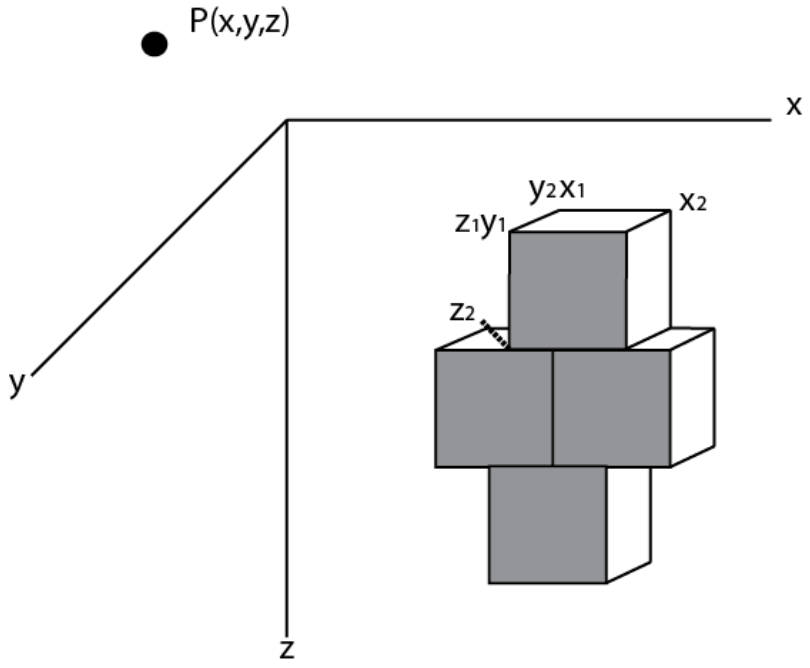


Figure 4.3 The geometry of a 3D rectangular prism method, approximating a 3-dimensional mass. Diagram modified from Blakely (1995).

For a rectangular prism with a constant density ρ, the vertical component of gravity determined from equation (4.6) is given by:

$$g_z = G_\rho \iiint_{z_1 y_1 x_1}^{Z_2 y_2 x_2} \frac{z'}{(x'^2+y'^2+z'^2)^{3/2}} dx'dy'dz' \tag{4.7}$$

After integrating over the volume, the analytic solution is:

$$g_z = G_\rho \sum_{i=1}^{2}\sum_{j=1}^{2}\sum_{k=1}^{2} \mu_{ijk}\left[z_k arctan\frac{x_i y_j}{z_k R_{ijk}} - x_i \log\left(R_{ijk}+y_j\right) - y_j \log(R_{ijk}+x_i)\right] \tag{4.8}$$

where G is the gravitational constant and

$$R_{ijk} = \sqrt{x_i^2 + y_j^2 + z_k^2} \qquad \text{and} \qquad \mu_{ijk} = (-1)^i(-1)^j(-1)^k \tag{4.9}$$

By summing the results of equation (4.8) with a corresponding density for each prism, the vertical gravitational attraction can be calculated. This method may not be the most practical as it makes unnecessary calculations for boundaries where two side by side prisms have the same density (Blake, 1995).

4.3.3 Gravity Interpretation

The gravity dataset provided by CGS had a 1 km line spacing. To provide a more localized interpretation that would not be affected by regional gravity patterns or very deep structures a residual gravity map was created and used for the 2D and 3D forward models in this study. Oasis Montaj was used to calculate the residual Bouguer gravity map.

To enhance features closer to surface a residual gravity map was created and used for 2D and 3D forward modelling. Generally features closer to surface or smaller in size have shorter wave lengths compared to deeper larger anomalies (Musset and Khan, 2000). A regional gravity map was produced by calculating a 3 x 3 Hanning filter on the original Bouguer gravity map. The regional gravity map shows the long wavelength patterns of the original Bouguer gravity map. This regional gravity map was then subtracted from the original Bouguer gravity map which produced a residual Bouguer gravity map. The residual Bouguer gravity map shows features closer to surface and shorter wavelength anomalies, which were previously hidden due to the longer wavelength regional patterns being a stronger feature. Figure 4.4 shows a comparison of the original Bouguer gravity map and residual Bouguer gravity map as well as the calculated regional Bouguer gravity map.

A crustal thickness map shows the thickening of the crust over the area of Bethlehem. The crustal thicknesses were collected by the South African Seismic Experiment (SASE), during the period 1997 – 1999 (Carlson *et al*., 1996 and James *et al*., 2003). These stations were spaced 100 km apart. The crustal thickness map of the Bethlehem region is gridding around 1 station point. Therefore the crustal thickness data was only used as an observation and not for any quantitative interpretation.

A 2D profile X-Y (Figure 4.5) of the regional Bouguer gravity data was modeled. This is model presents a 2D forward model of the upper crust, lower crust and mantle. This 2D forward model shows the regional Bouguer gravity does not affect the upper crust in which borehole, seismic and gravity interpretations were made for this study. The 2D forward model shows a smooth upwarp of the lower crust, whereas the mantle shows a slightly more undulating surface. The densities and constraints used for the forward model is taken from James et al. (2003) and Niu and James, (2002). These models and densities were closest to the Bethlehem region.

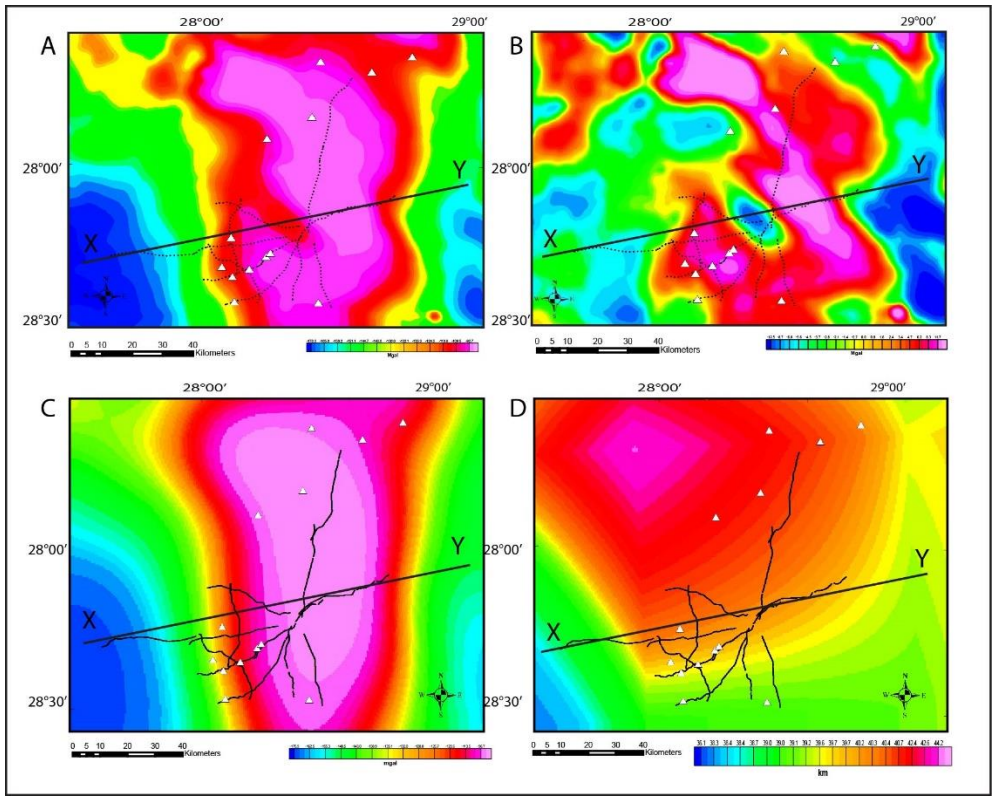


Figure 4.4 Map A – original Bouguer gravity map, Map B – residual Bouguer gravity map, Map C – calculated regional Bouguer gravity map and Map D – crustal thickness map, overlain with borehole data (white triangles and seismic lines (black lines). Profile line X - Y (black) used for forward modelling in figure 4.5.

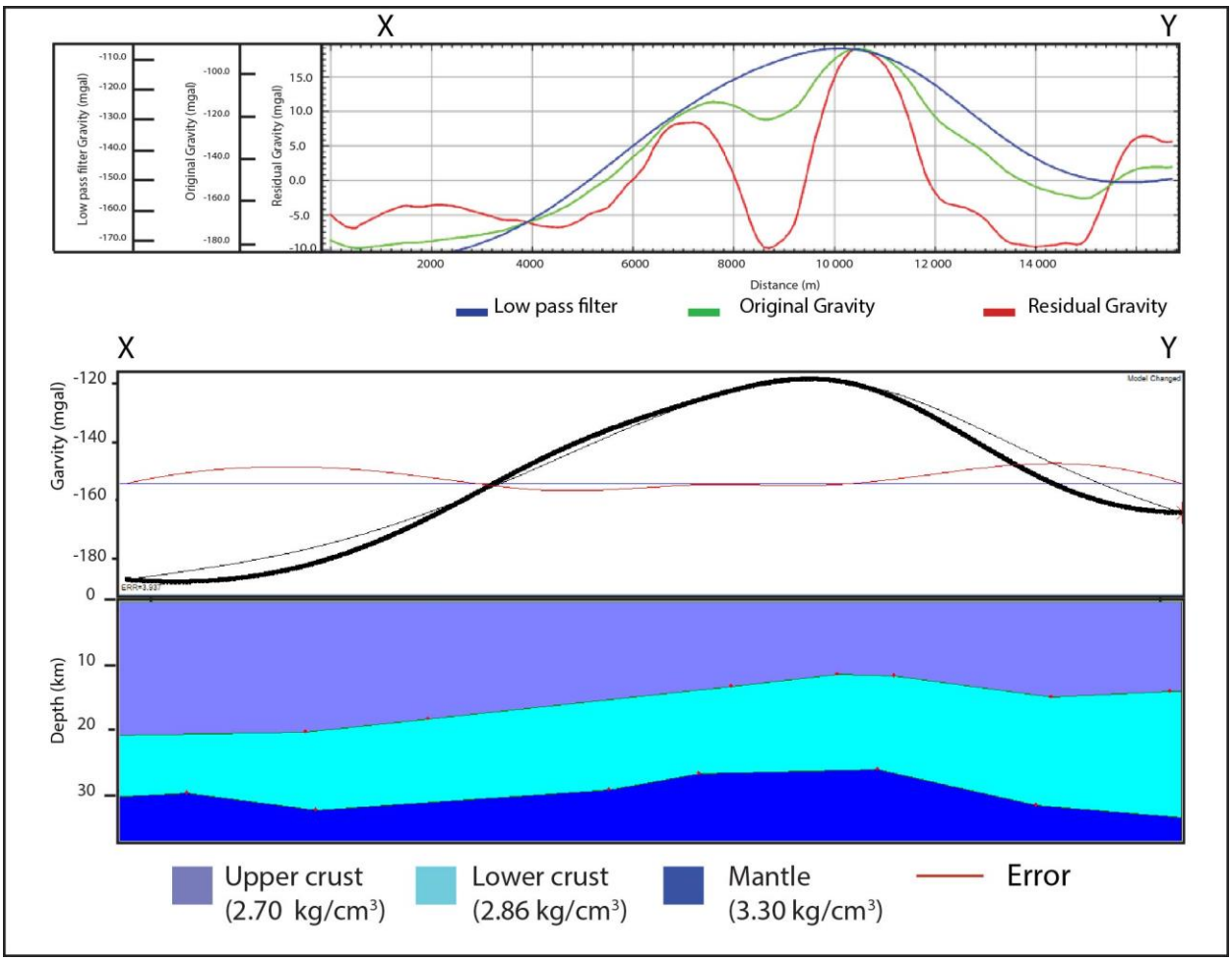


Figure 4.5 Profile X-Y showing the removal of regional gravity data. Above image shows Profile X-Y of the original gravity data (green line) compared to regional gravity data (blue line) and residual gravity data (red line). The residual gravity map was used for 2D and 3D forward modelling for this study.

The theory and methods presented above were used in software and interpretation of data to determine a well constrained, consistent 2D and 3D model of the Bethlehem area. The results are presented in Chapter 5.

5 Results

The seismic and 2D gravity forward model results are presented below. A final illustration is presented, to combine the fault interpretations from seismic and gravity data (Figure 5.17 and Figure 5.18).

5.1 Seismic Results

12 Seismic lines were interpreted for the Bethlehem study area. The seismic sections are described in terms of the 4 major contacts which include; Karoo Supergroup, Ventersdorp Supergroup, Central Rand Group, West Rand Group and basement. These contacts are used to constrain the 2D forward gravity models and to define and constrain the 3D geological model.

Magnetic and borehole data is included in the seismic interpretation to show where boreholes coincide with seismic data (Figure 5.1). These boreholes were used to determine the dolerite sills within the Karoo Supergroup. The seismic sections can be divided into two areas; the south western region which has majority of the seismic sections and cross over seismic lines that allow for a more constrained interpretation. The north eastern region which has few seismic sections and boreholes which made constraining the interpretation difficult.

The seismic results area presented as the south western region and north eastern region. A description of how each lithology was interpreted in these regions is given, which is followed by the figures of each seismic section in that region. A description of individual seismic sections can be found in Appendix A. The gravity map (Figure 5.1) is used as the base map for the seismic line locations because the Bethlehem gravity high can be used as a reference location, as well as correlation to gravity structures which can be made with the seismic interpretation. The magnetic map shows features close to surface and was used to correlate locations of sills with seismic sections (figure 5.1).

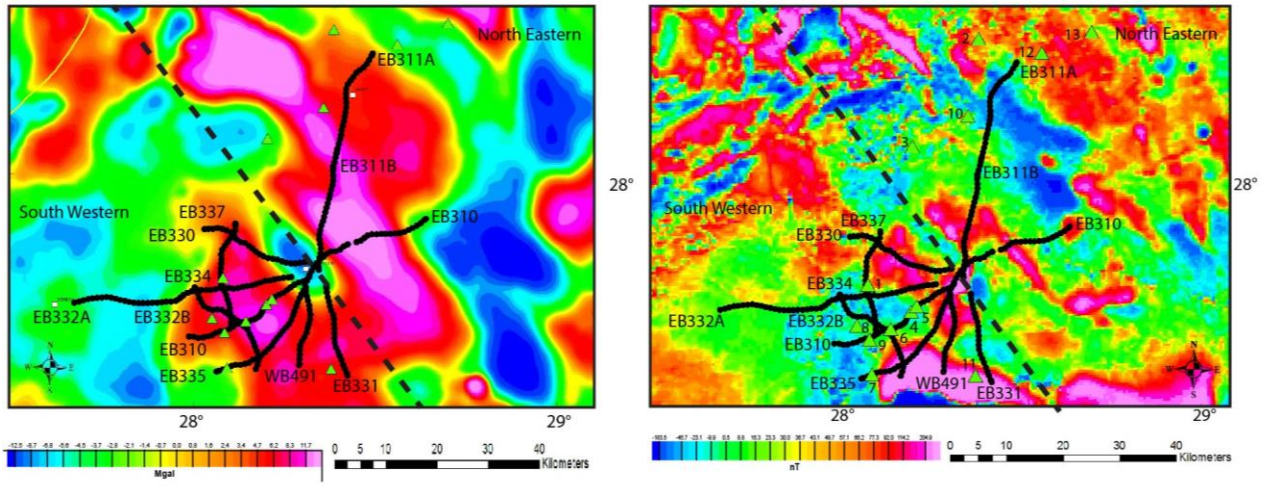


Figure 5.1 Location map of seismic lines interpreted for this study overlaid on the residual gravity map (left) and magnetic map (right) of the Bethlehem region. Seismic lines are centered on the town of Bethlehem. Most of the lines end at the town, crossing one side of the anomaly except for EB310 which runs across the anomaly. EB310 is also split into 3 parts A, B and C. The boreholes are represented by green triangles. The south western region and north eastern regions are separated by dashed line

5.1.1 Seismic results of south western region

In the south western region of the Bethlehem study area the seismic sections cover a large area with a fair amount of detail. Figures 5.2 – 5.9 shows each seismic section with and without interpretation. 2 seismic sections (EB334 and EB 337) cross-cut several other seismic sections which creates a well constrained interpretation in the south western region. Borehole data were used to constrain depth of reflectors. However, the constant velocity depth conversion meant depth recorded in boreholes may not be the same as the seismic section depth.

Two faults were interpreted in the south western region which are described as follows.

Fault B – Interpreted in EB330, EB332 and EB310 (Figure 5.2, 5.3 and 5.4) is a north northwest trending normal fault, dipping towards the west. Fault B uplifts the granite to the east and truncates the West Rand Group to the west of the fault.

Fault C – Interpreted in EB310 (Figure 5.4) is a north northwest trending normal fault, dipping towards the east. Fault C uplifts the granite to the west of the fault and truncates the West Rand Group to the east of the fault.

The basement granite suite is distinguished in the seismic sections by a homogeneous layer of reflectors as mentioned in Chapter 4. No boreholes in the south western region intersect West Rand Group and basement. Therefore the West Rand Group – basement boundary is only defined by the change in amplitude of reflectors from closely packed strong reflectors to a homogeneous seismic package. This boundary is not as constrained as the Karoo, Ventersdorp or Central Rand interfaces. The basement is at a depth of 5 km in the south western region and gradually shallows towards the east shown in EB330, EB332, EB310 and EB335. In seismic section EB310 the granite has been uplifted by normal faults B and C to lie beneath the Karoo to form a ridge trending north northwest. Within the granite layer strong reflectors are observed at a depth of 5.5 km. These strong reflectors are visible in sections EB330, EB332, EB310 and EB337 all at the same depth.

The West Rand Group was defined by a package of closely spaced, strong internal reflectors, due to the shale and quartzite layering within the group. This is described in chapter 4. This type of package was observed clearly in sections EB310C, EB335, EB334. However, not all seismic sections show this distinguishing reflector package. In these cases such as EB332, WB491 and EB331, cross cutting seismic sections and the closest boreholes were used to approximate the Central Rand Group – West Rand Group interface.

The second difficulty is interpreting the base of the West Rand Group. There is no distinct reflector to mark this interface, due to the sedimentary/felsic base of the West Rand Group having similar Vp and ρ to the granite. However the granite basement produces a homogeneous package on seismic sections and this was used as the boundary between the West Rand Group and granite basement. This is seen in seismic sections EB330 and EB310. The West Rand Group thickness ranges from 2 km to 5 km in the south western region. The base of the West Rand Group is at a depth of 5 km and is tilted towards the east observed in section EB322 and EB310A. The West Rand Group continues to shallow toward the east where it truncates the Central Rand Group and Ventersdorp Supergroup, creating a lithological contact change. This contact is observed in section EB332, EB310, EB330, EB334, EB335 and EB337. To the south of the region seismic sections EB331 and WB491 show the West Rand Group underlying the Karoo Supergroup at a thickness of 2 km. The boundary for the West Rand Group in seismic section EB331 and WB491 have the least constraint of all the seismic sections. To the east of the region the West Rand Group is truncated by faults B and C on the west and east respectively, as the basement has been uplifted to underlie the Karoo.

The Central Rand Group – West Rand Group interface was difficult to constrain. With the exception of one borehole, there was no interception of the boundary between Central Rand and West Rand or the base of the Witwatersrand Supergroup in the borehole data.

The Central Rand Group is only interpreted in the south western region. Seismic sections EB322, EB337, EB334 and EB335 shows the Central Rand tilting upwards towards the north east, where it is truncated by the Karoo. The thickness of the Central Rand Group ranges from 1 to 2.5 km where it is pinched out and truncated by the West Rand Group. The truncation of the Central Rand Group is confirmed in boreholes 9 and 6 on seismic section EB310 which shows Central Rand Group underlying Ventersdorp Supergroup in borehole 9 and West Rand Group underlying Ventersdorp Supergroup in borehole 6.

The Ventersdorp – Witwatersrand contact is fairly sparse and only appears on the western and southern ends of seismic sections EB330, EB322, EB310, and EB335. Boreholes 9 and 7 show the base of the Ventersdorp Supergroup ranging from approximately 2000 m to 2500 m from surface which corresponds to sections EB332 and EB335 respectively. In the south western region the Ventersdorp Supergroup unconformably overlies the West Rand Group in sections EB310, EB335. The Ventersdorp Supergroup is otherwise overlying the Central Rand Group and is tilted upwards in an easterly direction, where it is truncated by the Karoo. This is shown in sections EB310, EB335 and EB334.

The base of the Karoo is clearly imaged on all seismic sections due to its low velocity and density compared to the underlying layers. The depth of the interface across the south western section is between 1000 m – 1500 m. The Karoo interface is fairly horizontal, truncating all underling layers creating an angular contact with the Ventersdorp Supergroup, Central Rand Group, West Rand Group and basement. These angular contacts are clearly visible in seismic section EB332 where the Ventersdorp – Central Rand Group interface and Central Rand Group - West Rand Group interface are truncated by the Karoo interface.

Within the Karoo Supergroup borehole data were used to determine the location and structure of dolerite sills on seismic sections EB310 and EB337. Boreholes 9, 6, 4 and 5 are positioned along seismic section E310. These boreholes show 2 dolerite sills at depths of approximately 600 m and 1 km with varying thicknesses of 40 m – 180 m and 40 m to 100 m respectively. Seismic section EB337 has one borehole with a dolerite intrusion at a depth of 500 m and thickness of 100 m.

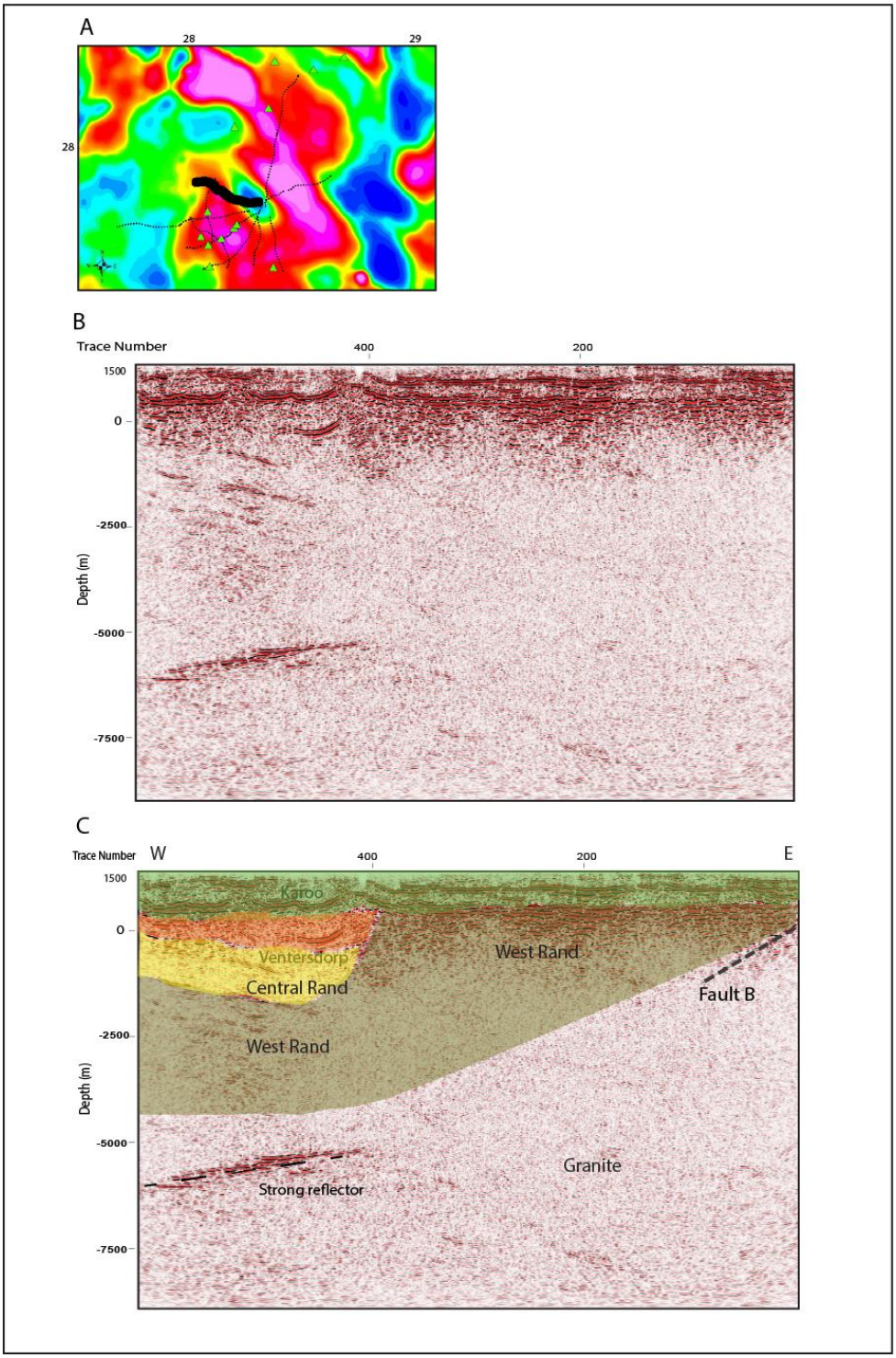


Figure 5.2 Gravity map (A) shows location of the seismic line. Seismic section EB330 with no interpretation (B) and interpretation (C). There are no boreholes close to this seismic line. Fault B uplift granite and tilts West Rand Group.

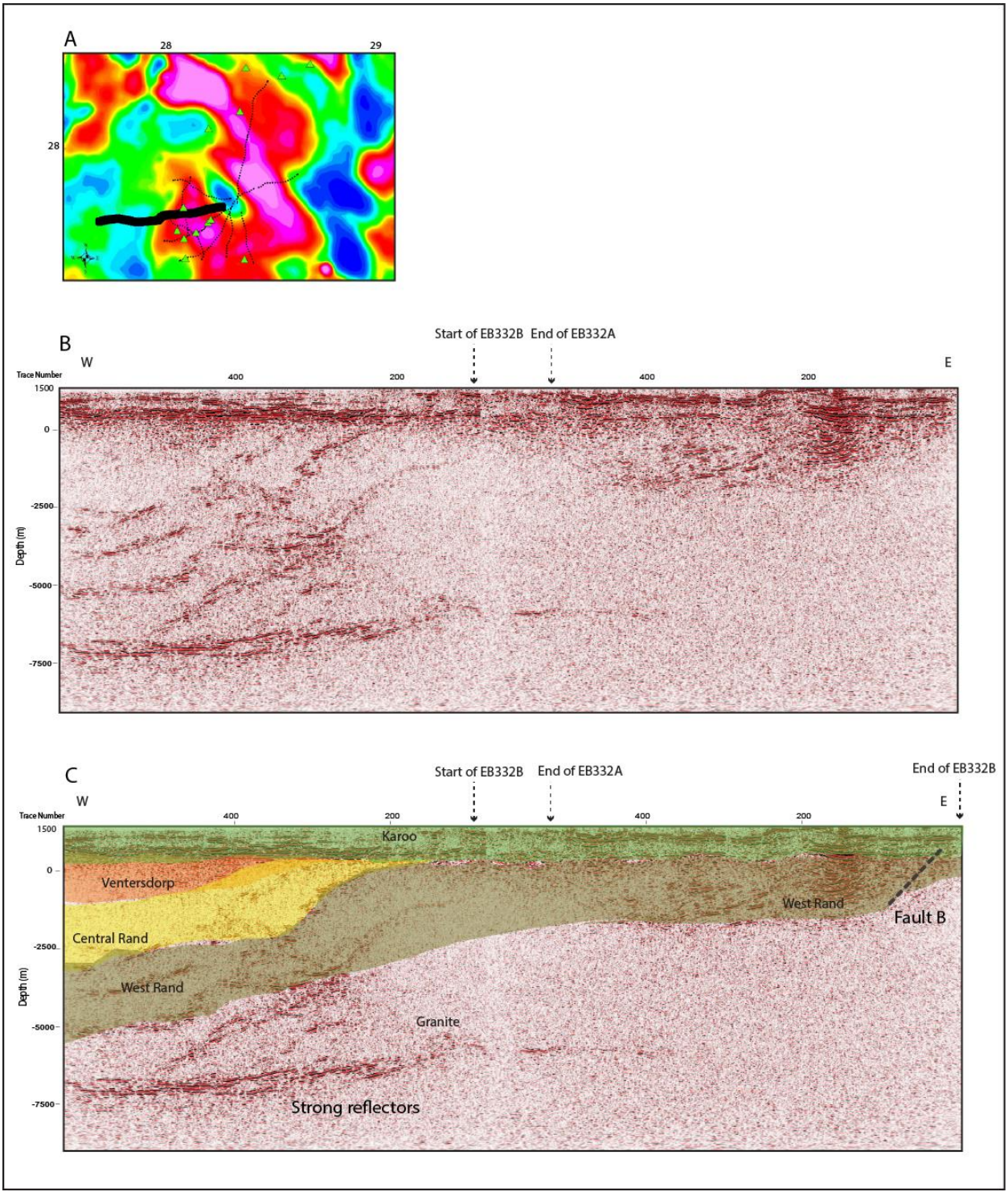


Figure 5.3 Gravity map (A) shows location of seismic section EB332. Seismic section EB332 with no interpretation (B) and interpretation (C). This line was separated into A and B. There are no boreholes close to this seismic line.

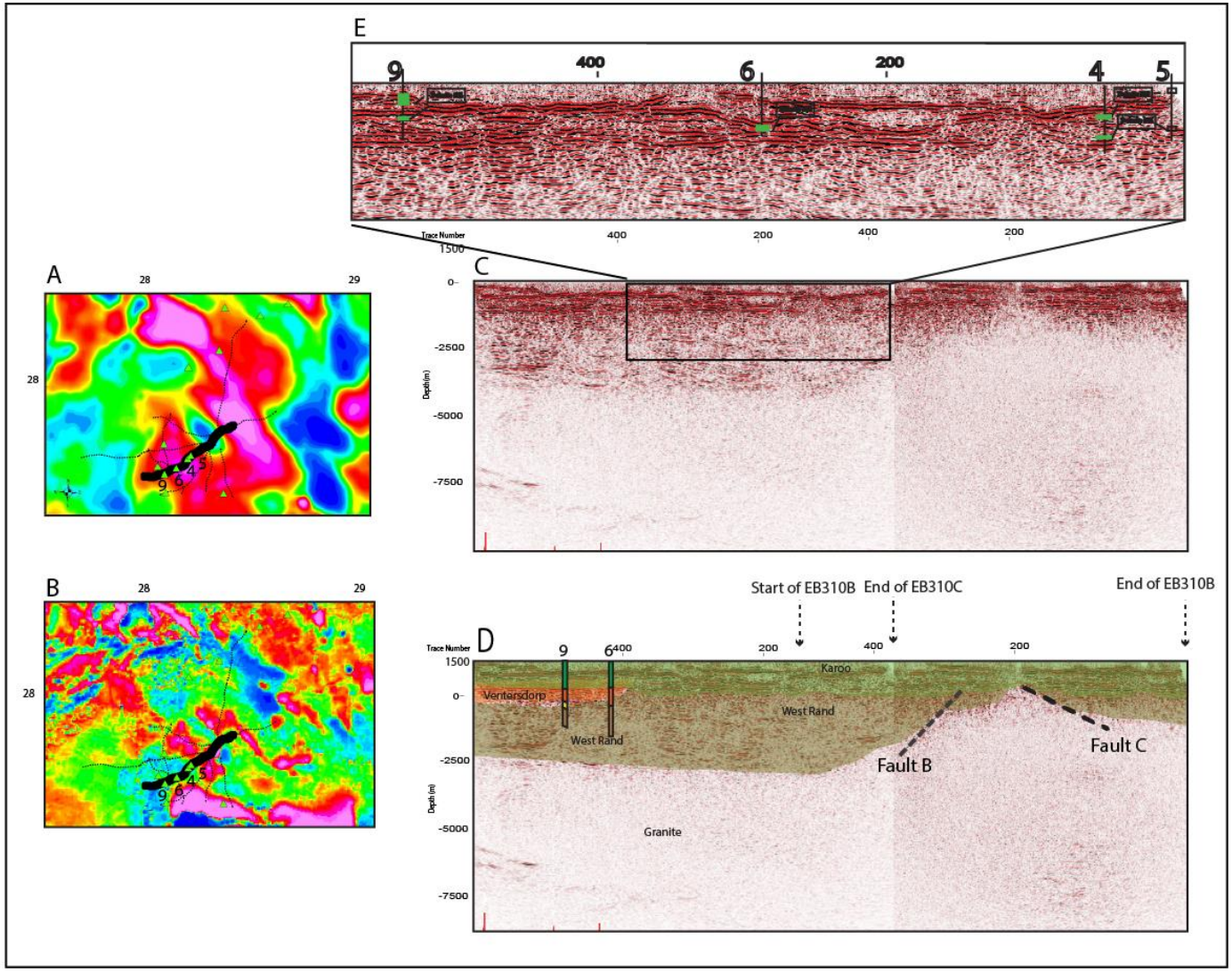


Figure 5.4 Gravity map (A) and magnetic map (B) shows location of seismic line and borehole for EB310. Seismic section EB310 C and B with no interpretation (C) and interpretation (D).This line was split into 3 parts section EB310 C and B on the south western side and EB310 A on the north eastern side. Boreholes 9 and 6 go deeper than the Karoo and are shown in the interpreted seismic section. Boreholes 9, 6, 4 and 5 also show dolerites which are shown in (E).

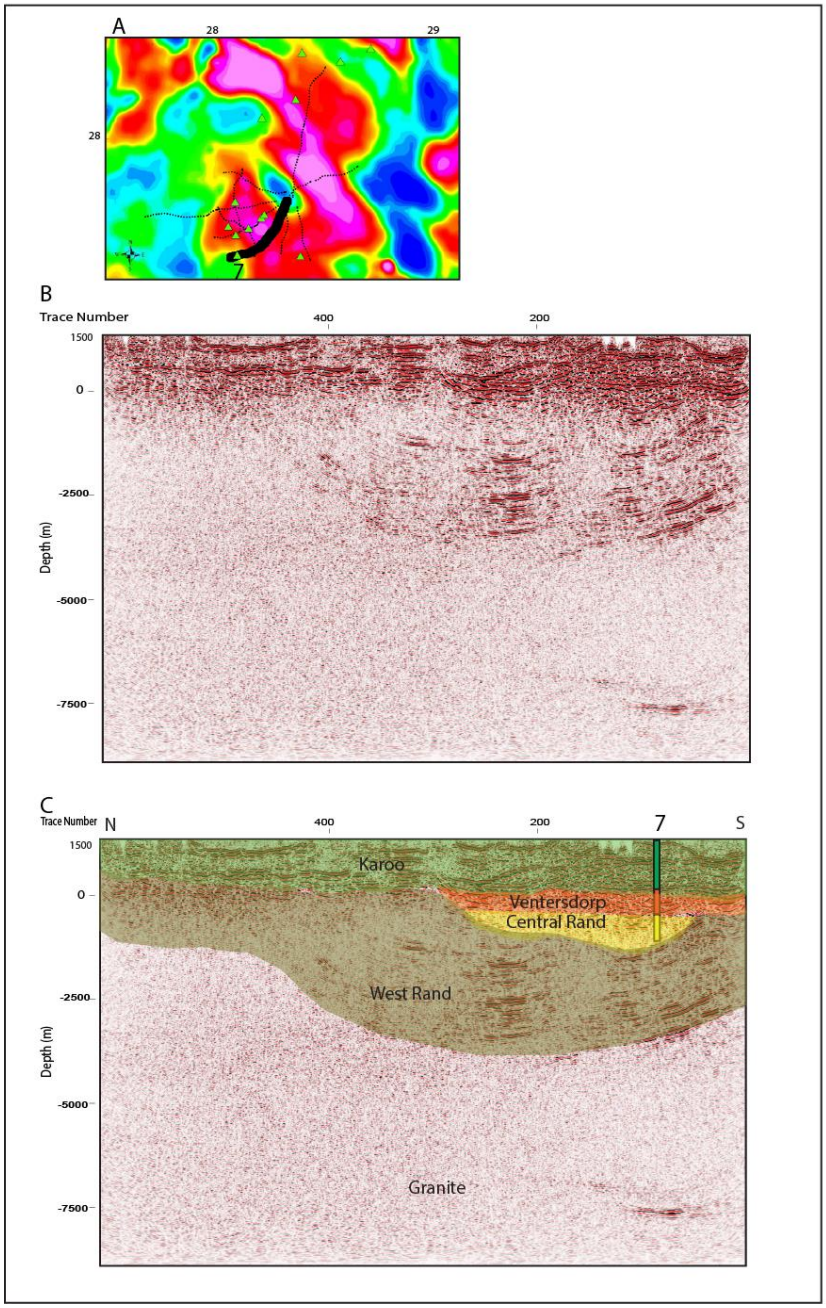


Figure 5.5 Gravity map (A) shows the location of seismic section and boreholes. Seismic section EB335 with no interpretation (B) and interpretation (C). Borehole 7 which overlies seismic section EB335 is shown in (C).

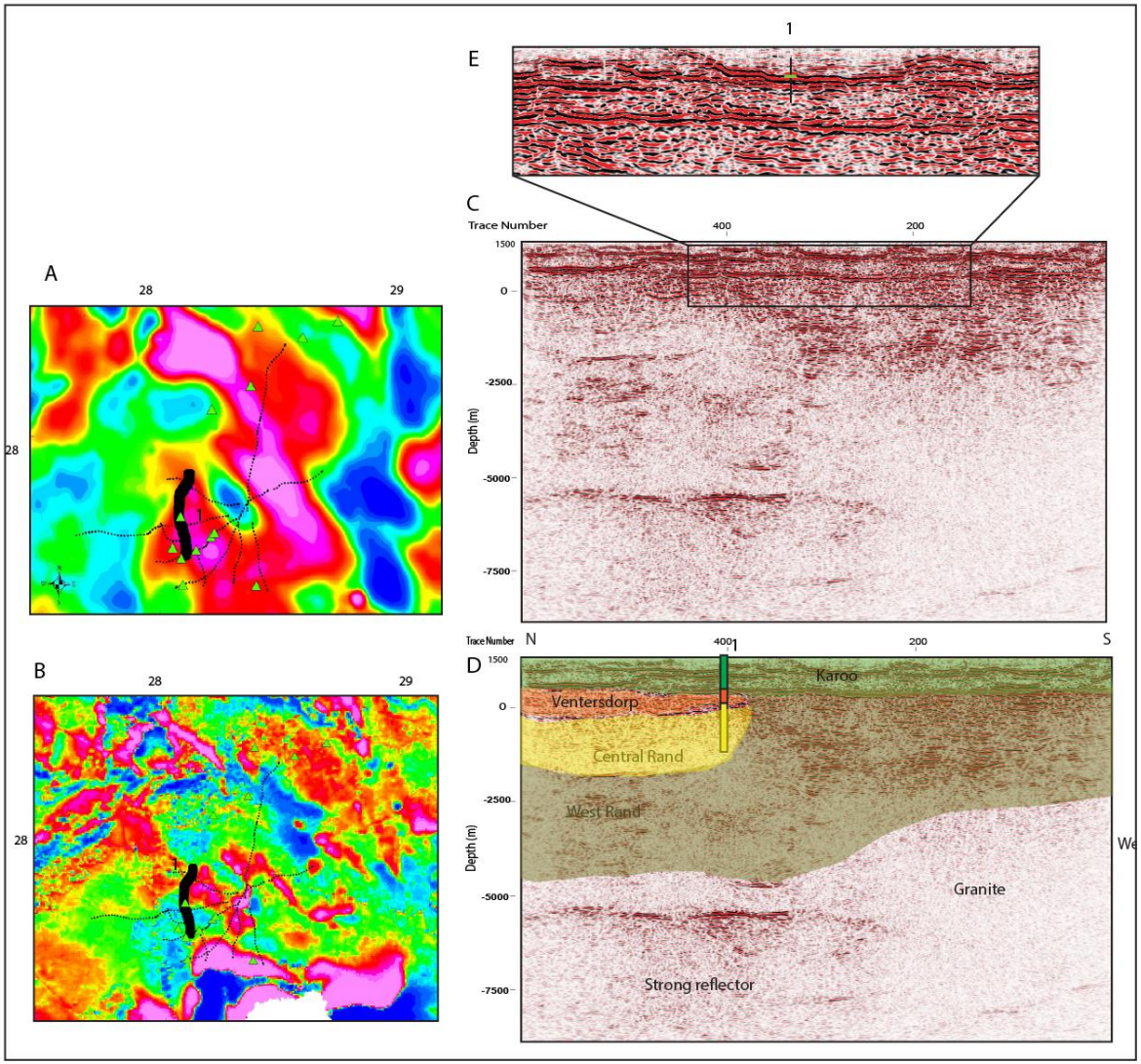


Figure 5.6 Gravity map (A) and magnetic map (B) shows the location of seismic section and boreholes. Borehole1 which overlies. Seismic section EB337 with no interpretation (C) and interpretation (D). Seismic section EB335 is shown in (D). Borehole 1 also shows dolerite intrusions and is shown in image (E).

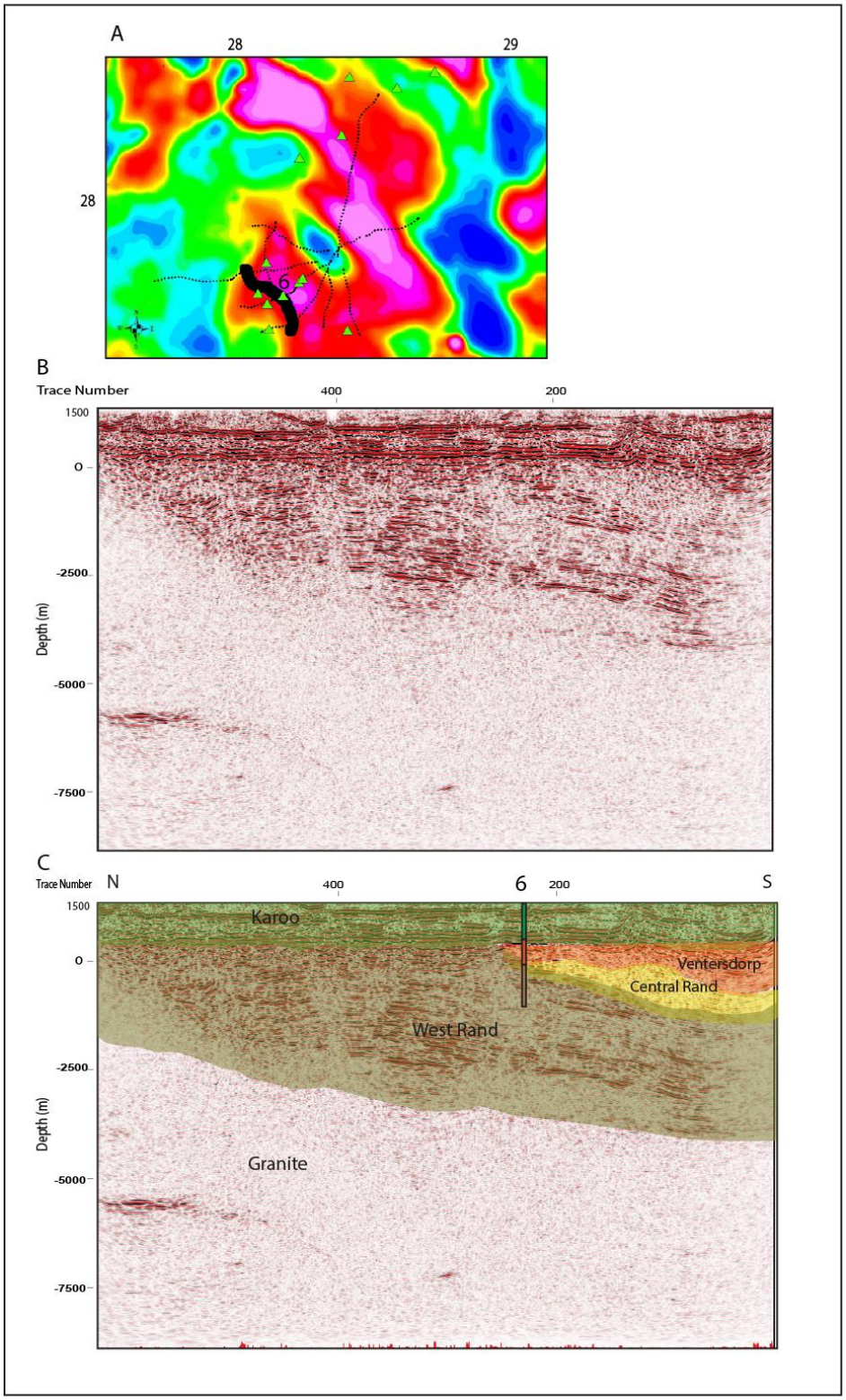


Figure 5.7 Gravity map (A) shows the location of seismic section and boreholes. Seismic section EB334 with no interpretation (B) and interpretation (C). Borehole 6 which overlies seismic section EB334 is shown in (C).

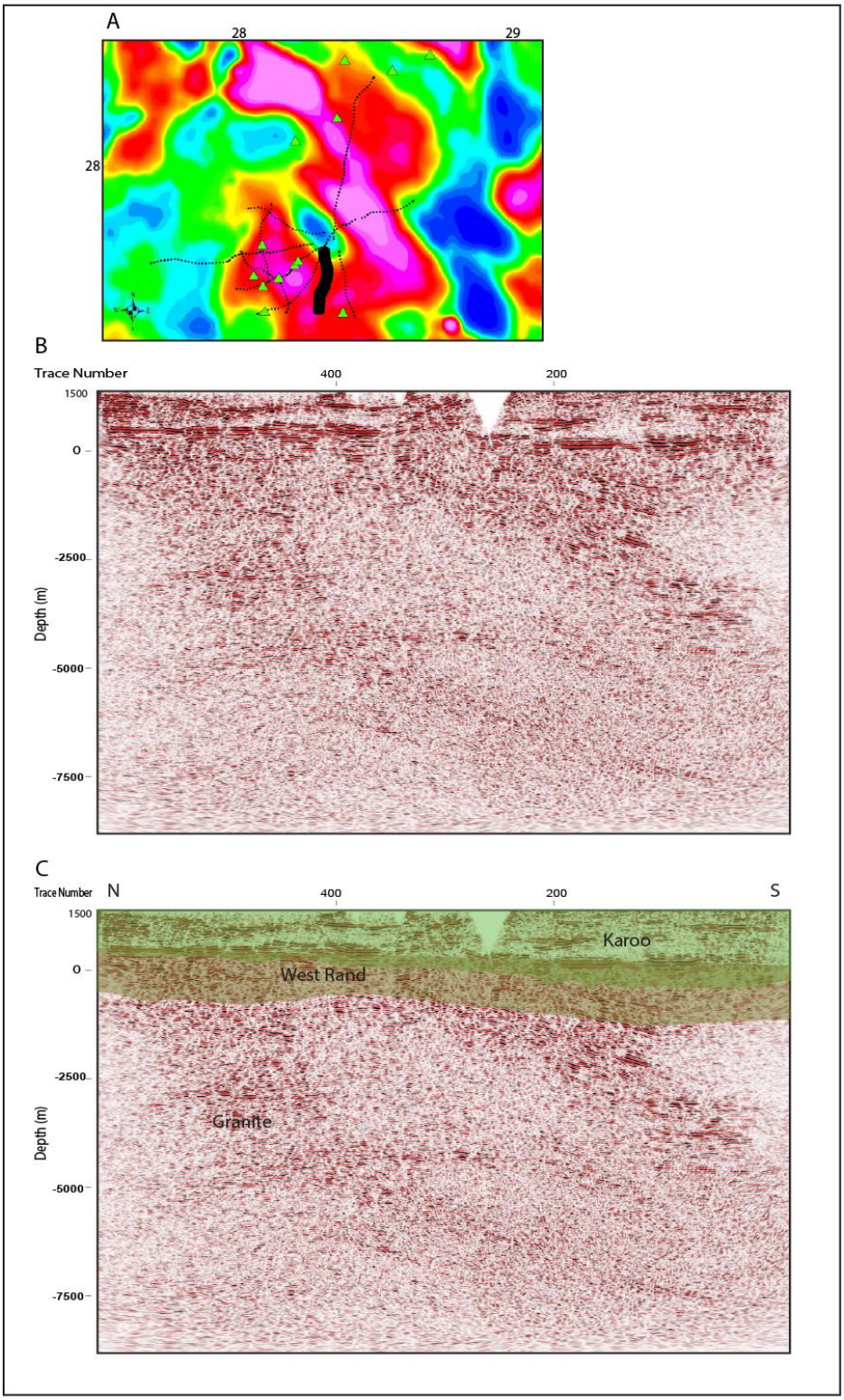


Figure 5.8 Gravity map (A) shows location of seismic line. Seismic section WB491 with no interpretation (B) and interpretation (C). There are no boreholes close to this seismic line.

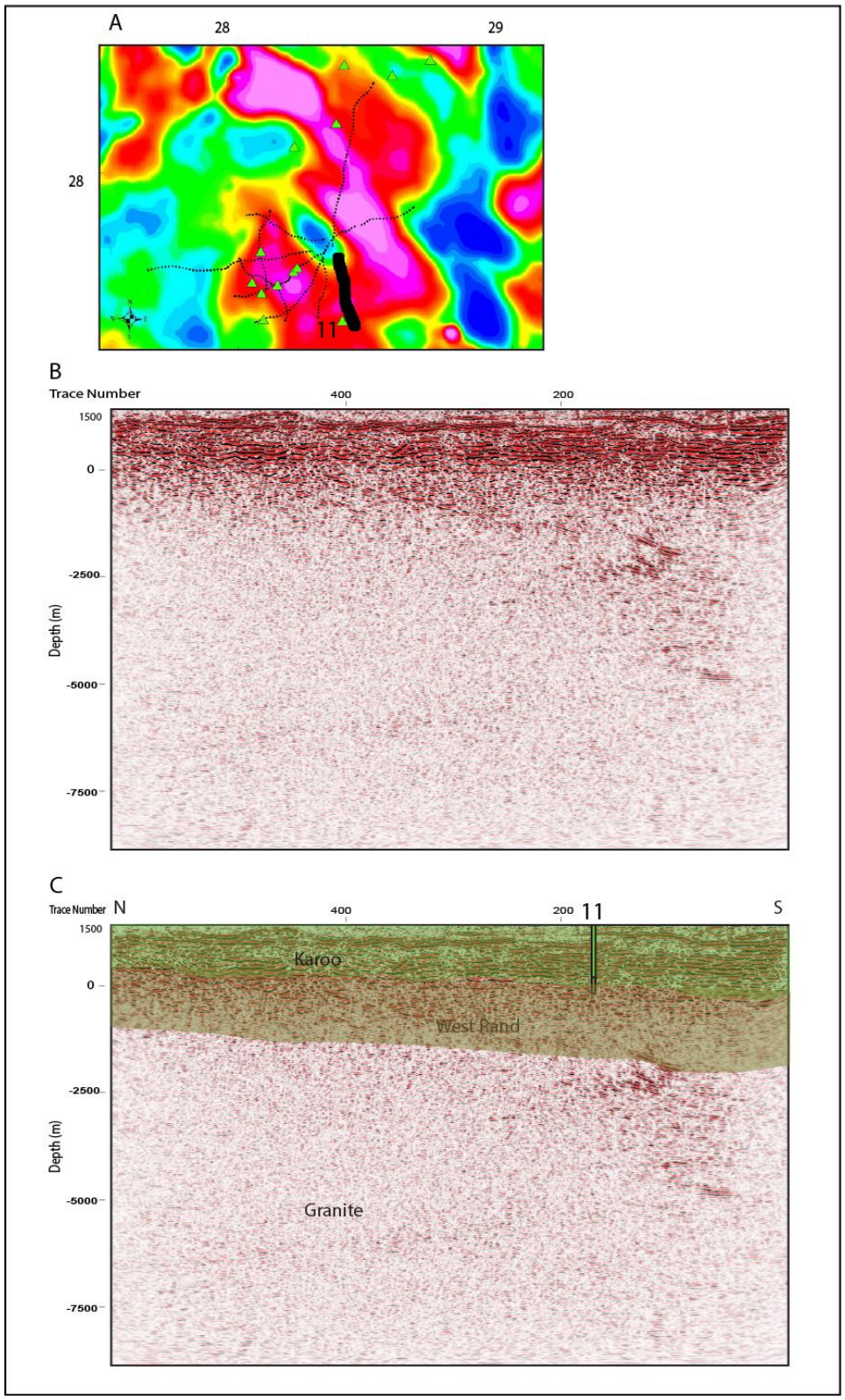


Figure 5.9 Gravity map (A) shows location of seismic line. Seismic section EB331 with no interpretation (B) and interpretation (C). Borehole 11 is shown in interpreted seismic section (B).

5.1.2 Seismic results of north eastern region

The north eastern region has only 3 seismic sections to cover a large area, with very few boreholes. There are no cross cutting seismic lines to constrain reflectors and all boreholes near the seismic sections are less than 1 km deep, except for boreholes 2 and 3 which show the basement granite suite underlying the Karoo. With this in mind the seismic sections were interpreted with care when picking reflectors.

Seismic section EB310A was interpreted to have a thin layer of the West Rand Group underlying the Karoo. This was constrained by the continuation of the West Rand Group eastwards in line EB310 which slightly overlaps section EB310A. A very thin layer of West Rand Group was observed in seismic sections EB311. The West Rand Group – basement interface is not clear and an undulating surface was interpreted to show the West Rand Group was not a continuous thickness.

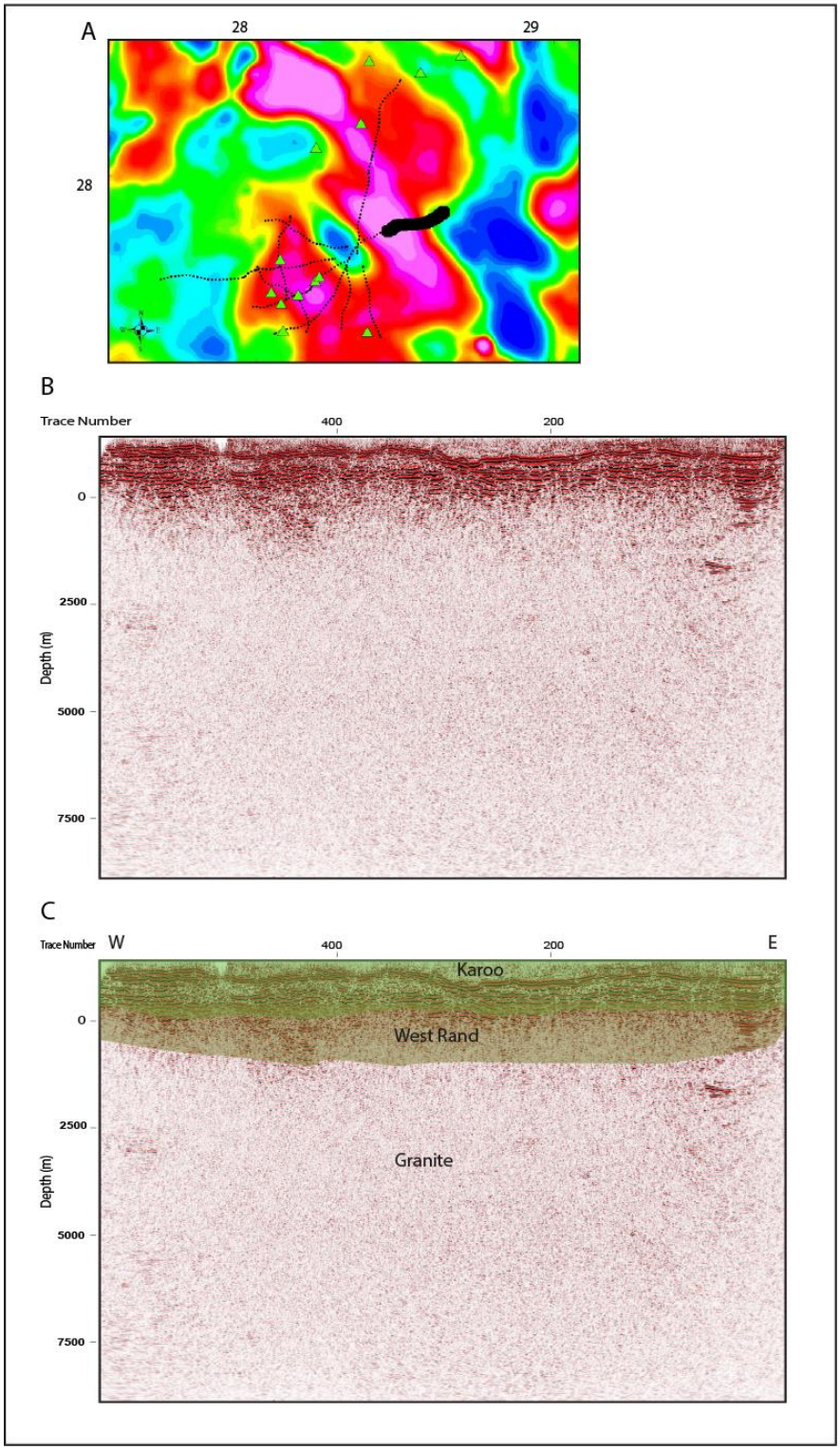


Figure 5.10 Gravity map (A) shows location of seismic line. Seismic section EB310A with no interpretation (B) and interpretation (C). There are no boreholes near his section.

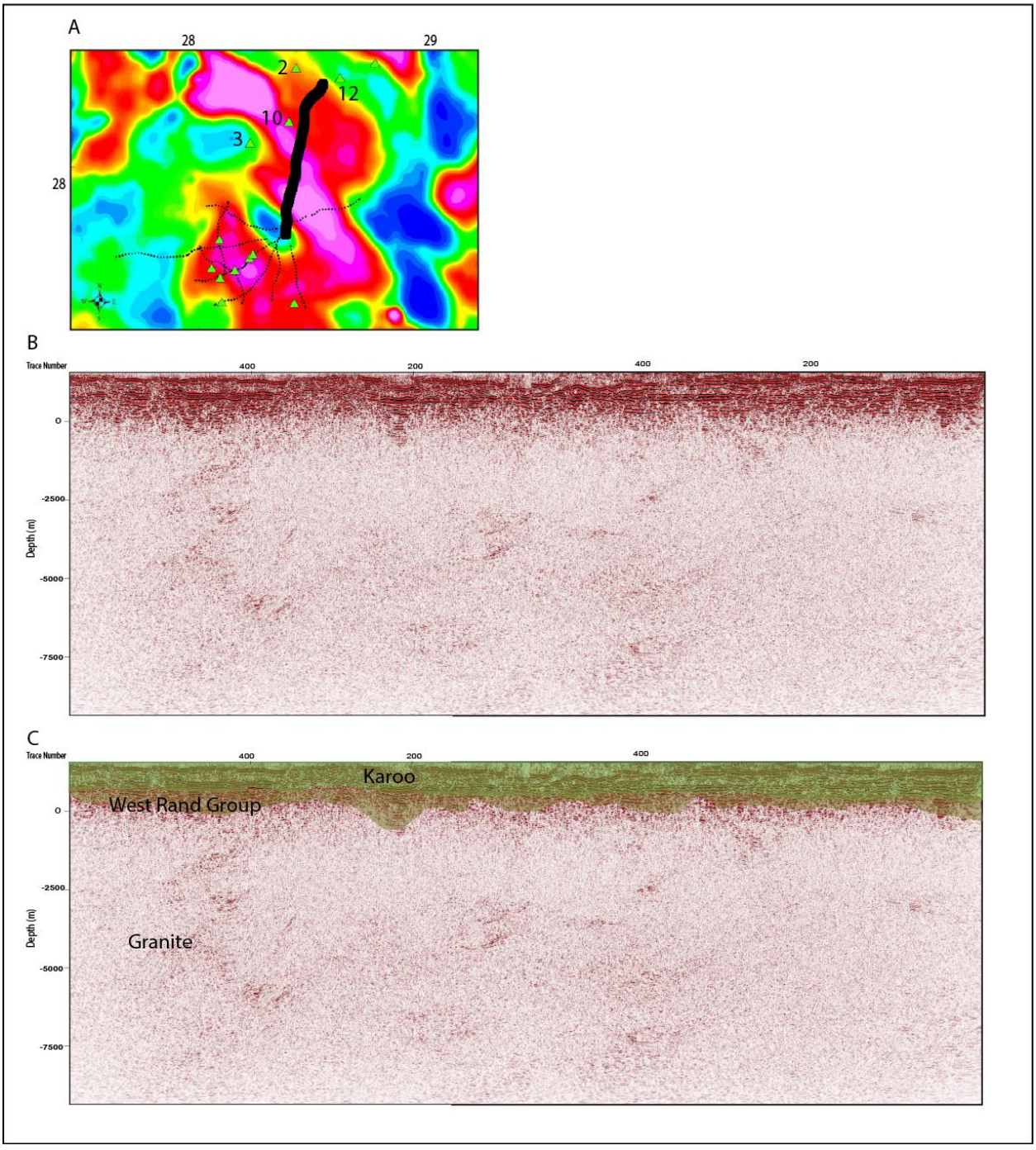


Figure 5.11 Gravity map (A) shows location of seismic line. Seismic section EB311 with no interpretation (B) and interpretation (C). Boreholes near this seismic line do not go deeper than the Karoo and are not shown.

5.2 Gravity Results

Four 2D potential field forward models were created over the Bethlehem study area to further constrain the 3D gravity model (Figure 5.12). The 2D forward model profiles were constrained by the interpreted seismic sections and borehole data. The gravity profiles were designed to cover a similar area of the seismic lines, so that the seismic lines could be efficiently used to constrain depths of lithologies. The 2D forward modelling was modelled using the residual gravity map described in Chapter 4, which enhances the Bethlehem gravity high and highlights the main highs and lows in the Bethlehem study area. The densities used in the models are Karoo Supergroup – 2.55 g/cm^3, Ventersdorp Supergroup – 2.88 g/cm^3, Central Rand Group 2.61 g/cm^3, West Rand Group – 2.91 g/cm^3 and basement – 2.67 g/cm^3. These were taken from literature seen in Chapter 3 and slightly modified during forward modelling to best interpret the Bethlehem study area. Figure 5.12 to 5.15 show the gravity models with location of profile and seismic data. A description of each model is provided after each figure.

A major difference in the 2D gravity profiles and seismic interpetations is the West Rand Group – basement boundary. This was expected as the interface could not be clearly intepreted and constrained in the sesimic sections as explained in Chapter 4. Profiles 1 – 4 all show an undulating boundary which is is very different to what is observed in the seisimc interpretation.

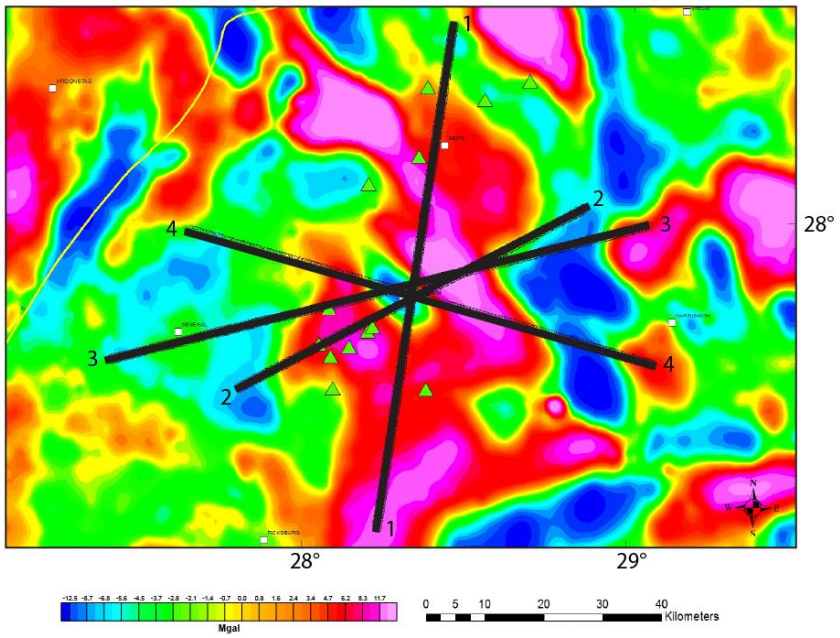


Figure 5.12 Location map of the 4 gravity profiles (Black lines) overlying the residual gravity map of the Bethlehem study area. Boreholes are represented by green triangles.

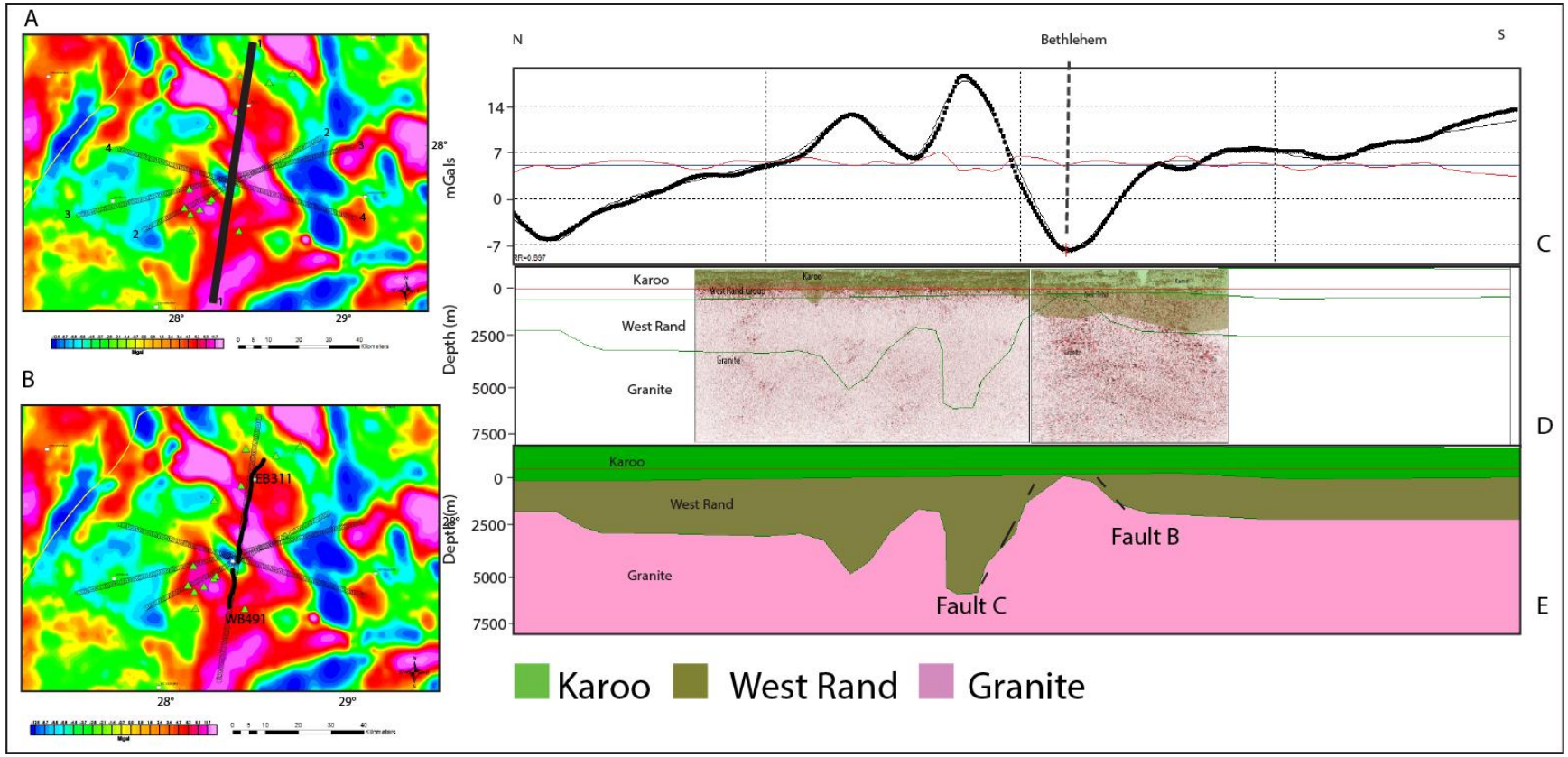


Figure 5.13 Location of gravity profile 1 overlain on the residual gravity map of Bethlehem (A). Location of seismic section EB331 and WB491 which corresponded with the gravity profile (B). First panel (C) shows 2D gravity profile with observed gravity anomaly and calculated gravity anomaly of model (thin black line). Second panel (D) shows correlating seismic sections used to constrain model. Third panel (E) shows 2D gravity model corresponding to the calculated gravity profile in first panel.

Gravity profile 1 shows a north - south profile crossing over both the south western and north eastern regions of the Bethlehem study area. The Karoo layer corresponds to the seismic section interpretation. However, the 2D model showed a much thicker West Rand Group layer compared to the seismic section as well as an undulating West Rand Group – basement contact. Whereas the seismic sections showed a fairly horizontal homogeneous layer with an unclear interface due to the lack of constraint and no strong reflectors. The northern section of profile 1 shows the West Rand Group has a depth ranging from 2.5 – 3 km corresponding with an increase in gravity. The highest gravity reading in profile 1 corresponds to fault C and shows a downthrown section of West Rand Group rocks reaching a depth of 5.5 km. This is followed by a gravity low corresponding to an uplifted section of basement rock by 2.5 km. The lowest gravity reading corresponds to granite underlying the Karoo Supergroup. The differences are density and size of displacement caused the change in gravity. At this change in gravity fault C and Fault B are normal faults which have uplifted the basement rock to form a ridge. These faults have been observed in seismic sections EB330, EB332 and EB310. On the south section of profile 1 the basement is at a depth of 2 km and the West Rand Group underlies the Karoo Supergroup with a thickness of 2 km.

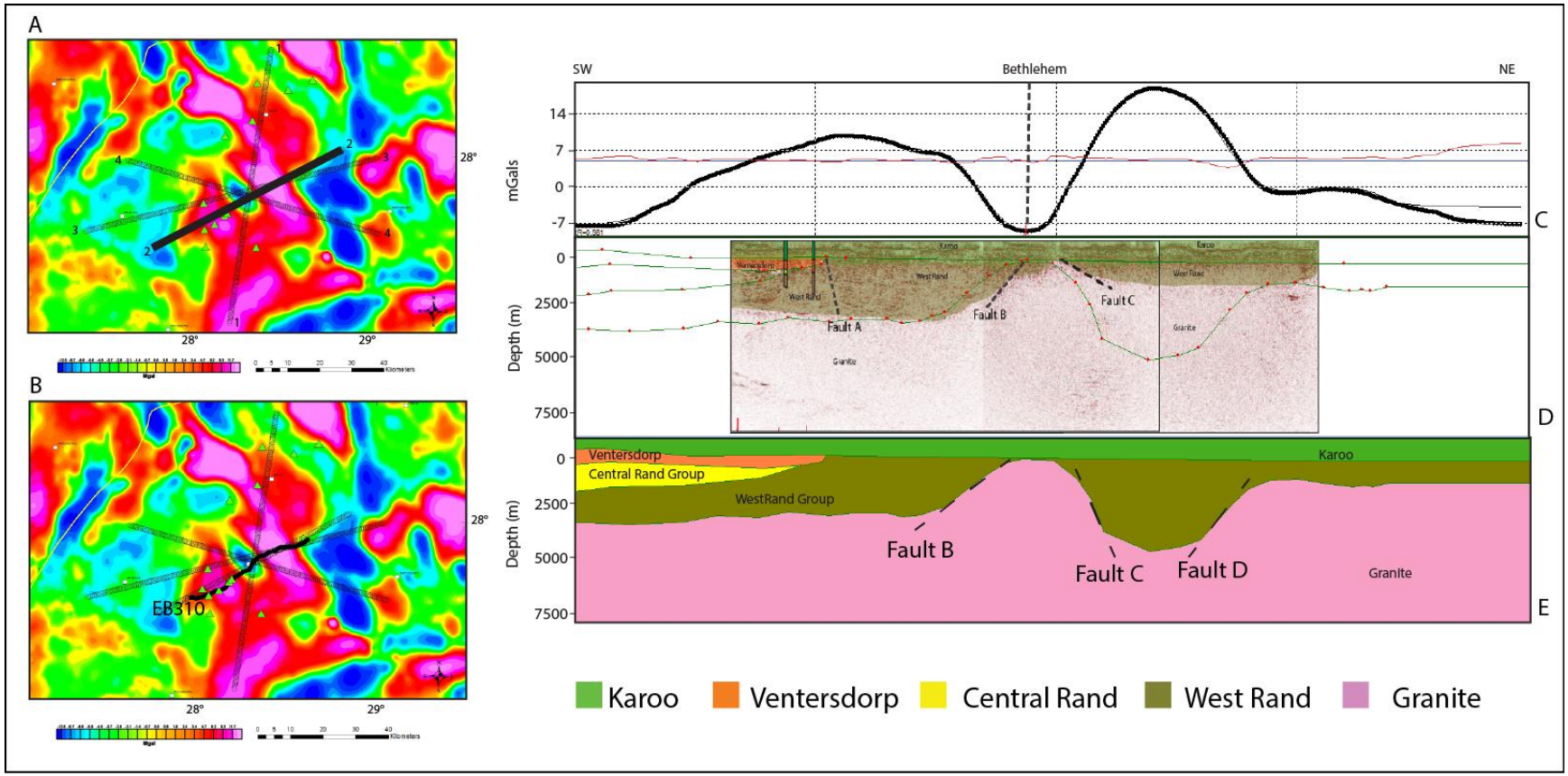


Figure 5.14 Location of gravity profile 2 overlain on the residual gravity map of Bethlehem (A). Location of seismic section EB310 which corresponded with the gravity profile (B). First panel (C) shows 2D gravity profile with observed gravity anomaly and calculated gravity anomaly of model (thin black line). Second panel (D) shows correlating seismic sections used to constrain model. Third panel (E) shows 2D gravity model which corresponds to calculated gravity profile in first panel.

Gravity profile 2 shows a southwest - northeast profile crossing over both the south western and north eastern regions of the Bethlehem study area. The Karoo Supergroup, Ventersdorp Supergroup and Central Rand Group layers of the 2D gravity model corresponds to the seismic section interpretation. The model shows a slightly thicker Karoo layer of 1.8 km and thin Ventersdorp layer of 500 m, pinching out towards the north east. The Central Rand Group has a thickness of 500 m and pinches out like the Ventersdorp. The Central Rand Group could not be interpreted in the seismic sections. Similar to profile 1, profile 2 shows an undulating West Rand Group – basement contact compared to that of the seismic section which showed a fairly horizontal homogeneous layer with an unclear interface. Normal faults, fault B and fault C correlate with seismic section EB310. The 2D forward model shows an uplifted basement of 2.5 km created by these faults. Similar to profile 1 to the northeast of Fault C shows a thick layer of downthrown West Rand Group rocks. This correlates with the highest gravity reading and the uplifted basement correlates with the lowest gravity reading. Fault B and Fault C are located at the change in gravity seen on the location map. North east of fault C the basement granite shows a second uplift in the basement and is described as fault D. Fault D is not observed in seismic sections. The uplifted basement east of Fault D is at a depth of 2.5km from surface and is overlain by a 1 km thick layer of West Rand Group rocks. Fault D corresponds to the gravity low in the northeast of profile 2.

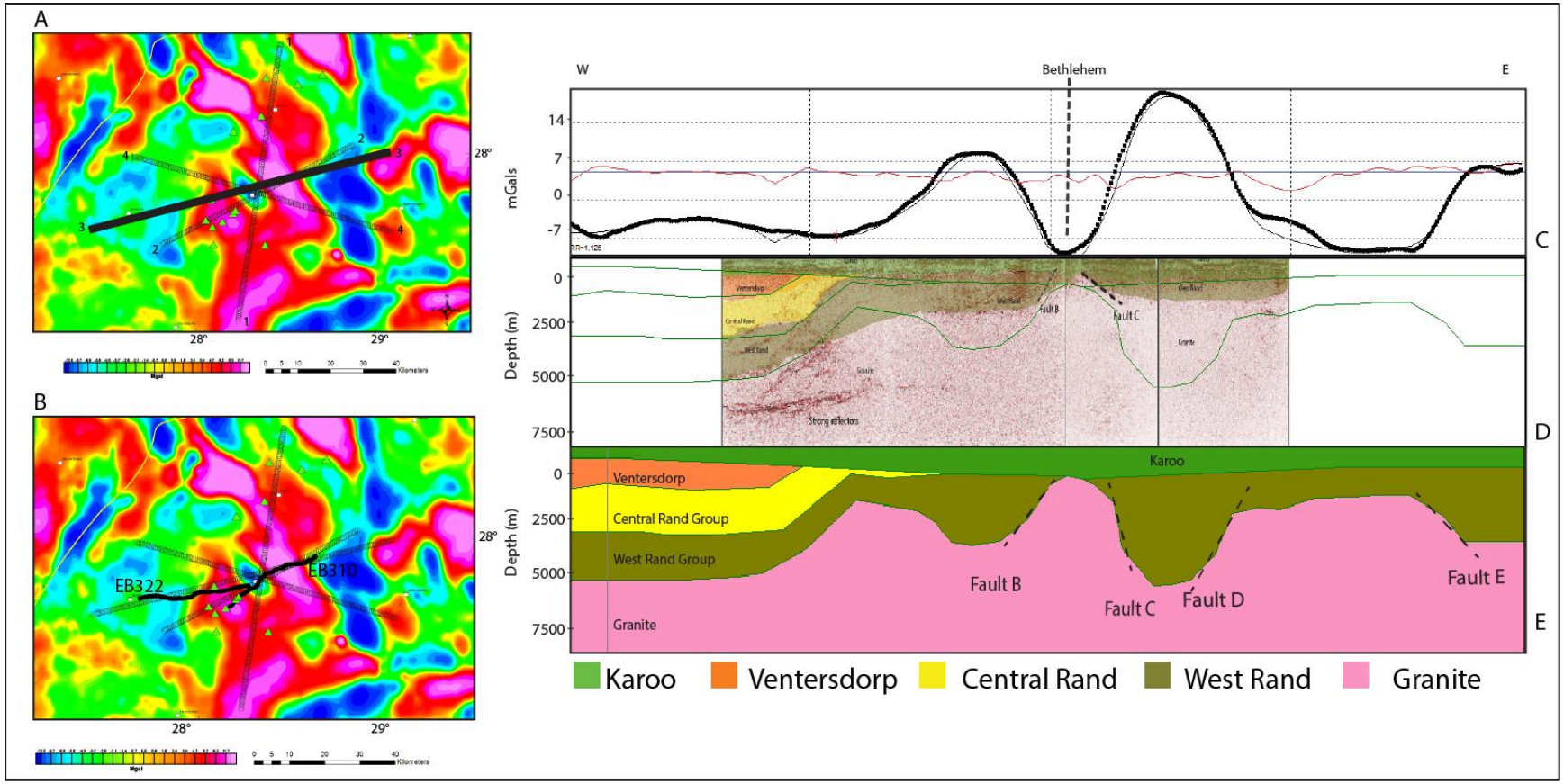


Figure 5.15 Location of gravity profile 3 overlain on the residual gravity map of Bethlehem (A). Location of seismic sections EB332 EB310 which corresponded with the gravity profile (B). First panel (C) shows 2D gravity profile with observed gravity anomaly and calculated gravity anomaly of model (thin black line). Second panel (D) shows correlating seismic sections used to constrain model. Third panel (E) shows 2D gravity model corresponding to the calculated gravity profile in first panel.

Gravity profile 3 shows a west - east profile crossing over both the south western and north eastern regions of the Bethlehem study area. The Karoo and Ventersdorp and Central Rand layers of the 2D gravity model corresponds fairly well to the seismic section interpretation. This shows a slightly thinner Karoo layer with a thickness of approximately 800 m in the west of the profile, 2 km thick section in the middle of the profile and finally thins out again to the east of the profile. The Ventersdorp layer is 1 km, and pinches out towards the east. The Central Rand layer has a thickness of 2.5 km eventually pinching out like the Ventersdorp. The Ventersdorp and Central Rand Group pinch and are truncated by the Karoo. On the west section of profile 3 major tilting of Ventersdorp, Central Rand Group, West Rand Group and basement is observed. This correlates to the tilting observed in the seismic interpretation of section EB332. Similar to profile 1 and 2, the 2D forward model shows an undulating West Rand Group – basement contact compared to that of the seismic section which showed a fairly horizontal homogeneous layer with an unclear interface. Fault B and C have uplifted the granite, creating a granite ridge, with thick West Rand Group sediments on either side. The granite ridge is in the same location as gravity profile 2, with the granite uplifted to underlie the Karoo layer. The thick layer of West Rand Group on either side of the ridge corresponds to the 2 gravity highs observed in profile 3. On the eastern section of profile 3 a second ridge of granite is modelled corresponding to a second smaller gravity low. This granite ridge is uplifted by normal faults D observed in profile 2 and Fault E. A thin layer of West Rand Group sediments overlies the second granite ridge.

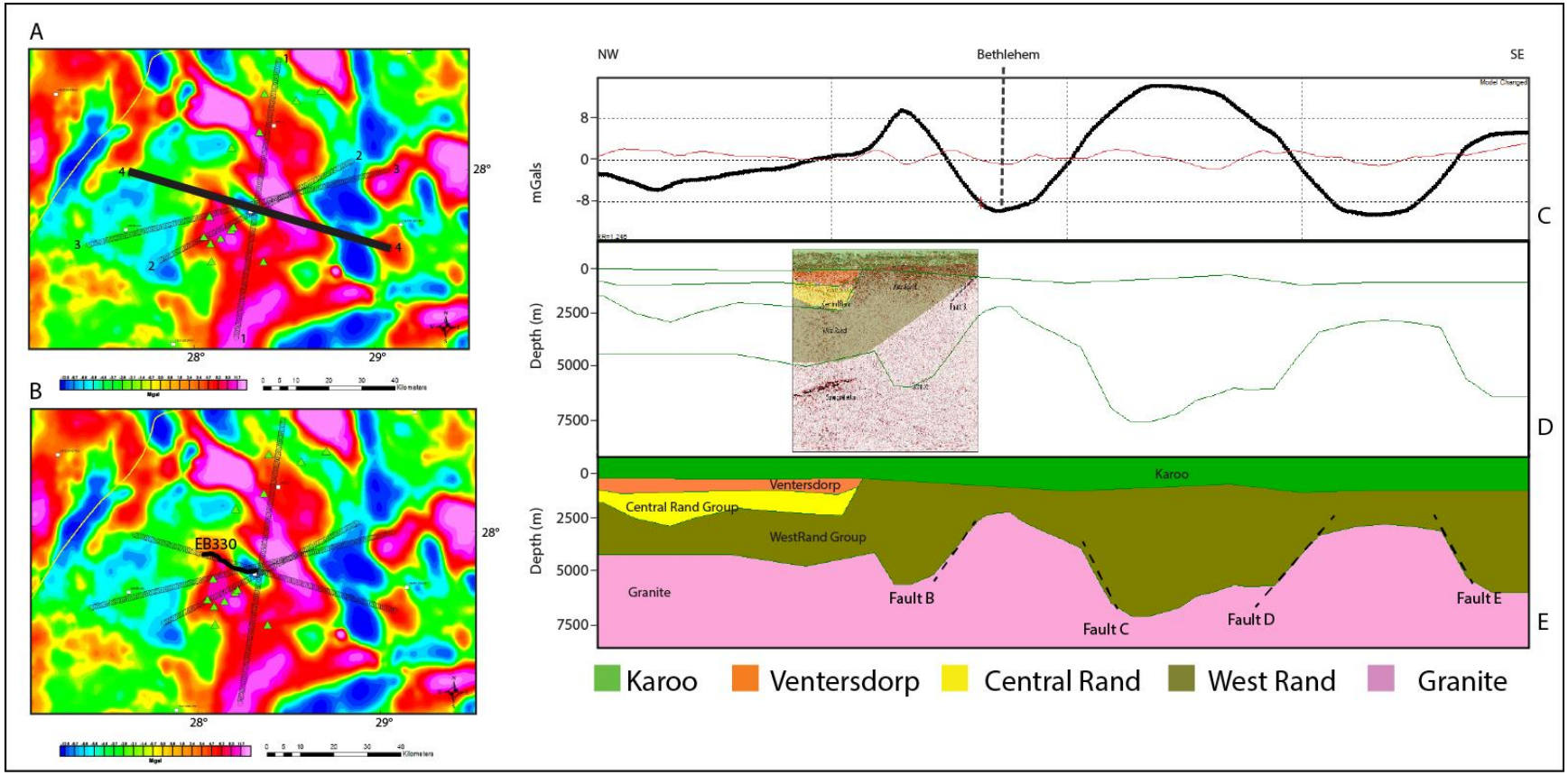


Figure 5.16 Location of gravity profile 4 overlain on the residual gravity map of Bethlehem (A). Location of seismic section EB330 which corresponded with the gravity profile (B). First panel (C) shows 2D gravity profile with observed gravity anomaly and calculated gravity anomaly of model (thin black line). Second panel (D) shows correlating seismic sections used to constrain model. Third panel (E) shows a 2D gravity model corresponding to the calculated gravity profile in first panel.

Gravity profile 4 shows a northwest - southeast profile crossing over both the south western and north eastern regions of the Bethlehem study area. Only the north western side of the profile has a seismic section to constrain modelling. The Karoo and Ventersdorp and Central Rand layers of the 2D gravity model corresponds fairly well to the seismic section interpretation. This shows a thick Karoo layer with a thickness of approximately 2 km – 1.5 km. The Ventersdorp layer is very thin, which eventually pinches out towards the northwest. The Central Rand layer has a thickness of 800 m. The Ventersdorp and Central Rand Group create a contact with the West Rand Group. Similar to profile 1, 2 and 3 the 2D model shows an undulating West Rand Group – basement contact compared to that of the seismic section which showed a fairly horizontal homogeneous layer with an unclear interface. Fault B and C have uplifted the granite, creating a granite ridge, with thick West Rand Group sediments on either side. The granite ridge is in the same location as gravity profile 2 and 3. In this profile the granite has not uplifted to the extent of profiles 2 and 3 where the basement has been uplifted to underlie the Karoo layer. The West Rand Group also appears to be much thicker than that of the other profiles. Fault D and E observed in profile 3 are also observe in this profile. Again the ridge created by fault D and E is much deeper and overlain by a thicker layer of West Rand Group rocks. Gravity profile 4 shows a much thicker West Rand Group layer and the uplift of the granite is not to the same extent compared to that of the other profiles. Profile 4 covers a larger area of the gravity high to the south east of fault C. The profile shows a large thick and deep layer of West Rand Group which corresponds to the high gravity reading.

To summarize the results of Section 5.1 and 5.2, figure 5.17 shows the location of faults. Faults B and C were interpreted seismic sections and gravity forward models. Faults D and E were interpreted in 2D forward models only. Faults B - E shows north northwest trending normal faults. The location and trend of faults B - E corresponds to the change in gravity from low to high and follows the same trend as the gravity anomaly. Fault B and C create a ridge of granite interpreted in both seismic and 2D forward models which underlies the Karoo Supergroup. The magnetic map shows faults B and C correspond to a magnetic high. The magnetic high surrounds the granite ridge which underlies the Karoo Supergroup. Fault D and E only interpreted in 2D forwarding modelling creates a second deeper granite ridge overlain by West Rand Group sediments. These 2 granite ridges correspond to the gravity low readings. A lithological contact is formed as the Ventersdorp Supergroup, Central Rand Group and West Rand Group are tilted to the west. The Ventersdorp and Central Rand Groups are pinched out and are truncated by the West Rand Group.

To create a better view of the faults interpreted in the seismic sections. The seismic sections were imported into google earth. This helped to understand the basement uplift. Figure 5.18 shows the south western and north eastern regions of the Bethlehem study area. The south western regions shows an area of low gravity. In this area the basement is deeper as well as the West Rand Group, Central Rand Group and Ventersdorp overlying the basement respectively. The north eastern region shows an area of high gravity. In this area we see a very shallow basement with only a thin layer of West Rand Group overlying the basement. The basement has been uplifted in the area of high gravity. This result has been consistently interpreted from the 2D seismic lines and 2D gravity forward models.

The results presented above were used to create the 3D geological model. The 3D geological model is presented on chapter 6.

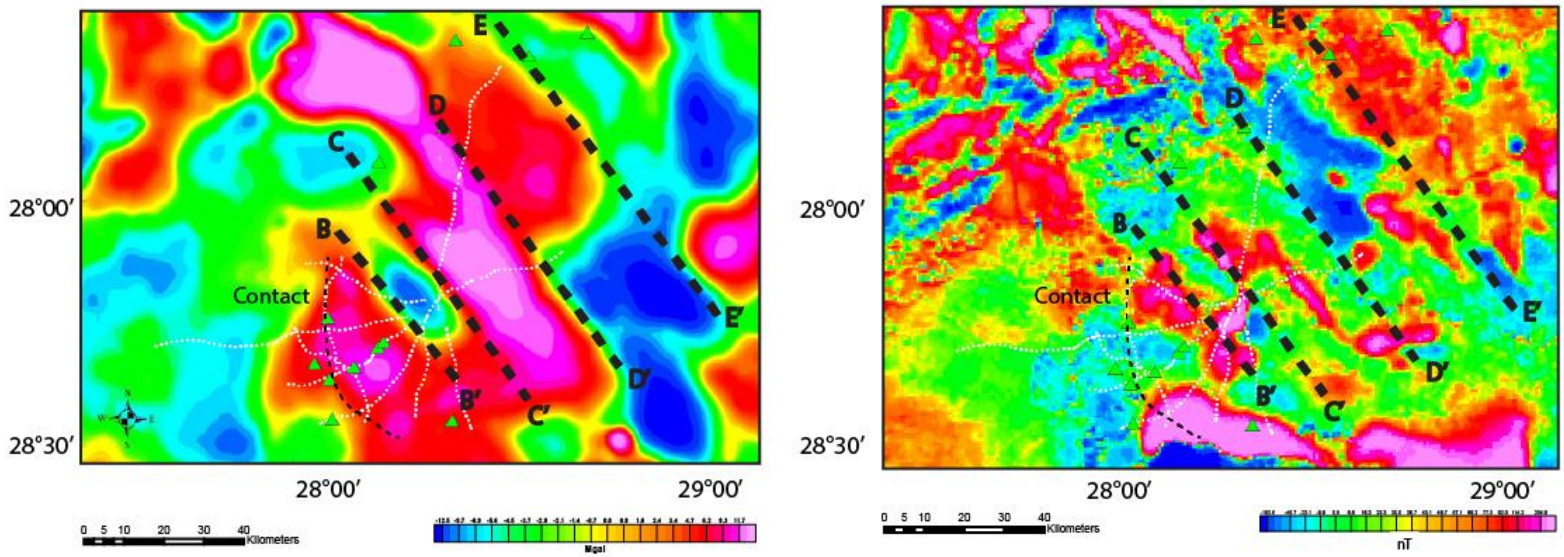


Figure 5.17 Location of seismic lines fault B and C and 2D gravity model faults C – E overlain on the residual gravity map (left) and Magnetic map (right). Green triangles are borehole locations and white lines are seismic line locations.

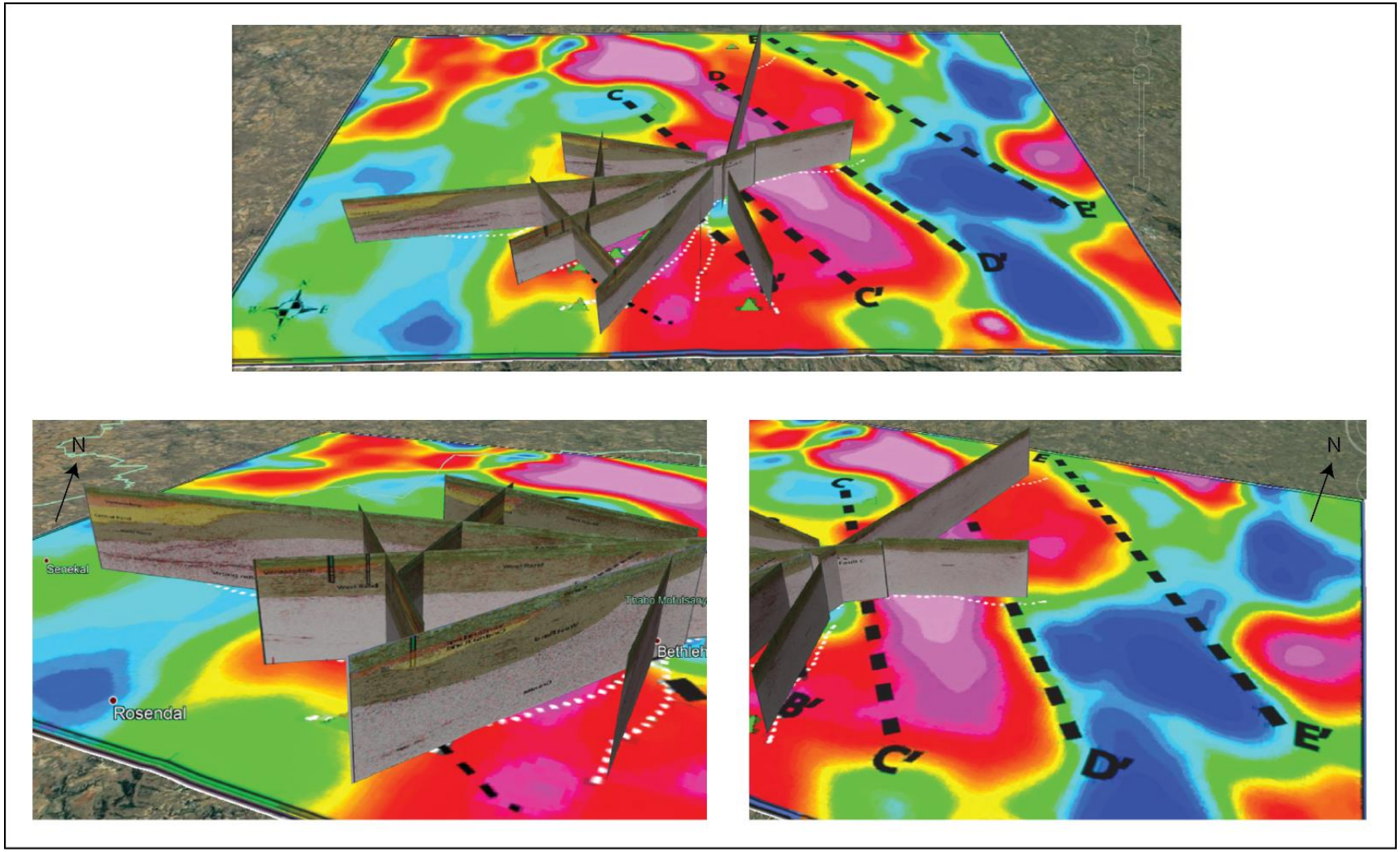


Figure 5.18 Google earth image of all seismic sections (top), the south western region (left) and north eastern region (right). Residual gravity map and Fault B, C shows how seismic section interpretation corresponds to observed data. Fault D and E interpreted only in 2D forward modelling and not in seismic sections are also drawn on map

6 3D Modelling

The creation of the 3D geological and gravity models presents the final integration of the seismic, gravity and borehole data for this study. The geological model focuses on the interpreted seismic data, with picked horizons imported into Leap Frog Geo to constrain each lithological boundary. The gravity model uses the geological model as a constraint along with the gravity grid.

6.1 3D Geological Model

Five volumes were created representing the lithological layers; Karoo Supergroup, Ventersdorp Supergroup, Central Rand Group, West Rand Group and basement suite. The geological model was created in Leapfrog Geo. The interpreted 2D reflection seismic sections are displayed in Figure 6.1. Each horizon was imported as a polyline and formed the wireframes for each geological volume. Faults interpreted from the 2D reflection seismic sections were recreated in Leapfrog Geo (Figure 6.1).

To create the five geological volumes, each wireframe defined a contact between two volumes. Interpolation between wireframes constrained the volume. In areas where there were limited or no data points, the interpolated surface volumes had greater uncertainty and unrealistic surface geometries. To better constrain these areas additional polylines were created to form reasonable geometries, which supported the 2D seismic interpretation and 2D gravity forward modelling.

3D surfaces were created for each contact during the interpolation process of each wireframe. During this process a number of iterations were done as constant refinements were required to create a realistic geological surface.

Faults created in Leap Frog Geo are not an accurate representation of what is interpreted in seismic sections. However, they are important as the faults show orientation and uplift of the West Rand Group and basement. Fig 6 shows the location and orientation of Faults B and C interpreted in seismic sections.

To keep a consistent constraint on the geological model the 2D forward model was not used during the model creation, as it does not cover a large enough area to constrain all the 2D seismic lines. This meant the undulating surface of the West Rand Group - basement contact is not shown in the 3D geological model. The 2D forward model was used as a constraint on the 3D gravity forward modelling.

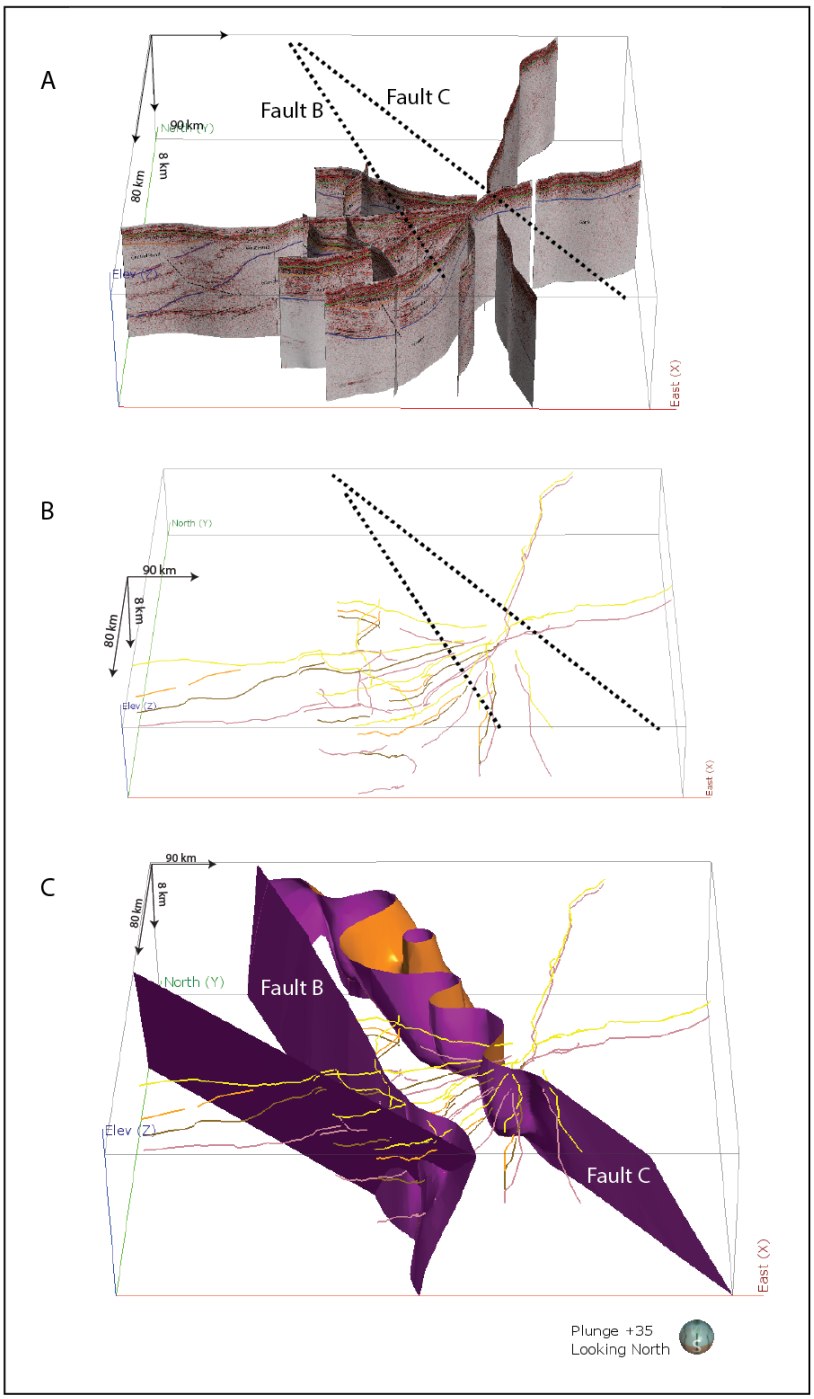


Figure 6.1 A 3D view of interpreted seismic lines, looking north and plunging at 35°shown in image (A). The imported seismic horizons which define the lithological boundaries. Key; pink – granite, brown – Central Rand, Orange – Ventersdorp, yellow – Karoo shown image (B). 4 Major faults interpreted from the 2D seismic lines and redrawn in Leapfrog Geo faults B and C shown in image (C).

6.2 Geological Volumes

The five geological models are most constrained on the south western and north eastern sections of the model. The south eastern section has very little data. Additional polylines were created to constrain the interpolation to match that of the south western and north eastern sections. The northwestern section has no seismic data and therefore polylines were created to extend the geological layers to fit the boundary. The depth of the volume was made the same as that of the seismic sections. The northwestern section was not used for the main interpretation. The Karoo volume is not shown as it covers the entire Bethlehem region.

6.2.1 Basement volume

Seismic interpretation defines the top of the basement as the West Rand Group – basement contact (Figure 6.2). As discussed in chapter 4 and 5 this contact was difficult to define due to the lack of a boundary reflector. The basement volume has a depth of 5 km in the southeast and shallows to 2 km in the northeast. The basement has one major uplift which elevates the north eastern section of the model by approximately 4 km. The basement is at its shallowest between fault B and fault C, creating a narrow ridge striking north northwest. It gradually gets deeper in a south eastern direction. Therefore the elevation of the basement in the north eastern half of the volume is several kilometers shallower than that of the south western half. Figure 6.2 displays the wireframes for the upper contact of the basement volume and the output volume of the basement layer.

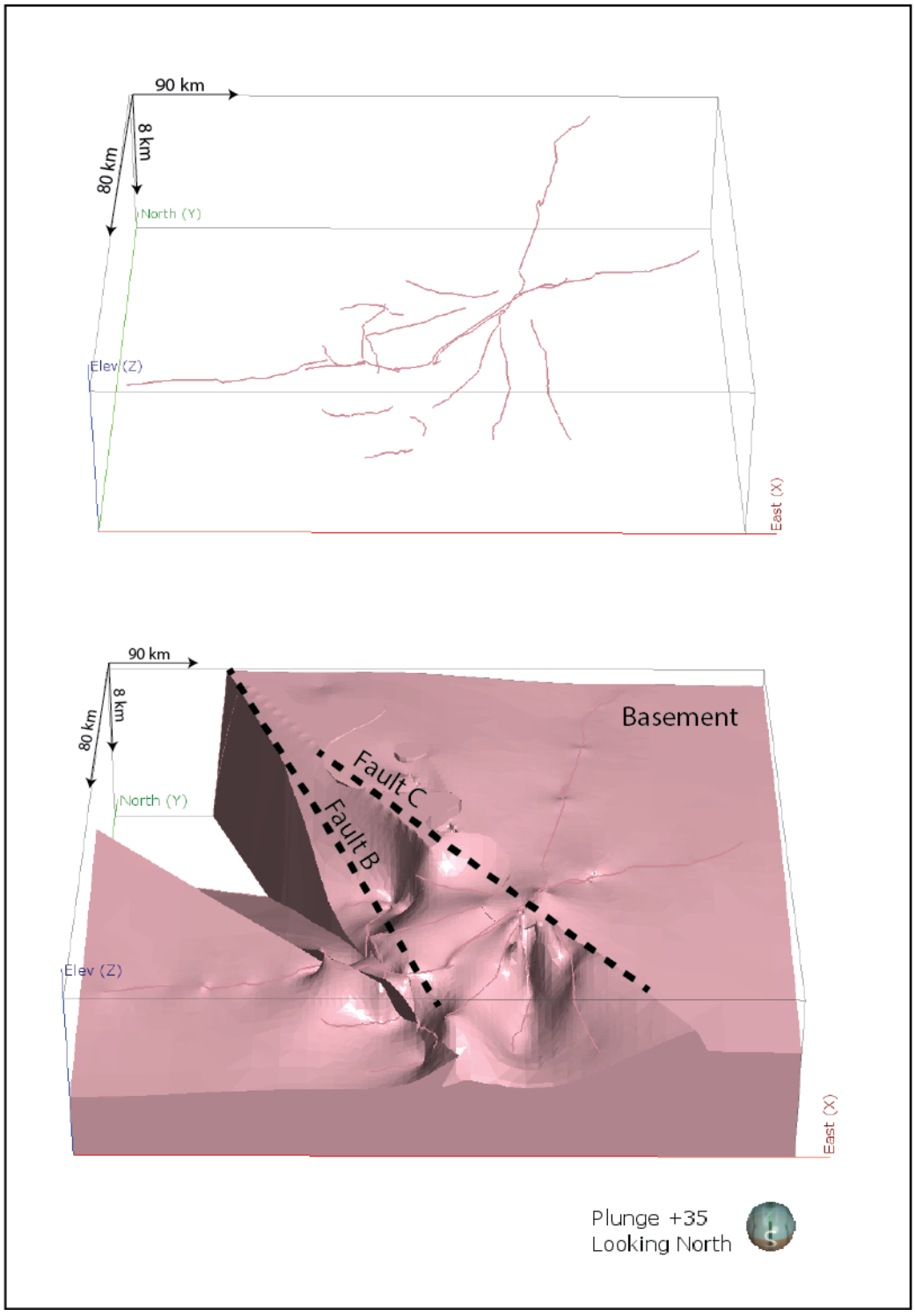


Figure 6.2 Model of basement volume. Upper contact wireframe (above). Pink lines represent the unconformable lithological contacts. Interpolated volume (below) with faults B and C labelled in dashed lines.

6.2.2 West Rand Group Volume

The upper contact displayed in Figure 6.3 is defined by the contact between the West Rand Group and Central Rand Group, which is only present in the south western section of the volume. In the north eastern section of the model the upper contact is defined as the West Rand Group – Karoo contact. The West Rand is thickest in the south western section approximately 4 km. The north eastern section of the volume is less than 1 km thick and uplifted by fault B and C, underlying the Karoo Supergroup.

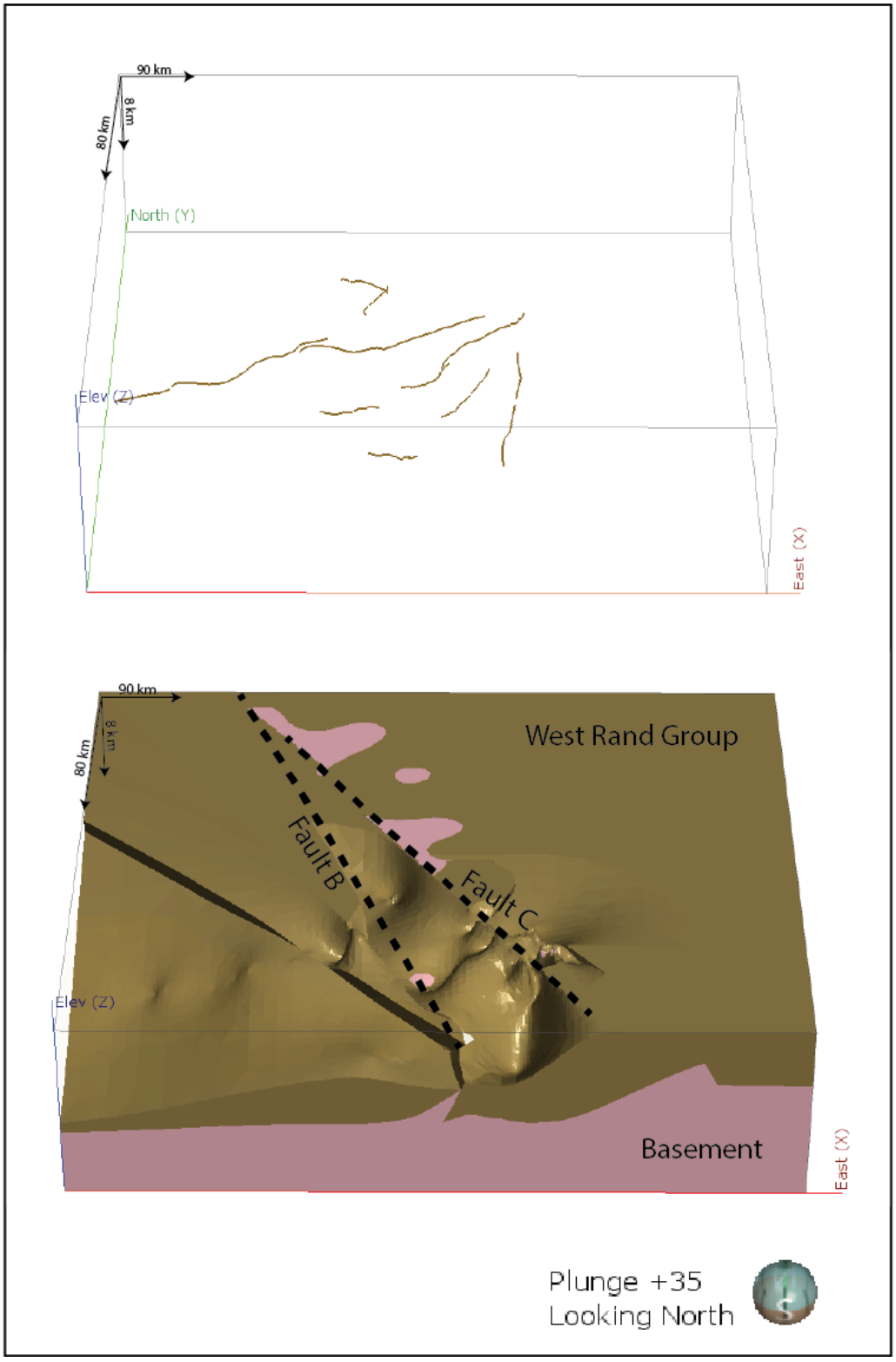


Figure 6.3 Model of West Rand Group volume. Upper contact wireframe of West Rand Group and Central Rand Group (above). Brown lines represent the unconformable lithological contacts. Interpolated volume (below) with faults shown in dashed lines.

6.2.3 Central Rand Group Volume

The Central Rand Group was only interpreted on the south western section of the volume. The base of the Central Rand Group volume is defined by the contact of the West Rand Group. The upper contact is defined by the contact between the Ventersdorp Supergroup and the Central Rand Group. The Central Rand Group is deepest at the south western corner of the volume and shallows moving toward the north east. Figure 6.4 shows the upper contact wireframe and interpolated volume.

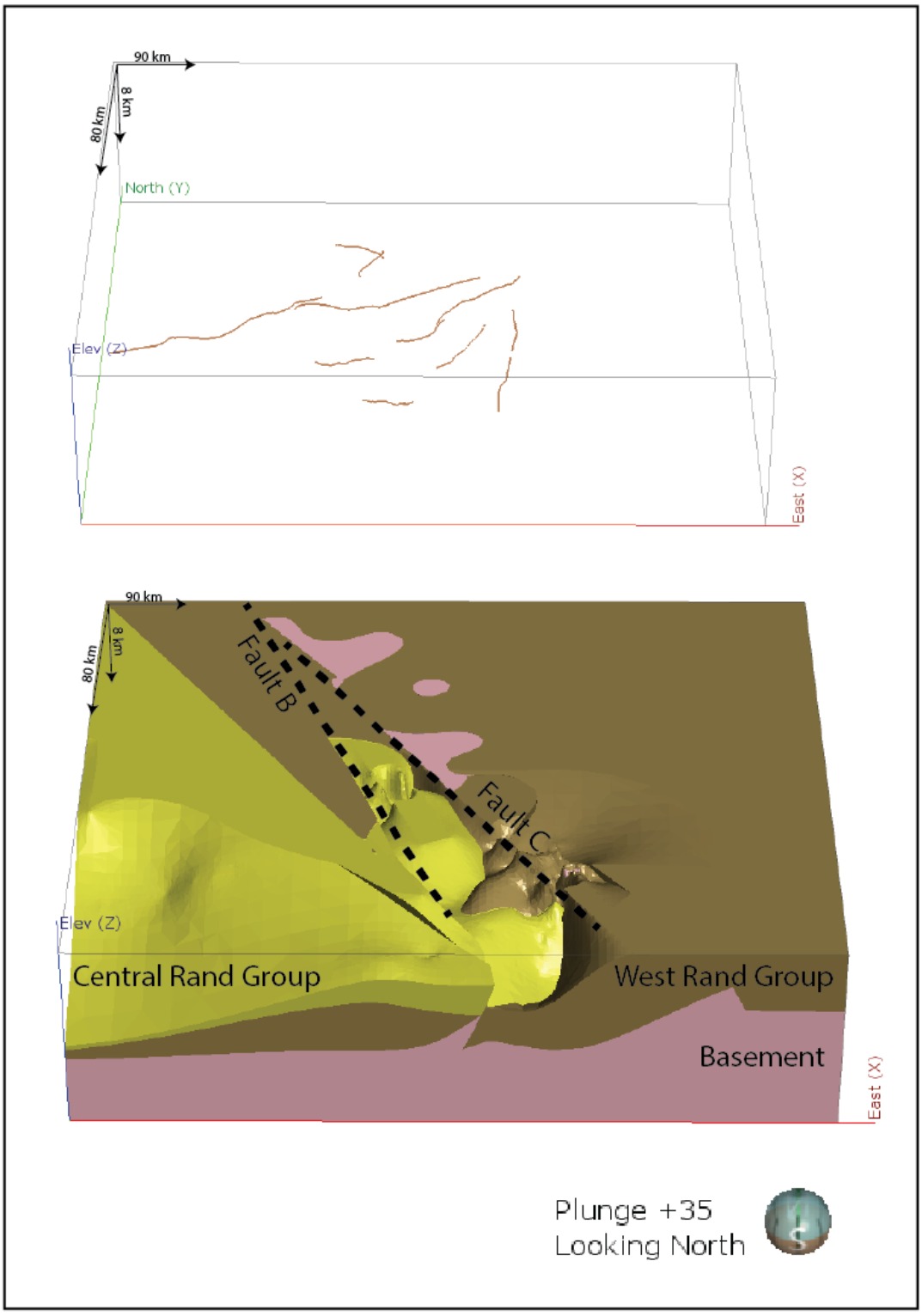


Figure 6.4 Model of Central Rand Group volume. Upper contact wireframe of Central Rand Group and Ventersdorp (above). Brown lines represent the unconformable lithological contacts. Interpolated volume (below) with faults shown in dashed lines.

6.2.4 Ventersdorp Supergroup Volume

The Ventersdorp Supergroup is the smallest layer in the volume in the Bethlehem region and shares a similar geometry to the Central Rand Group (Figure 6.5). The base contact is defined by the Central Rand Group Volume. The upper contact is defined by the contact between the Karoo and the Ventersdorp. The Ventersdorp volume only occurs in the south western section of the volume. The Karoo Supergroup truncates the Ventersdorp in several areas, this was interpreted in the 2D seismic sections. The fairly thin Ventersdorp layer gradually shallows from the south western corner of the volume towards the north east until it is truncated by the Karoo.

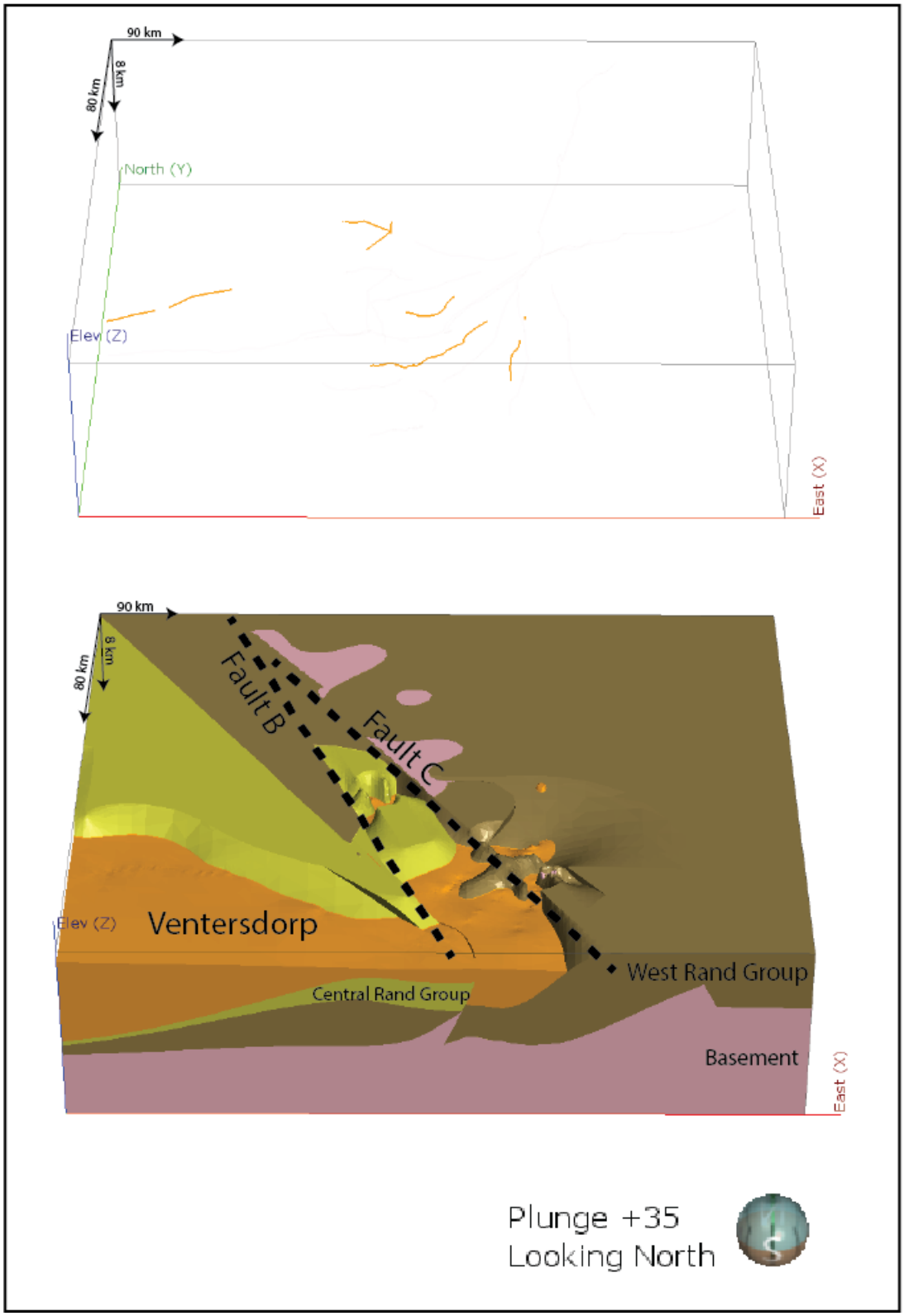


Figure 6.5 Model of Ventersdorp volume. Upper contact wireframe of Ventersdorp and Central Rand Group (above). Brown lines represent the unconformable lithological contacts. Interpolated volume (below) with faults shown in dashed lines.

6.3 3D Gravity Model

The 3D gravity model was created in PyGMI. The residual gravity map of the Bethlehem region was imported into PyGMI and was used as the observed gravity dataset see Figure 6.6. Each lithology required a density which is described in Chapter 3 i.e. basement – 2.67 g/cm^3, West Rand Group – 2.91 g/cm^3, Central Rand Group – 2.61 g/cm^3, Ventersdorp Supergroup – 2.88 g/cm^3 and Karoo Supergroup – 2.55 g/cm^3. The geological model was imported as a block model into PyGMI and used to integrate the seismic interpretation with the gravity interpretation.

The geological model was sectioned into 104 horizontal east - west 2D profiles. A few of these profiles are shown in figure 6.6 and 6.7. Each profile showed the model and its calculated gravity signal compared to that of the observed residual gravity dataset. The profiles are modified by selecting a lithology and drawing the geometry which would best fit the original gravity dataset.

Care was taken to modify with restraint so as to maintain the integrity of the interpreted seismic data, yet still create a geologically correct model. This was an iterative process that required a number of modifications and refinements.

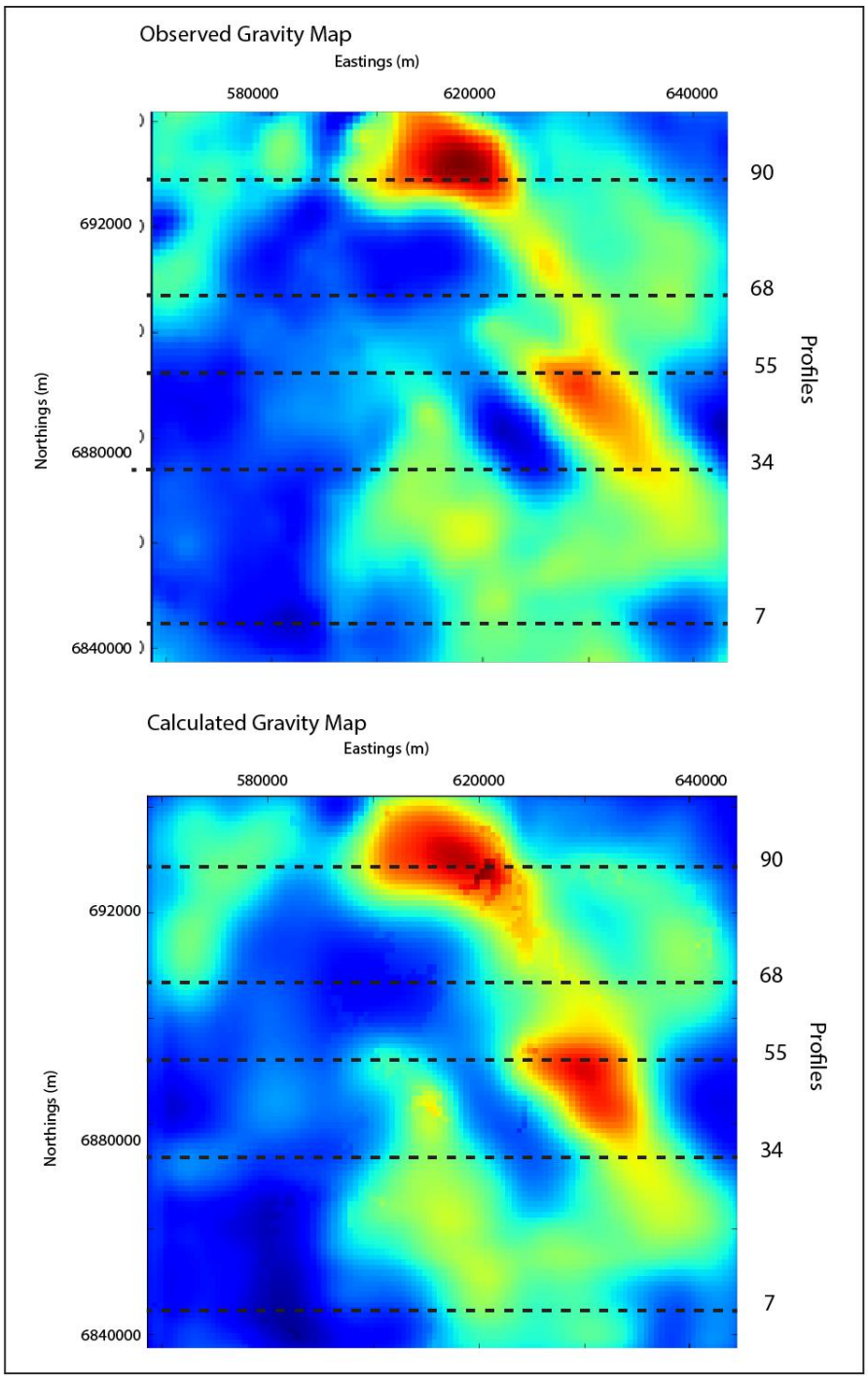


Figure 6.6 Map of observed gravity (above) and calculated gravity from forward model (below). Lines 7, 68, 55, 34, and 90 are the locations of profiles shown in figure 6.7.

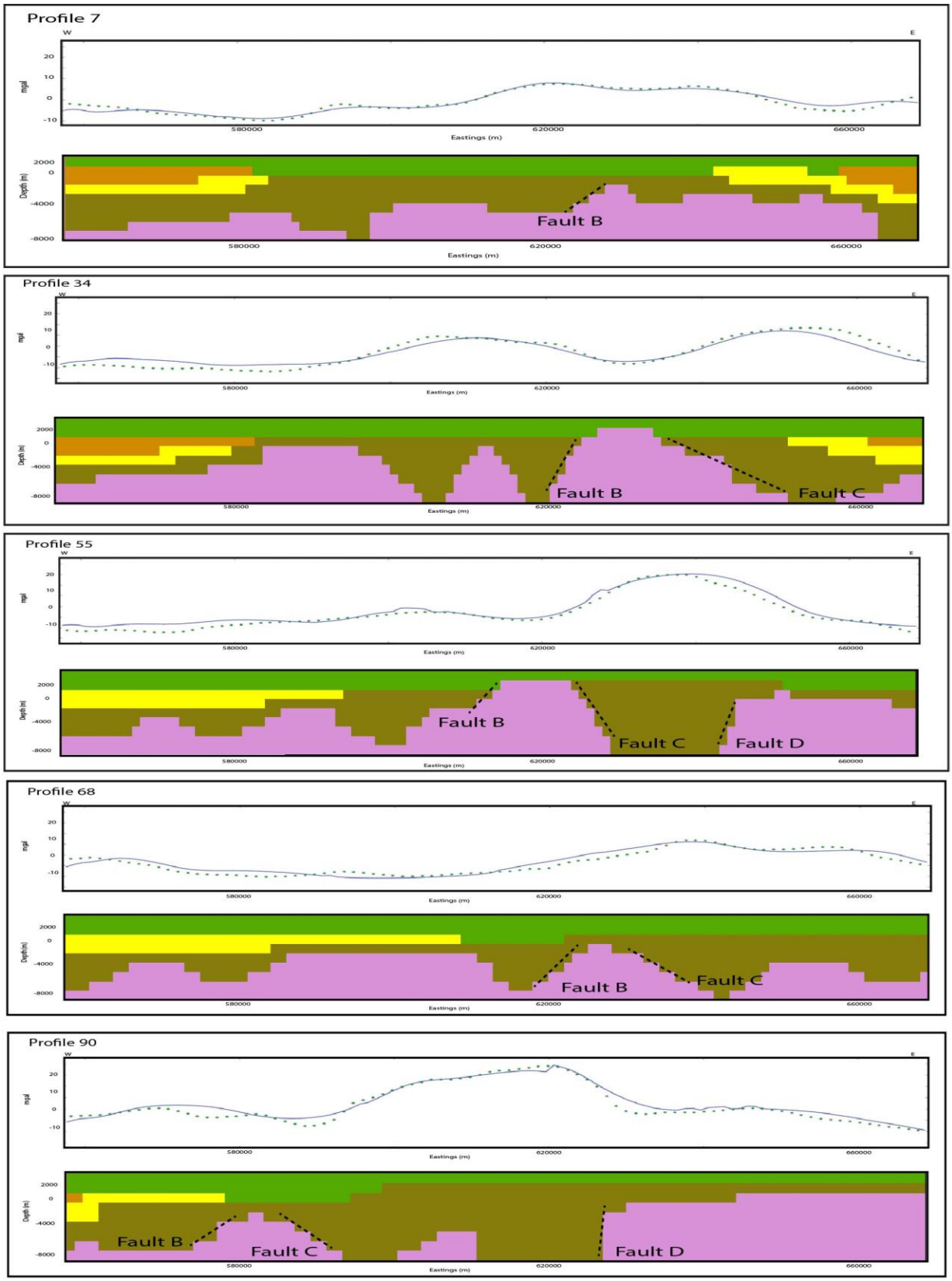


Figure 6.7 2D profiles from the 3D gravity model. Green dotted line shows observed residual gravity and blue line represents calculated gravity from model. Faults B, C and D correspond to seismic and 2D forward modelling interpretation.

6.4 Gravity Volumes

The gravity model has a depth of 8 km to be consistent with the 3D geological model and seismic sections. The densities of each lithology was consistent with the 2D gravity forward models. Similar to the geological model, the gravity model is mainly constrained in the south western and north eastern regions from seismic sections and borehole data.

The Karoo Supergroup overlies all 4 layers in the gravity model. The thickness of the layer is fairly constant, approximately 1.5 km. The Karoo layer is less thick in the central section of the Bethlehem study area surrounding the two ridges formed by the faults B, C and D. The layer also thickens in the ridge formed by these faults. The 1.5 km thickness of the layer is consistent with the interpretation of the 2D seismic lines and borehole data.

6.4.1 Basement Volume

The main structure seen in the north eastern section of the basement volume is a ridge created by fault B and C, with a northwest strike see Figure 6.8. Between faults C and D the basement layer is very deep and goes below the 8 km depth of the model. Normal faults B, C and D have uplifted the basement to form 2 ridges. These ridges were interpreted in the 2D seismic sections, 2D forward models and the 3D geological model. The low density of the basement rock would account for the lowest gravity readings when the basement is very shallow. This is consistent with the residual gravity dataset and profiles 34, 55 and 68 show the lowest gravity readings coinciding with the basement being very shallow.

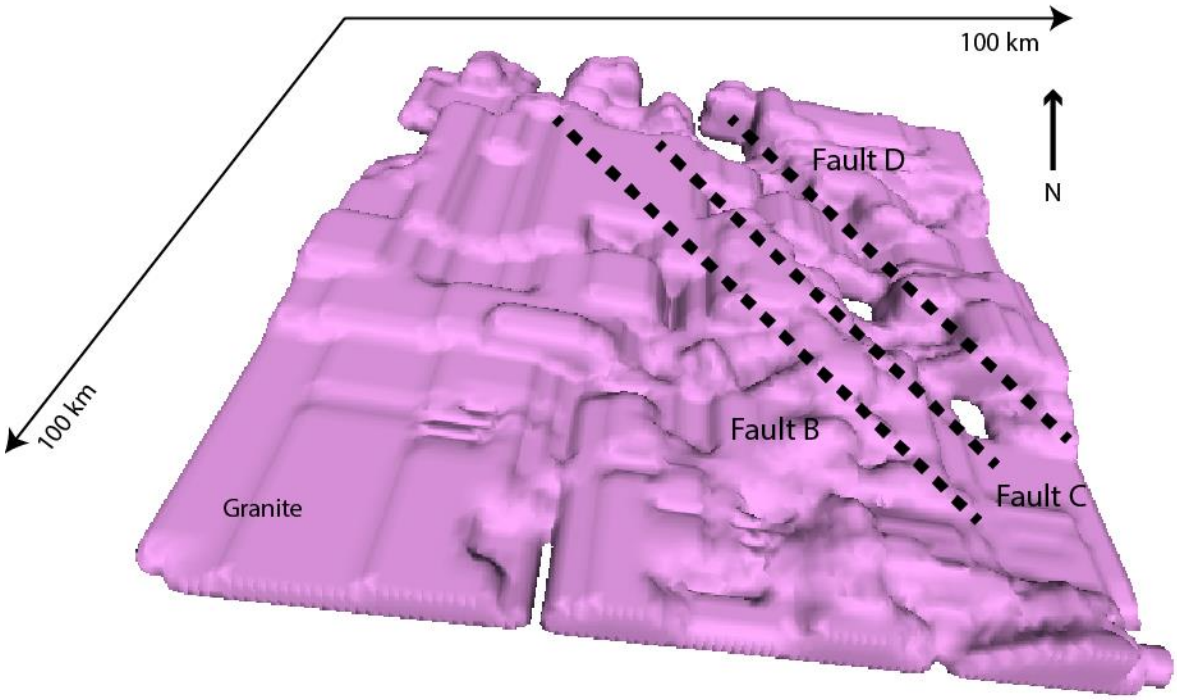


Figure 6.8 3D Model of basement volume. Dotted black lines show faults B, C and D.

6.4.2 West Rand Group Volume

The West Rand Group shows a fairly level surface. Where the top of the West Rand is deepest in the south western section of the model at approximately 7 km. In the north east region the West Rand Group is shallowest at a depth of 2 km and underlies the Karoo Supergroup. Faults B and C create a basement ridge which truncates the West Rand Group on the west of Fault B and east of Fault C. The thickest part of the West Rand Group, approximately 8 Km, is between Faults C and D. This thick layer of West Rand Group corresponds to the highest gravity reading in the Bethlehem study area. The West Rand Group has a high density compared to the basement, which would give a high gravity reading. The density and thickness of the West Rand Group layer next to the low density basement, gives a gravity reading that is consistent with the low-high-low gravity readings that are observed in the residual gravity dataset.

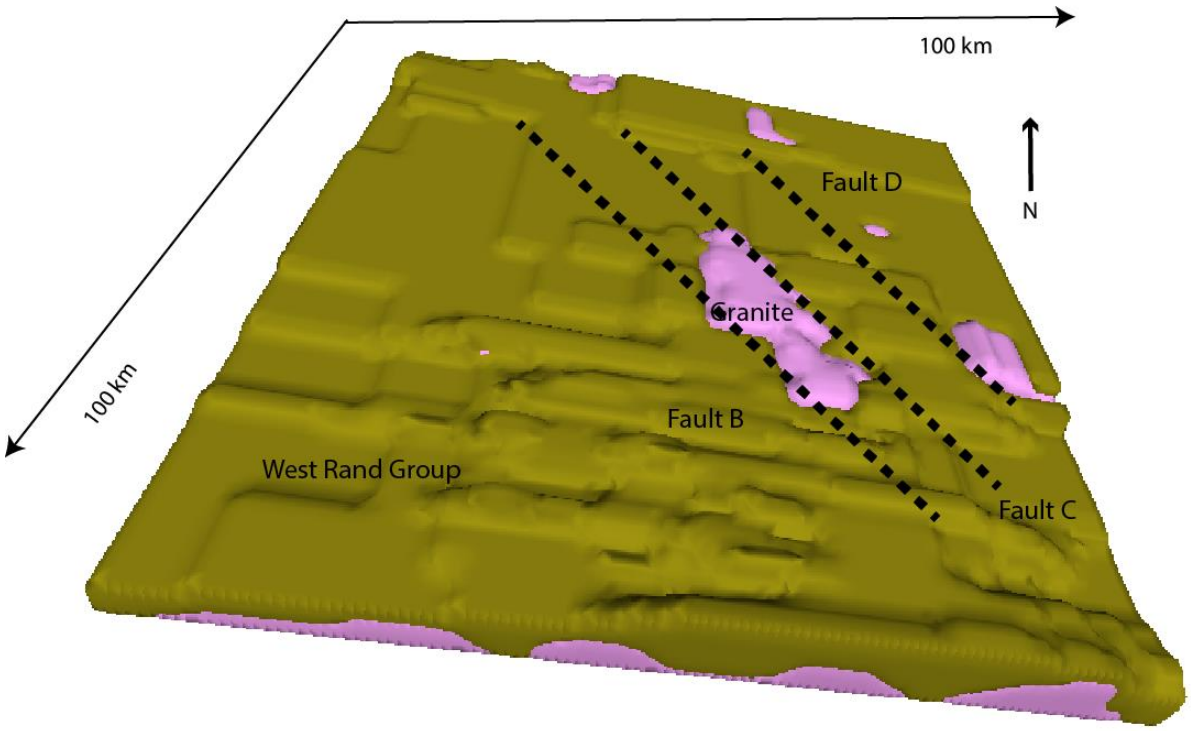


Figure 6.9 3D gravity West Rand Group volume with underlying basement (pink). Dotted black lines shows faults B, C, and D.

6.4.3 Central Rand Group Volume

The Central Rand Group occurs mainly on the western side of the model and partly on the south eastern side of the model. The layer is deepest on the western side and gradually shallows towards the east. This is consistent with the 2D seismic sections and 2D gravity forward models. The south eastern and north western section of the model shows a small deposition of Central Rand Group. No seismic or borehole data were available in this area and therefore less constraint on the extent and thickness of the Central Rand Group was available. A lithological contact between the Central Rand Group and West Rand Group is observed towards the center of the model. This is consistent with the 2D seismic interpretation. At this point the Central Rand Group is tilted and pinched out by the Karoo Supergroup.

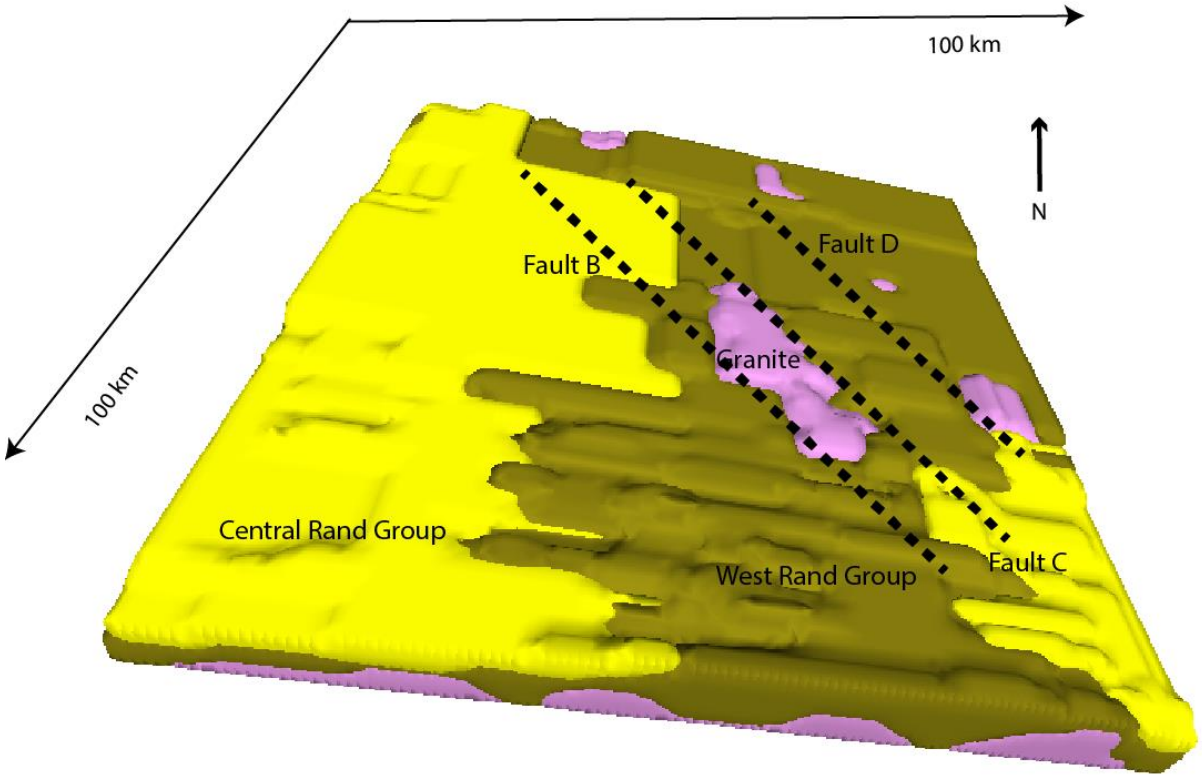


Figure 6.10 3D gravity model of Central Rand Group volume (yellow), with underlying West Rand Group (brown) and basement (pink).

6.4.4 Ventersdorp Supergroup Volume

The Ventersdorp Supergroup covers the smallest area. Only occurring on the western and south eastern edges. The Ventersdorp layer is very thin, less than 1 km thick. Similar to the Central Rand Group, the Ventersdorp Supergroup is tilted towards the east and is pinched out and truncated by the Karoo Supergroup.

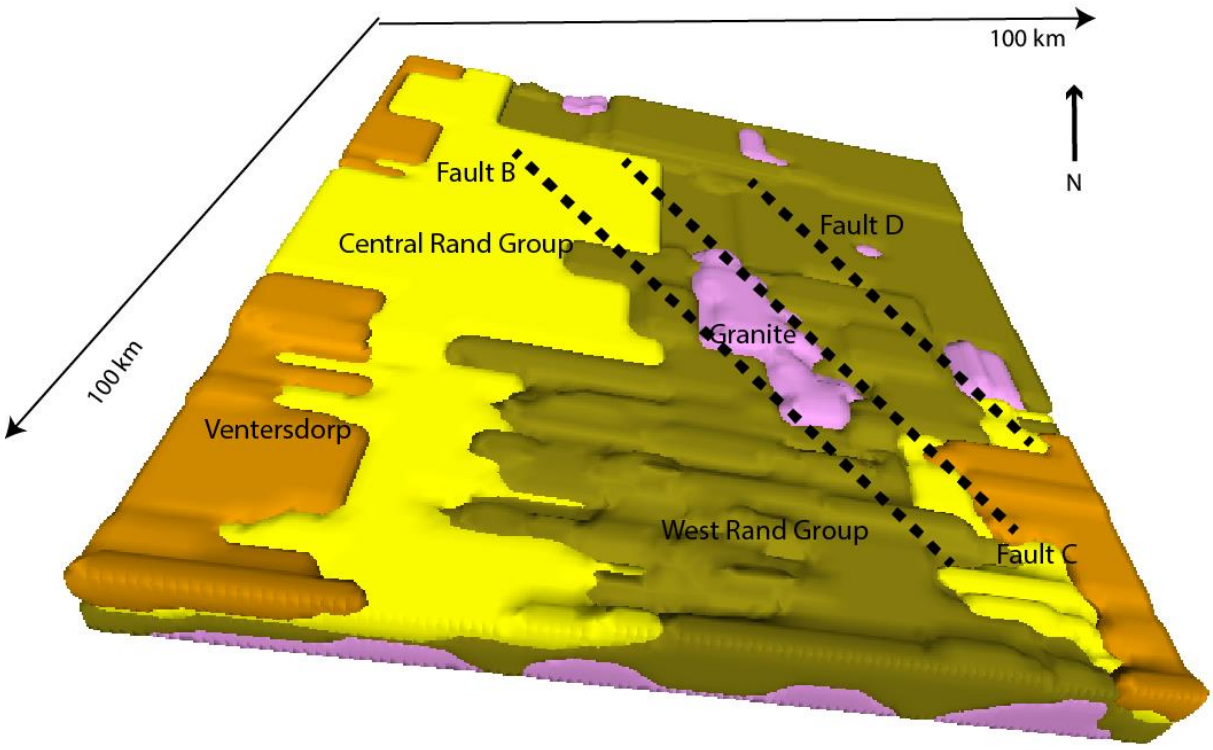


Figure 6.11 3D gravity model of the Ventersdorp Supergroup (orange), with underlying Central Rand Group (yellow), West Rand Group (brown) and basement (pink).

7 Discussion

This study investigates the Bethlehem sub-basin through integration and 3D modelling of several geophysical datasets. A 3D geological model and 3D gravity forward model were created through analysis of 13 boreholes, 12 2D reflection seismic sections, regional magnetic qualitative analysis and 2D gravity forward modelling. The integration of data included borehole depths that constrained interpretation of seismic reflectors for each lithology. Large scale magnetic interpretations integrated with borehole data constrained dolerite sills that were picked on 2D seismic sections. 2D seismic interpretations were used to constrain the depth of each lithology unit in the 2D gravity forward models. As well as constrain the surfaces created for the 3D geological models.

7.1 Stratigraphy of the Bethlehem study area

The south eastern edge of the Witwatersrand basin is overlain by the Karoo Supergroup. Boreholes shows the major stratigraphic units present in the Bethlehem study area are the basement, West Rand Group, Central Rand Group, Klipriviersberg Group and Karoo Supergroup.

The basement – West Rand Group interface was difficult to interpret in seismic sections. The top of the basement was determined by the change in amplitude of reflectors from closely spaced strong reflectors to a homogeneous transparent package. The basement – West Rand Group interface differed considerably in seismic sections and 2D and 3D gravity forward models. The final 3D forward model shows an undulating basement – West Rand Group interface, controlled by 4 normal faults (Figure 5.17 and Figure 6.8). Lastly an interesting feature observed in seismic sections is a strong reflector within the basement layer. The cause of this strong reflector is unknown and could not be correlated with modelling and interpretation from this study. However, it is fairly consistent and continuous in several seismic sections in the south western area of the Bethlehem study area. These strong reflections occur at the same depth, amplitude, and orientation. A reflection at this depth requires a large reflection coefficient. Some suggestions for this reflection could be deformation of the basement or an intrusion. Further research and observation into this anomaly would need to be carried out to provide more information and interpretation of this feature.

The West Rand Group was interpreted as a package of closely spaced reflectors on seismic sections. The south western region of the study area showed a distinct close reflector package which was interpreted as the West Rand group. The north western region of the study area had no boreholes that drilled into the West Rand Group. As well as no distinctive reflector package that is associated with the West Rand Group. 2D gravity forward models were used to constrain a thin layer of West Rand Group rocks approximately 1 km

thick that underlies the Karoo Supergroup in the north eastern region. 3D gravity forward modelling showed an undulating basement – West Rand Group interface.

The Ventersdorp Supergroup and Central Rand Group interface were only interpreted in the south western area of the seismic sections. Both lithologies are tilted in an easterly direction and tends to pinch out and truncated by the Karoo Supergroup. The 3D gravity forward model which covered a larger area than the seismic sections showed the Ventersdorp Supergroup and Central Rand Group also deposited on the eastern section of the Bethlehem study area. These thin layers are tilted towards the west and pinch out as it is truncated by the Karoo. Seismic and gravity forward modelling is consistent in that Ventersdorp Supergroup or Central Rand Group is not present in the central and northern section of the Bethlehem study area.

The Karoo Supergroup had the strongest reflectors and showed consistently through all 12 seismic sections and 13 boreholes with a depth range from 1 km – 1.7 km. This depth was also consistent in 3D gravity forward modelling. The Karoo Supergroup was thinner in sections where Ventersdorp Supergroup and Central Rand Group where present and thicker in areas where the basement and West Rand Group were underlying the Karoo. Seismic sections also interpreted dolerites within the Karoo. These dolerites where constrained by boreholes and showed dolerite sills scattered throughout the Bethlehem study area.

Transvaal and thicker units of the Witwatersrand Supergroup and Ventersdorp Supergroup could have been deposited in the Bethlehem area. Through uplift and deformation of the basement and Witwatersrand Supergroup, erosion has removed these layers. The lack of the Dominion Group is consistent with the interpretation of the south eastern section of the Vredefort Impact as a shallowing basement, no Dominion Group and thinning Witwatersrand Supergroup which is observed in (Molezzi, 2017).

7.2 Structural Features

The structural features of the Bethlehem study are illustrated in Figure 7.1 and 7.2. Four faults B, C, D and E, created 2 granitic ridges and horst and graben structures. Thus preserving thick successions of West Rand Group rocks within the grabens and uplifting granite ridges close to surface.

Figure 7.1 presents a chart showing a timeline of deposition of the Witwatersrand basin and how the interpretation of the Bethlehem study area correlates with it. Figure 7.1 also shows tectonic events from literature that have occurred in the Witwatersrand basin.

Figure 7.2 shows a diagram of faults B to E interpreted in the Bethlehem study area on a gravity map, magnetic map and a gravity map of a greater area surrounding the Bethlehem study area. This map shows the correlation of faults and the greater Bethlehem area.

Fault B - Interpreted in borehole, seismic and 2D and 3D gravity forward models. A north northwest trending normal fault, dipping to the west and uplifting the basement by 2.5 km to the east.

Fault C - Interpreted in seismic sections and in 2D and 3D forward modelling. Is a north northwest trending normal faulting, dipping to the east. Fault C shows a downthrown West Rand Group layer by 3 km to the east of the fault. This downthrown block of West Rand Group is the thickest layer of West Rand Group rock in the Bethlehem study area.

Fault D – Interpreted only in 2D and 3D forward modelling is a north northwest trending normal fault, dipping to the west, has uplifted the basement by 2km.

Fault E – Interpreted 2D and 3D gravity modelling is a normal fault trending north northwest and dipping east, uplifts granite 2 km to the west of the fault. Created a deeper granite ridge with Fault D.

7.3 3D gravity forward model

The 3D gravity forward model is a 100 x 100 km model created through a combination of all datasets and models used for this study. The model shows a large north northwest granite ridge which was interpreted in seismic sections controlled by fault B and C that underlies the Karoo Supergroup. To the east of this ridge is a smaller granite ridge trending north northwest and is controlled by fault D and E which is deeper and is overlain by West Rand Group rocks. These ridges and valleys create horst and graben structures that correlate with the gravity lows and highs observed in the residual gravity map (Figure 7.2). A thick layer of West Rand Group rocks is preserved in the graben between the 2 granite ridges (faults C and D). This graben trends north northwest and correlates with the gravity high which trends north northwest. Finally the gravity readings on the western section of the Bethlehem study area are lower than the eastern section. This is due to the occurrence of a thicker layer of Central Rand Group rocks and deeper West Rand Group compared to a very shallow and undulating surface of West Rand Group and basement rocks observed in the eastern region.

Fault B and C also show a central uplift of the basement trending north northwest, similar to what is seen in the south eastern section of the Vredefort dome, where granite has been uplifted in a south east direction (Molezzi, 2017). However Bethlehem is 155 km away from the Vredefort dome and more studies focused on the area need to be conducted to determine a correlation and structural relationship between these two structures. Studying a larger area around Bethlehem is required to determine the extent of the Witwatersrand basin units and why some of these units are not continued in the Bethlehem study area such as the Transvaal Supergroup which is discussed in borehole data from McCarthy et al. (2018).

7.4 Timeline of events

For this study no age dating is provided and the timeline for faults cannot be accurately interpreted. Literature of the surrounding area and main Witwatersrand basin are used to determine a timeline of events.

Fault B, C, D and E occur after the deposition of the Ventersdorp Supergroup. Horst and grabens structures are indicative of extensional and rifting environments. The Witwatersrand basin went through major continental rifting during the Klipriviersberg deposition and further extensional collapse during the deposition of the Platberg Group resulting in major graben formation, listric faulting of older structures and second and third order faulting of older rift structures defined by (Dankert and Hein, 2010 and Manzi et al., 2013). This period of time is described by Manzi et al. (2013) as the Hlukana – Platberg Event.

It is suggested from this study that faults B to E occurred during the extensional period and deposition of the Platberg Group. During the Vredefort Impact (2023 Ma) there is a possibility that faults B to E were reactivated, uplifting the basement for a second time which would be consistent with the south eastern section of the Vredefort dome basement modelled by Molezzi, (2017).

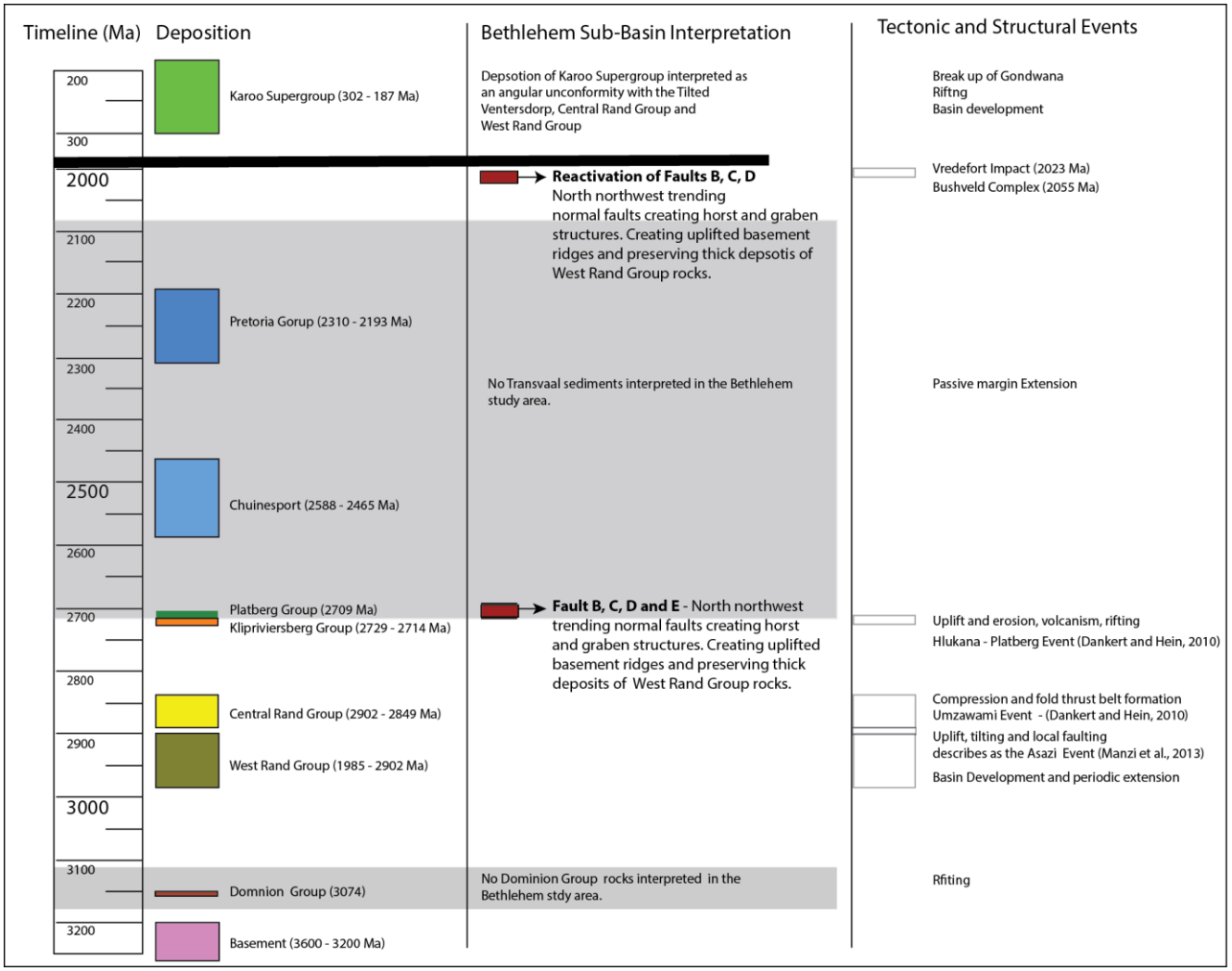


Figure 7.1 Chart showing the deposition of the Witwatersrand basin, Bethlehem tectonic events which have occurred and tectonic events in the Witwatersrand basin in literature. Areas shaded in grey shows deposition that did not occurred in the Bethlehem study area (Johnson et al., 2006; Dankert and Hein, 2010; Manzi et al., 2013; Molezzi, 2017).

7.5 Bethlehem gravity anomaly

The Bethlehem gravity high is approximately 80 km west to east and 100km north to south. The gravity anomaly shows a 90 mgal change in gravity compared to the surrounding areas. The main cause of the Bethlehem gravity high is a northwest trending horst and graben system created by normal faults B, C, D, and E. These faults have created 2 granite ridges described in Section 7.2. These highs and lows are created due to the contrast of higher density West Rand Group rocks surrounding lower density basement granite. The horst and graben system uplifts the granite ridge 2.5 km to underlie the Karoo Supergroup and is surrounded by West Rand Group rocks ranging in thickness from 1 km to 5 km in the graben. The northeast area of the Bethlehem sub-basin has a shallower basement and West Rand Group that underlies the Karoo Supergroup compared to the south western region which has a larger deposit of Central Rand and Klipriviersberg rocks, with a deeper West Rand Group and Basement. The 3D gravity modelling agrees with published work that the Bethlehem region has an uplifted basement as well as a further uplifted NW trending granite ridge which underlies the Karoo Supergroup (Ainslie et al., 1994, Wilsher, 1987; Corner et al., 1989). This study shows that the high gravity reading is produced by a thick layer of West Rand Group rocks preserved in grabens surrounding a horst of basement underlying the Karoo Supergroup. The contrast of dense West Rand Group rocks compared to a less dense basement granite is large enough to produce the change in gravity that is observed. This differs from previous studies that suggest the gravity high is caused by a denser warped basement (Wilsher, 1987; Corner et al., 1989). This study shows by removing the regional gravity a series of north northwest trending faults are observed instead of one main axis from previous literature. Finally this study agrees with the latest theory by Ainslie et al., 1994 that horst and graben structures have preserved thick successions of West Rand Group rock in the Bethlehem area.

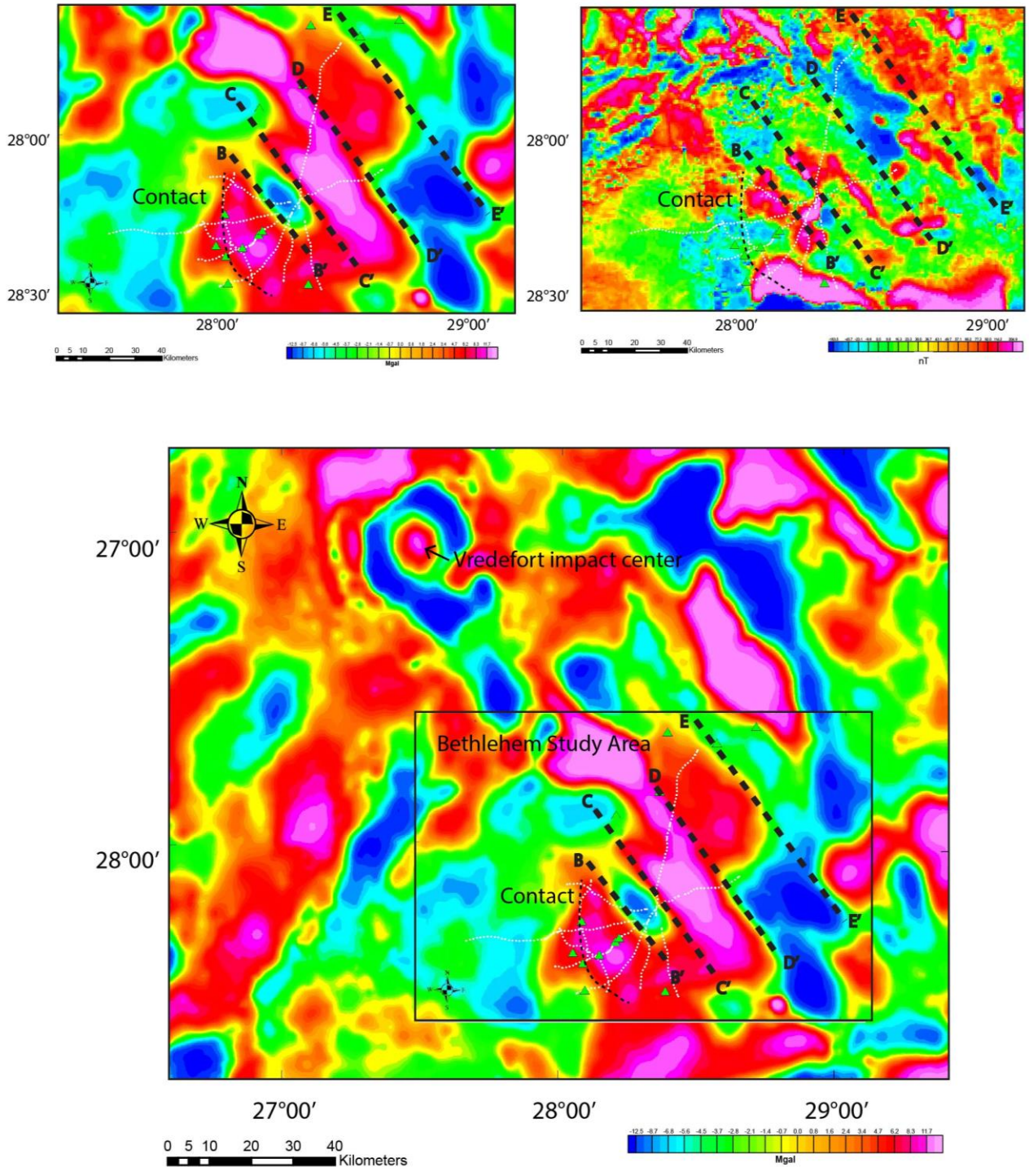


Figure 7.2 Residual gravity map of the Bethlehem study area, TMI map of the Bethlehem study area and a greater region surrounding the Bethlehem study area. Seismic lines shown in (white), boreholes (green triangles) and faults B, C, D and E in dashed white lines.

8 Conclusion

A 3D geological model and 3D gravity model were creating using borehole data, 2D reflection seismic sections, magnetic data and gravity data. These geophysical datasets collected over a period from the1960s to early 1990s were reinterpreted and used to determine the structure and geology of the Bethlehem sub-basin as well as the cause of the Bethlehem gravity anomaly. These geophysical datasets were reinterpreted using the latest software providing a 3D geological and geophysical view of the Bethlehem sub-basin.

Borehole data were used to constrain the depths of lithologies in 12 seismic reflectors. Seismic reflectors were used to constrain lithology depths on 2D gravity forward models as well as depths of lithology surfaces in a 3D geological model. The constant velocity conversion meant a distortion of depth at a deeper level which was taken into account during the interpretation of reflectors. The results of the 3D geological model showed four major faults B, C, D and E. which have uplifted the granite basement forming 2 north northwest trending ridges with uplifted West Rand Group rocks surrounding the granite ridges.

The 3D geological model was used to constrain depth of lithologies in the 3D gravity forward model. The result of the 2D and 3D gravity forward models showed the granite basement has 2 horst and graben structures. A major granite ridge (horst) seen in the 3D geological model underlies the Karoo Supergroup as well as a second granite horst to the east is deeper and overlain by West Rand Group rocks. These horst and grabens are seen in the northern and north eastern sections of the Bethlehem study area which correlate with the gravity highs and lows observed in the residual gravity map. The south western section shows a deeper granite basement which is undulating and is overlain by thicker units of West Rand Group, Central Rand Group, Ventersdorp Supergroup and Karoo Supergroup.

References

Ainslie, L., Andreoli, M.A.G. and Antoine, L.A.G., 1994. Witwatersrand Basin Analysis and Its Uranium Resources Evaluation. Unpublished progress report 1, Earth and Environmental Technology Department, University of the Witwatersrand, Johannesburg, 13.

Antoine, L.A.G. Nicolaysen, L.O. and Niccol, S.L., 1989. Processed and enhanced gravity and magnetic images over the Vredefort structure and their interpretation. Tectonophysics, 171, 63 – 74.

Beach, A. and Smith, R., 2007. Structural geometry and development of the Witwatersrand Basin, South Africa: In: Ries A. C., Butler R. W. H. and Graham R., (Eds). Deformation of the continental crust: The Legacy of Mike Coward, Geological Society, Special Publication, 272, 533-542.

Blakely, R.J., 1995. Potential Theory in Gravity and Magnetic Applications. Cambridge University Press, Cambridge.

Carlson, R.W., Grove, T.L., de Wit, M.J. and Gurney, J.J., 1996. Program to study crust and mantle of the Archean Craton in Southern Africa. EOS, Trans. Am. Geophys. Union, 77(29): 273, 277.

Catuneanu, O., Wopfner, H., Eriksson, P.G., Cairncross, B., Rubidge, B.S., Smith, R.M.H. & Hancox, P.J., 2005. The Karoo basins of south-central Africa, Journal of African Earth Sciences, 43, 211–253

Corner, B., Wilsher, W.A., du Plessis, J.G., Durrheim, R.J., Nicolaysen, L.O. and du Plessis, A., 1986a. Bouguer Gravity Map of the Witwatersrand Basin. Department of Geophysics, University of the Witwatersrand, Joahnnesburg.

Corner, B., Durrheim, R.J. and Nicolaysen L.O., 1986c. The structural framework of the Witwatersrand Basin as revealed by gravity and aeromagnetic data. Extended Abstracts, Geocongress 86, Geological Society of South Africa, 27-30.

Corner, B., Durrheim, R.J. and Nocolaysen, L.O., 1990. Relationships between the Vredefort structure and the Witwatersrand basin within the tectonic framework of the Kaapvaal craton as interpreted from regional gravity and aeromagnetic data. Tectonophysics, 171, 49 – 61.

Corner, B., Niccol, S.L.,Wilshire,W.A. and Durrheim, R.J., 1986b. Aeromagnetic map of the Witwatersrand Basin – total field intensity upward continued by 500 m. Department of Geophysics, University of the Witwatersrand, Johannesburg.

Corner, B. and Wilsher, W.A., 1989. Structure of the Witwatersrand Basin derived from interpretation of aeromagnetic and gravity data. In: G.D. Garland (Editor), Proceedings of Exploration 87, Ontario Geological Survey, Special Volume 3:532-546

Dankert, B. T. and Hein, K.A.A., 2010. Evaluating the structural character and tectonic history of the Witwatersrand Basin. Precambrian Research 177, 1-22.

De Beer, J.H., 2015. (Editor). The History of Geophysics in Southern Africa, SUN MEDIA, Stellenbosch.

De Wet, J.A.J. and Hall, D.A., 1994. Interpretation of the Oryx 3D seismic survey: Proceedings of the XVth CMMI Congress. South African Institute of Mining and Metallurgy 3, 259–270.

Duncan, A.R. and Marsh, J.S., 2006. The Karoo Igneous Province. in The Geology of South Africa, pp. 461-499, eds. Johnson, M. R., Anhaeusser, C. R. & Thomas, R. J. Geological Society of South Africa and Council for Geoscience.

Frimmel, H.E., 2005. Archaean atmospheric evolution: evidence from the Witwatersrand gold fields, South Africa. Earth-Science Reviews 70, 1–46.

Frimmel, H. E. and Minter, W. E. L., 2002. Recent developments concerning the geological history and genesis of the Witwatersrand gold deposits, South Africa. Society of Economic Geologists, Special Publication, 9, 17-45.

Frimmel, H. E., 2014. A giant Mesoarchean crustal gold-enrichment episode: possible causes and consequences for exploration, in Kelley, K., and Howard, G., eds., Building Exploration Capability for the 21st Century. Society of Economic Geologists, Special Publication No. 18, 209-234.

Gordon-Welsh, J.F., Kleywegt, R.J., Venter, C.P., du Plessis, A., Beukes, J.H.T. and du Plessis, J.G., 1986. Regional gravity surveys by the Geological Survey - data acquisition, reduction and presentation. Ann. Geol. Surv. S. Afr., 20: 59-68.

James, D.E., Niu, F. and Rokosky, J., 2003. Crustal structure of the Kaapvaal Craton and its significance for early crustal evolution. Lithos, 71: 413-429.

Johnson, M.R., van Vuuren, C.J., Visser, J.N.J., Cole, D.I., Wickens, H.d.V., Christie, A.D.M., Roberts, D.L. and Brandl, G., 2006. Sedimentary rocks of the Karoo Supergroup in The Geology of South Africa, pp. 461-499, eds.

Jones, M.Q.W., 2003. Thermal properties of stratified rocks from Witwatersrand gold mining areas. Journal of the South African Institute of Mining and Metallurgy 26 (3), 173-186.

Hales, A.L. and Gough, D.I., 1962. Isostatic anomalies and crustal structure. In: The gravity survey of the Republic of South Africa. Geological Survey of South Africa, Handbook 3.

Kearey, P., Brooks, M. and Hill, I., (2002). An introduction to geophysical exploration, 3rd edition. Oxford, Blackwell Science, 272.

Krahmann, R., 1936. The geophysical magnetometric investigations on the West Witwatersrand Areas between Randfontein and Potchefstroom, Transvaal. Transactions of the Geological Society of South Africa, 39, 247-275.

Leaman, D.E., 1984. Notes on microbarometer elevation determinations. Exploration Geophysics, 15: 53-59.

Malehmir, A., Durrheim, R., Bellefleur, G., Urosevic, M., Juhlin, C. and White, D., 2012. Seismic methods in mineral exploration and mine planning: A general overview of past and present case histories and a look into the future. Geophysics, 77 (5), WC173-WC190.

Manzi, M.S.D., Hein, K.A.A., Durrheim, R.J., King, N., 2014. The Ventersdorp Contact Reef model in the Kloof Gold Mine as derived from 3D seismics, geological mapping and exploration borehole datasets. International Journal of Rock Mechanics and Mining Sciences 66, 97-113.

Manzi, M. S. D., Hein, K. A. A., King N. and Durrheim R. J., 2013. Neoarchaean tectonic history of the Witwatersrand Basin and Ventersdorp Supergroup: New Constraints from high resolution 3D seismic reflection data. Tectonophysics 590, 94–105.

Mcarthy, T.S., Corner, B., Lombard, H., Beukes, N.J., Armstrong, R.A. and Cawthorn, R.G., 2018. The pre-Karoo geology of the southern portion of the Kaapvaal Craton, South Africa. Geological Survey of South Africa.

Molezzi, M., 2017. Modelling The Witwatersrand Basin: A Window Into Neoarchaean - Palaeoproterozoic Crustal-Scale Tectonics. MSc thesis, University of the Witwatersrand, Johannesburg, 156.

Mussett, A. E. and Khan, M. A., 2000. Looking into the Earth: an Introduction to Geological Geophysics. Cambridge: Cambridge University Press, 492.

Nkosi, N.Z., Manzi, M.S.D., Drennan, G.R., Yilmaz, H., 2017. Experimental measurements of seismic velocities on core sampels and their dependence on mineralogy and stress; Witwatersrand Basin (South Africa). Studia Geophysica et Geodaetica 61, 115-144.

Niu, F., James, D.E., 2002. Fine structure of the lowermost crust beneath the Kaapvaal craton and its implications for crustal formation and evolution. Earth and Planetary Science Letters 200, 121-130.

Pretorius, C.C., Muller, M.R., Larroque, M. and Wilkens, C., 2003. A review of 16 years of hardrock seismics on the Kaapvaal Craton. In: D.W. Eaton, B. Milkereit and M.H. Salisbury (Editors), Hardrock Seismic Exploration. Society of Exploration Geophysicists, Geophysical Developments Series, 10:247-268.

Pretorius, C.C., Steenkamp, W.H., Smith, R.G., 1994, Developments in data acquisition, processing and interpretation over ten years of deep vibroseismic surveying in South Africa: Proceedings of the 15th Congress of the Council for Mining and Metallurgical Institutions. South African Institute of Mining and Metallurgy 3, 249–258.

Pretorius, C.C., Jamieson, A.A. and Irons, C., 1989. Seismic exploration in the Witwatersrand Basin, Republic of South Africa. In G.D. Garland (Editor), Proceedings of Exploration 87, Ontario Geological Survey, Special Volume 3, 241-253.

Pretorius, C.C., Jamison, A.A., Irons. C., 1987. Seismic exploration in the Witwatersrand Basin, RSA. Exploration '87. Proceedings Geophysical Methods: advances in the state of the Art, 22, 241-253.

Pretorius, D.A., Brink, W.C.J., Fouche, J., 1986. Geological map of the Witwatersrand Basin. In: Anhaeusser, C.R., Maske, S. (Eds.), Mineral Deposits of Southern Africa, vol. I. Geological Society of South Africa, Johannesburg.

Robb, L. J. and Meyer, M. F., 1995. The Witwatersrand Basin, South Africa: Geological framework and mineralization processes. Ore Geology Reviews, 10, 67-94

Robb, L. J., Charlesworth, E. G., Drennan, G. R., Gibson, R. L and Tongu, E. L., 1997. Tectonometamorphic setting and paragenetic sequence of Au-U mineralisation in the Archaean Witwatersrand Basin, South Africa, Australian Journal of Earth Sciences: An International Geoscience Journal of the Geological Society of Australia, 44 (3), 353-371.

Roux, A.T., 1970. The application of geophysics to gold exploration in South Africa. In: L.W. Morley (Editor), Mining and Groundwater Geophysics 1967. Proceedings of the Canadian Centennial Conference, Ontario. Economic Geology Report 26, Geological Survey of Canada, 425-438.

SACS (South African Committee for Stratigraphy)., 1980. Stratigraphy of South Africa, Part I. Compiled by L.E. Kent. Lithostratigraphy of the Republic of South Africa, South West Africa/Namibia, and the Republics of Boputhatswana, Transkei and Venda. Handbook Geological Survey of South Africa, 8, 690.

Salisbury, M. and Snyder, D., 2007. Application of seismic methods to mineral exploration. In: Goodwell, W. D. (Eds.), Mineral deposits of Canada: a synthesis of major deposit types district metallogeny, the evolution of geological provinces and exploration methods. Geological Association of Canada Mineral Deposits Division Special Publication, 5, 971-982.

Stettler, E.H., Fourie, C.J.S. & Cole, P., 2000. Total magnetic field intensity map of the Republic of South Africa (in 4 panels), Council for Geoscience, Pretoria.

Talwani, M., Worzel, J.L. and Landisman, M., 1959. Rapid Gravity Computations for Two-Dimensional Bodies with Application to the Mendocino Submarine Fracture Zone. Journal of Geophysical Research, 64(1): 49-59.

Weder, E.E.W., 1994. Structure of the area south of the central rand gold mines as derived from a gravity and vibroseis surveys: Proceedings of the XVth CMMI Congress. South African Institute of Mining and metallurgy 3, 271-281.

Wilsher, W.A., 1987. A structural interpretation of the Witwatersrand Basin through the application of automated depth algorithms to both gravity and aeromagnetic data. Unpublished. MSc thesis, University of the Witwatersrand, Johannesburg, 70.

Veeken, P. C. H., 2007. Seismic stratigraphy, basin analysis and reservoir characterisation. The Boulevard, Langford Lane, Kidlington, United Kingdom, Elsevier, 37, 509.

Appendix A

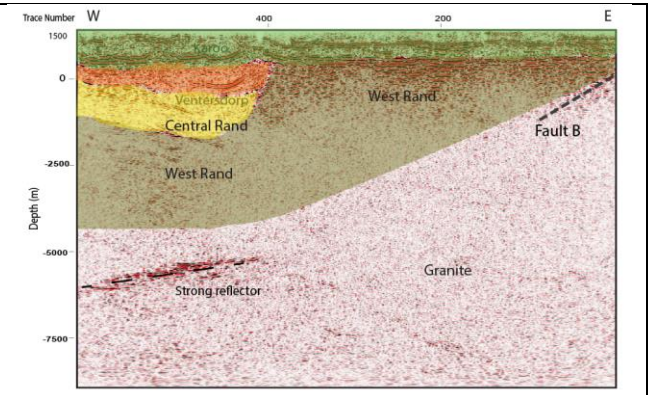
Table 1	**Line EB330**	
Faults	Interpretation	
Fault B Normal fault in north east direction which tilts West Rand Group and granite upwards to east		
Major Contact Reflector	**Borehole intersections – No boreholes lie on seismic line. Borehole 1 is closest.**	**Reflector interpretation**
Base of Karoo Supergroup	Base of Karoo at 1.1 km	Karoo shows a thickness of 1.7 km. Karoo overlies Ventersdorp in this area. Base of Karoo decreases in thickness and overlies the West Rand Group.
Base of Ventersdorp Supergroup	Base of Ventersdorp at 1.5 km	Ventersdorp Supergroup has a thickness less 400 m. Ventersdorp is tilting upwards towards the west and pinches out at the west end of seismic section.
Base of Central Rand Group	Intersects Central Rand Group at 1.5 km but does not intersect base.	Central Rand Group has a thickness of 800m. It follows the same tilt as Ventersdorp Supergroup.
Base of West Rand Group	Does not intersect	The base of the West Rand Group is defined by the change in reflectors from closely packed small reflectors. The West Rand Group is tilted in the same direction as Central Rand Group and Ventersdorp. Fault B tilts West Rand upwards in easterly direction.
Granite	Does not intersect	Granite is interpreted as homogeneous texture.Fault B uplifts the granite. An unknown strong reflector occurs within the granite layer.

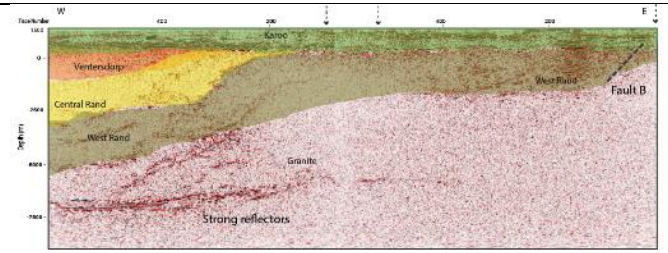
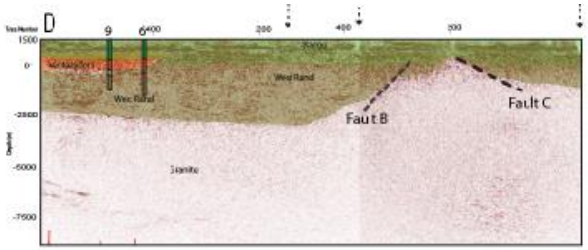
Table 2	**Line EB322**	
Faults	Interpretation	
Fault B	Normal fault which tilts West Rand Group and granite upwards to east.	
Small fault	Fault shows break in boundary reflectors	
Major Contact Reflector	**Borehole intersections – No boreholes lie on seismic line. Borehole 1 is closest.**	**Reflector interpretation**
Base of Karoo Supergroup	Base of Karoo at 1.1 km	Base of Karoo is fairly horizontal with a thickness of 1.4 km.
Base of Ventersdorp Supergroup	Base of Ventersdorp at 1.5 km	Ventersdorp Supergroup has a thickness 1.5 km. Ventersdorp is tilting upwards towards the east and pinches out at the base of Karoo Supergroup.
Base of Central Rand Group	Intersects Central Rand Group at 1.5 km but does not intersect base.	Central Rand Group has a thickness of 2 km. It follows the same tilt as Ventersdorp and pinches out as it reaches the Karoo.
Base of West Rand Group	Does not intersect	The base of the West Rand Group is defined by the change in reflectors from closely packed small reflectors and fairly homogeneous layer beneath defined as granite. The West Rand Group has a thickness of 2.5 km fairly consistently. The West Rand Group is tilted in the same direction as Central Rand Group and Ventersdorp. The West Rand Group is fairly horizontal until Fault B tilts West Rand upwards in easterly direction. This is seen in seismic section EB330.
Granite	Does not intersect	Granite is interpreted as homogeneous texture. Granite underlies West Rand Group and follows the same tilt. Ranging from a depth of 7 km in west to 2.5 km.The basement is then uplifted and underlies West Rand Group at 2.2 km. Granite is tilted like the West Rand Group at Fault B.

Table 3	**Line EB310**	
Faults	Interpretation	
Fault B	Normal fault in north east direction which tilts West Rand Group and granite upwards to east	
Fault C	Normal Fault in south west direction uplifts West Rand Group and Granite.	
Major Contact Reflector	**Borehole intersections – Borehole 4, 5, 6, 9 intersect EB310 C, B. boreholes 4 and 5 do not go below Karoo boreholes 9 and 6 are shown on interpreted seismic section.**	**Reflector interpretation**
Base of Karoo Supergroup	Base of Karoo at 1.30 km and 1.28 km	Base of Karoo is fairly horizontal with a thickness of 1.3 km.
Base of Ventersdorp Supergroup	Base of Ventersdorp at 1.9 km and 2.2 km	Ventersdorp Supergroup has a thickness approximately 2 km. Ventersdorp is tilting upwards towards the east and pinches out at the base of Karoo Supergroup.
Base of Central Rand Group	Central Rand Group less than 200 m only intersected by borehole 9.	Central Rand Group is not interpreted in this section. Borehole 9 intersects Central Rand Group however the resolution of the seismic section discussed in chapter 4 may not be able to pick up this layer especially if it is not continuous.
Base of West Rand Group	Does not intersect base. Borehole 6 shows West Rand Group underlies Ventersdorp at 2.2 km. Borehole 9 shows West Rand Group underlies Central Rand Group at 2.1 km.	The base of the West Rand Group is defined by the change in reflectors from closely packed small reflectors and fairly homogeneous layer beneath is defined as granite. The West Rand Group has a thickness of 2.5 km fairly consistently on the east. West Rand Group is fairly horizontal until Fault B tilts West Rand upwards in easterly direction until is pinches out as it reaches the Karoo Supergroup. On the west of Fault C the is no West Rand Group and to the east of Fault C there is a thin layer of West Rand Group 1 km thick. And is fairly horizontal.

Granite	Does not intersect	Granite is interpreted as homogeneous texture. Granite underlies and is fairly horizontal. Granite is tilted like the West Rand Group at Fault B until it underlies the Karoo Supergroup at 1.3 km. On the west of Fault C granite is tilted towards the west forming a ridge in a northerly direction.

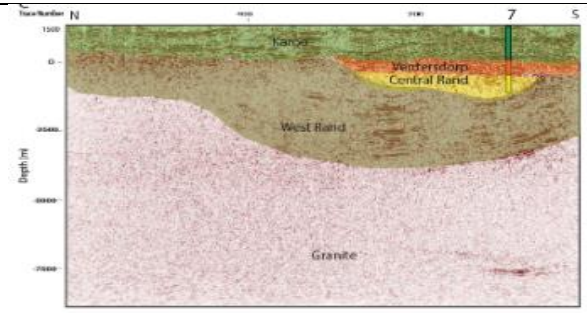
Table 4	**Line EB335**	
Faults	Interpretation	
none		
Major Contact Reflector	**Borehole intersections – Borehole 7 lies on EB335**	**Reflector interpretation**
Base of Karoo Supergroup	Base of Karoo at 1.5 km	Base of Karoo is fairly horizontal with a thickness of 1.5 km.
Base of Ventersdorp Supergroup	Base of Ventersdorp at 2.6 km	Ventersdorp Supergroup has a thickness approximately 1 km. Ventersdorp is tilting upwards towards the north and pinches out at the base of Karoo Supergroup.
Base of Central Rand Group	Central Rand Group 1 km thick does not reach base of Central Rand	Central Rand Group has lenticular shape and pinches out on both ends.
Base of West Rand Group	Does not intersect	The base of the West Rand Group is defined by the change in reflectors from closely packed small reflectors and fairly homogeneous layer beneath defined as granite. The West Rand Group has a thickness of 2.3 km fairly consistently on the east. West Rand Group appears to show a tilt. It was noted that this could be due to over migration and not a geological feature.
Granite	Does not intersect	Granite is interpreted as homogeneous texture.

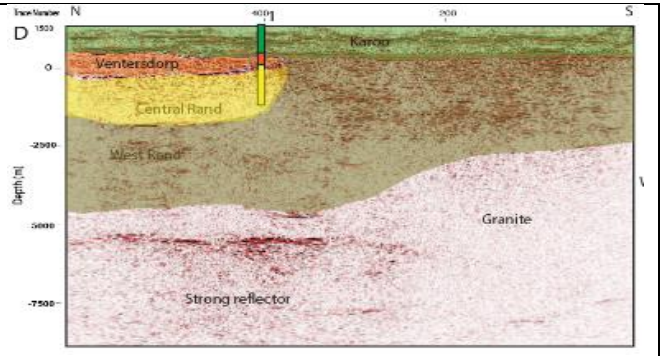
Table 5	**Line EB337**	
Faults	Interpretation	
none		
Major Contact Reflector	**Borehole intersections – Borehole 1 lies on EB337**	**Reflector interpretation**
Base of Karoo Supergroup	Base of Karoo at 1.1 km	Base of Karoo is fairly horizontal with a thickness of 1 km.
Base of Ventersdorp Supergroup	Base of Ventersdorp at 1.5 km	Ventersdorp Supergroup has a thickness approximately 0.5 km. Ventersdorp is tilting upwards towards the north and pinches out at the base of Karoo Supergroup.
Base of Central Rand Group	Central Rand Group 1 km thick does not reach base of Central Rand	Central Rand Group has a thickness of 1 km. It follows the same tilt as Ventersdorp Supergroup.
Base of West Rand Group	Does not intersect	The base of the West Rand Group is defined by the change in reflectors from closely packed small reflectors and fairly homogeneous layer beneath defined as granite.
Granite	Does not intersect	Granite is interpreted as homogeneous texture.

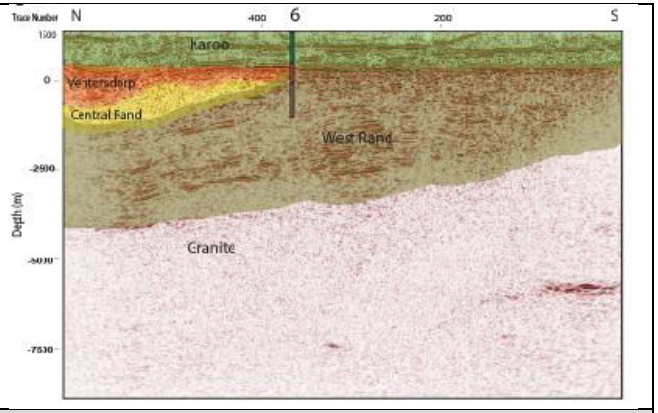
Table 6	**Line EB334**	
Faults	Interpretation	
No faults interpreted		
Major Contact Reflector	**Borehole intersections – Borehole 6 lies on EB334**	**Reflector interpretation**
Base of Karoo Supergroup	Base of Karoo at 1.2 km	Base of Karoo is fairly horizontal with a thickness of 1 km.
Base of Ventersdorp Supergroup	Base of Ventersdorp at 2.2 km	Ventersdorp Supergroup has a thickness approximately 1 km. Ventersdorp is tilting upwards towards the north and pinches out at the base of Karoo Supergroup.
Base of Central Rand Group	Does not intersect.	Central Rand Group has a thickness of 0.3 km. It follows the same tilt as Ventersdorp Supergroup.
Base of West Rand Group	Does not intersect base. West Rand underlies Ventersdorp Supergroup.	The base of the West Rand Group is defined by the change in reflectors from closely packed small reflectors and fairly homogeneous layer beneath is defined as granite. The West Rand Group has a thickness of 2.7 km fairly consistently on the east. West Rand is tilted to the north and underlies Karoo on south.
Granite	Does not intersect	Granite is interpreted as homogeneous texture. Granite follows same trend as West Rand Group.

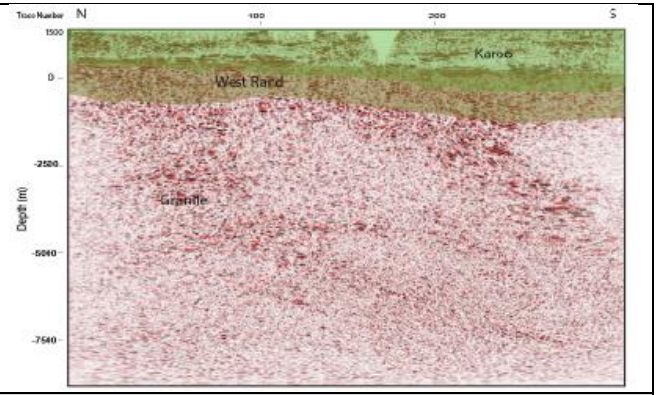
Table 7	**Line WB491**	
Faults	Interpretation	
No Faults interpreted		
Major Contact Reflector	**Borehole intersections – No boreholes lie on seismic section. Borehole 11 closest**	**Reflector interpretation**
Base of Karoo Supergroup	Base of Karoo at 1.7 km	Base of Karoo is fairly horizontal with a thickness of 1.3 km in the north to 1.7 in the south of section.
Base of Ventersdorp Supergroup	Does not intersect	No Ventersdorp interpreted.
Base of Central Rand Group	Does not intersect.	No Central Rand interpreted
Base of West Rand Group	Does not intersect base. West Rand underlies Karoo Supergroup	The base of the West Rand Group is defined by the change in reflectors from closely packed small reflectors and fairly homogeneous layer beneath defined as granite. The West Rand Group has a thickness of 2 km fairly consistently.
Granite	Does not intersect	Granite is interpreted as homogeneous texture. Granite follows same trend as West Rand Group.

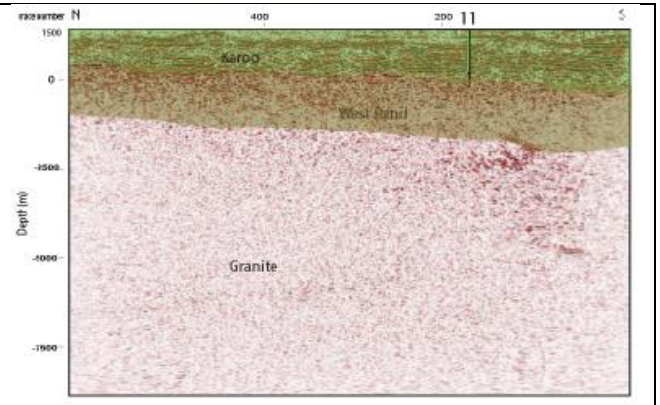
Table 8	**Line EB331**	
Faults	Interpretation	
No Faults interpreted		
Major Contact Reflector	**Borehole intersections – Borehole 11 lies on seismic section.**	**Reflector interpretation**
Base of Karoo Supergroup	Base of Karoo at 1.7 km	Base of Karoo is fairly horizontal with a thickness of 1.3 km in the north to 1.7 in the south of section.
Base of Ventersdorp Supergroup	Does not intersect	No Ventersdorp interpreted.
Base of Central Rand Group	Does not intersect.	No Central Rand interpreted
Base of West Rand Group	Does not intersect base. West Rand underlies Karoo Supergroup	The base of the West Rand Group is defined by the change in reflectors from closely packed small reflectors and fairly homogeneous layer beneath defined as granite. The West Rand Group has a thickness of 1.8 km fairly consistently.
Granite	Does not intersect	Granite is interpreted as homogeneous texture. Granite follows same trend as West Rand Group.

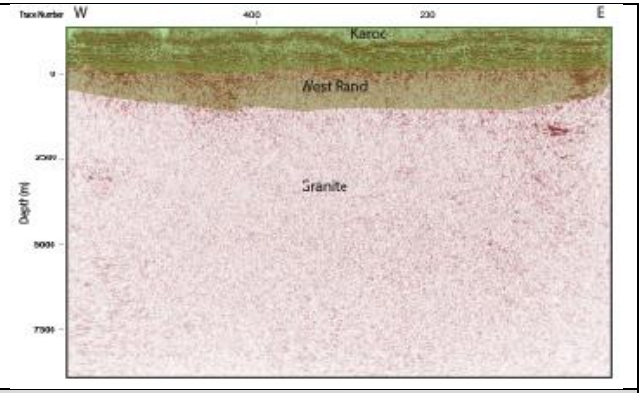
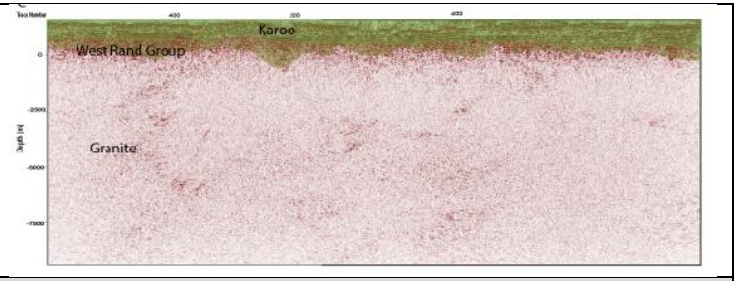
Table 9	**Line EB310A**	
Faults	Interpretation	
No Faults interpreted		
Major Contact Reflector	**Borehole intersections – No Boreholes close to EB310A**	**Reflector interpretation**
Base of Karoo Supergroup		Base of Karoo is fairly horizontal with a thickness of 1.4 km.
Base of Ventersdorp Supergroup		No Ventersdorp interpreted.
Base of Central Rand Group		No Central Rand interpreted
Base of West Rand Group		The base of the West Rand Group is defined by the change in reflectors from closely packed small reflectors and fairly homogeneous layer beneath defined as granite. The West Rand group was horizontal but a boundary was very difficult to interpret as no clear package was visible.
Granite		Granite is interpreted as homogeneous texture. Granite follows same trend as West Rand Group.

Table 10	**Line EB311**	
Faults	Interpretation	
No Faults interpreted		
Major Contact Reflector	**Boreholes 2, 3, 10 and 12 close to EB311**	**Reflector interpretation**
Base of Karoo Supergroup	Base of Karoo 900 m.	Base of Karoo is fairly horizontal with a thickness of 1.4 km.
Base of Ventersdorp Supergroup	No intersected	No Ventersdorp interpreted.
Base of Central Rand Group	Not intersected	No Central Rand interpreted
Base of West Rand Group	Not intersected	The base of the West Rand Group is defined by the change in reflectors from closely packed small reflectors and fairly homogeneous layer beneath defined as granite. The boundary for the West Rand group is not visible, however 2D gravity profiles were used to help interpret a very thin undulating layer of West Rand Group which was not a consistent layer that in which granite could break up the West Rand.
Granite	Boreholes 2, 3 and 10 intersected granite beneath Karoo Supergroup.	There were no obvious indication of granite underlying the Karoo Supergroup. A very thin layer of West Rand Group is present with possibility of granite breaking West Rand Group layer.